UCLA
UCLA Electronic Theses and Dissertations

Title
Disorders of iron regulation and their treatment

Permalink
https://escholarship.org/uc/item/86x151fv

Author
RAMOS, Emiio

Publication Date
2012

Peer reviewed|Thesis/dissertation

eScholarship.org Powered by the California Digital Library
University of California

UNIVERSITY OF CALIFORNIA
Los Angeles

Disorders of iron regulation and their treatment

A dissertation submitted in partial satisfaction of the
requirements for the degree Doctor of Philosophy
in Biochemistry and Molecular Biology

by

Emilio Ramos

2012

ABSTRACT OF THE DISSERTATION

Disorders of iron regulation and their treatment

by

Emilio Ramos

Doctor of Philosophy in Biochemistry and Molecular Biology

University of California, Los Angeles, 2012

Professor Sabeeha Merchant, Chair

In vertebrates, hepcidin is the peptide hormone that homeostatically regulates the body's supply of elemental iron, an indispensible reactant in many biological processes. Worldwide over a billion people are affected by diseases associated with iron imbalance. These conditions can be categorized as disorders in which hepcidin responds physiologically and disorders in which hepcidin is dysregulated. In the former, lack of dietary iron appropriately suppresses hepcidin to maximize dietary iron absorption capacity. Iron-restricted anemia can develop, nevertheless, if the iron content of food is not sufficient. In the latter, inappropriate hepcidin stimulation by cytokines, during chronic inflammation for example, reduces plasma iron and anemia results despite adequate levels of dietary and body iron.

Iron absorption depends on the interaction between hepcidin and its receptor, the iron exporting channel, ferroportin. When hepcidin activity is insufficient, iron pathways saturate and excess iron intoxicates the organs in which it accumulates. When plasma iron levels need to be reduced, hepcidin is secreted by the liver into circulation where it finds ferroportin and initiates its internalization and degradation. Plasma iron flow is thus blocked from the principle ferroportin-expressing cell types including, but not limited to, enterocytes, macrophages of the spleen and liver and hepatocytes until an unknown signaling mechanism suppresses hepcidin production to allow iron to flow to sites of need.

How the liver moderates hepcidin production in response to increased body iron is still not completely understood, but Chapter 1 of this dissertation, describes the use of mouse models of hepcidin deficiency to define two signals that independently regulate hepcidin production. Chapter 2 builds on a collaboration described in Chapter 3, and details the

optimization and use of hepcidin mimetics to treat iron overload caused by hepcidin deficiency. Chapter 4 is another collaboration that elucidates novel signaling pathways that suppress hepcidin and their connection to iron overload in conditions that damage cells of the liver.

The dissertation of Emilio Ramos is approved

Tomas Ganz

Manuel Penichet

Catherine Clarke

Guillaume Chanfreau

Sabeeha Merchant, Committee Chair

Con todo el corazón para María del Rosario.

TABLE OF CONTENTS

Abstract of the Dissertation ii

Acknowledgements vii

Vita viii

Overview: Iron homeostasis 1

Chapter 1: **Summary** 17
References 18
Paper: Evidence for Distinct Pathways of Hepcidin Regulation by Acute and Chronic Iron Loading in Mice 19

Chapter 2: **Summary** 38
References 39

Paper: Inhibition of Hepcidin Transcription by Growth Factors 40

Chapter 3: **Summary** 50
References 51
Paper: Minihepcidins are rationally designed small peptides that mimic Hepcidin activity in mice and may be useful for the treatment of iron overload 52

Chapter 4: Optimization of mini hepcidins yields peptides that prevent iron overload in mouse models of hemochromatosis 72
References 85

Concluding remarks 109

Acknowledgements

I would like to make an attempt to thank a few special people that made contributions- direct and indirect, personal and professional- to this work. In no particular order I would like to give thanks to:

Guillaume Chanfreau, Cathy Clarke, Sabeeha Merchant and Manuel Penichet for dutifully serving on my committee.

Tomas Ganz, for taking- and giving me- a chance and allowing me to join your home away from home. I knew research leads to discovery, but I never expected our research would lead me to discover myself. I will be forever grateful.

Elizabeta Nemeth for her unwavering support. Your sheer enthusiasm for life has been a consistent source of inspiration in my life.

Peter Ruchala for allowing me the satisfaction of playing "peptide chemist."

The rest of the Ganz lab, those past and present, for years of friendship.

Léon Kautz for making indispensible contributions at the lab bench, even before we knew each other.

Adam Rosenthal for recommending the Ganz lab when looking for a rotation. Your friendship is one of the things I will joyfully take with me from my time at UCLA.

También quiero agradecer a los héroes de mi vida.

A mi amigo y hermano Adrián Alejandro le quiero desear unas especiales, pero muy grandes.

A mis hermanos Mario, Isabel y Sylvia- gracias por todo y por siempre.

A mis padres Emilio y María Elena por trabajar sin falta todas las madrugadas que no tuve que trabajar.

A Ramiro, mi segundo padre pero un primer amigo.

Y a ti, corazón, por mi felicidad.

VITA

Emilio Ramos

2006	Bachelor of Science
	Biology
	University of California, San Diego
2006-2012	Graduate Student
	Department of Chemistry and Biochemistry-
	University of California, Los Angeles
2007-2010	Cellular and Molecular Biology Training Program trainee

Presentations

2009	Plenary Session Speaker
	BioIron Conference- Porto, Portugal
2011	Plenary Session Speaker
	BioIron Conference- Vancouver, Canada
2011	Oral Presentation- Winner of Promising Young Investigator award
	9th Australian Peptide Association meeting

Publications

1. Ramos E, Kautz L, Rodriguez R, Hansen M, Gabayan V, Ginzburg Y, et al. Evidence for distinct pathways of hepcidin regulation by acute and chronic iron loading in mice. Hepatology. 2011;53:1333–1341.

2. Goodnough JB, Ramos E, Nemeth E, Ganz T. Inhibition of hepcidin transcription by growth factors. Hepatology (Baltimore, Md.) [Internet]. 2012 [cited 2012 Mar 18];Available from: http://www.ncbi.nlm.nih.gov/pubmed/22278715

3. Preza GC, Ruchala P, Pinon R, Ramos E, Qiao B, Peralta MA, et al. Minihepcidins are rationally designed small peptides that mimic hepcidin activity in mice and may be useful for the treatment of iron overload. J. Clin. Invest. 2011;121:4880–4888.

Review of Iron Homeostasis

Elemental iron

In the earth's oxidizing atmosphere, the electrochemical potential of the Fe^{3+}/Fe^{2+} redox pair makes iron a versatile element that is used by almost all life forms to facilitate fundamental cellular processes. As a component of the cytochromes of the electron transport chain iron is essential for energy production and in hemoglobin and myoglobin iron enables oxygen storage and delivery to tissues. At physiological pH 7, ferrous iron (Fe^{2+}) is relatively soluble at 10^{-1} M but this form is not stable in the oxidizing environment of the earth's atmosphere. In contrast, the solubility of the stable ferric iron (Fe^{3+}) form is only 10^{-18} M making iron acquisition by living organisms a challenge. To restrict iron from randomly reacting with nearby biomolecules, organisms evolved protective mechanisms in the form of iron-carrying and iron storage proteins that limit the reactivity of the element. If the capacity of the organism to sequester iron in an unreactive state is exceeded or impaired, ferrous ions may react with hydrogen peroxide to form reactive oxygen species (e.g. Fenton's reaction below) which are damaging to cell membranes, proteins and DNA. Prolonged exposure to reactive iron ions leads to progressive organ failure as seen in patients with inherited or clinically acquired iron overload. This introduction will provide general information about iron physiology as it relates to humans, diseases which are caused by iron imbalance and their treatment.

Fenton's reaction: $Fe^{2+} + H_2O_2 \rightarrow Fe^{3+} + OH^- + OH^\cdot$ (1)

Iron Physiology

Normal iron physiology in humans centers on acquiring sufficient iron from the environment to replace losses, storing and transporting iron in a chemically inert state, and safely

delivering iron for incorporation within prosthetic groups and eventually proteins that catalyze redox reactions or store oxygen. The most common iron containing prosthetic groups are heme and iron-sulfur clusters. Heme consists of a pyrrole group whose four aromatic nitrogen rings are arranged in a ring and coordinate a single iron atom at the center. Heme groups are most commonly found in hemoglobin, myoglobin and cytochrome C oxidase, the last complex of the respiratory chain. Iron sulfur cluster (Fe-S) proteins contain rhombic arrangements of 2 or more iron atoms coordinates to sulfur atoms, typically donated by cysteine residues (2). Fe-S proteins have a wide range of reduction potentials (-700 mV to 400 mv) which makes them well-suited to function in complexes I-III of the electron transport chain (3).

A typical human adult has about 3-5 grams of total body iron: 60% of iron is found in circulating hemoglobin, 10% in myoglobin in muscles, 20% is stored in liver cells (hepatocytes and Kupffer cells) within the cage-like storage protein, ferritin, and the remainder is divided between enzymes such as cytochromes, peroxidases, catalase and others (4) (**Figure 1**). To replenish the daily loss of 1-2 mg of iron from mucosal cell sloughing, sweat and urine excretion, duodenal enterocytes must absorb an equal amount of iron. Iron absorption takes place at the apical surface of duodenal enterocytes either through the apical channel DMT1 that imports inorganic iron from plant-derived foods or through a poorly characterized apical heme transporter which takes up heme from animal sources. About 4 mg of iron circulates bound to diferric plasma transferrin which typically uses about 30% of its iron-carrying capacity and brings iron to most cells through the transferrin/transferrin receptor 1 cycle. The largest iron consumer in the body is the bone marrow which requires 20-25 mg of iron per day for the production of hemoglobin. Thus, the plasma iron pool can only sustain the production of new red blood cells for 3 to 4 hours if iron is not replenished. Red pulp macrophages of the spleen

continuously recycle 20-25 mg of iron per day into plasma by erythrophagocytosing old red blood cells. During increased iron demand, after blood loss for example, iron can be mobilized from ferritin stores in the liver.

The mechanism of systemic iron regulation

The body loses small amounts of iron per day in the urine and stool and more significantly through blood loss in menstruating women, but iron excretion is not known to be regulated. In cases of acute iron excess, for example after accidental ingestion of iron containing supplements, the body cannot significantly compensate by increasing the excretion of iron. Transferrin iron-carrying capacity is quickly saturated and highly toxic non-transferrin bound iron (NTBI) circulates which causes organ damage and the formation of scar tissue, fibrosis (5). To prevent excessive iron absorption, the liver secretes a peptide hormone, hepcidin, into plasma (6). Hepcidin is composed of 25 amino acids and includes 4 disulfide bonds which have been shown to be important for interaction with its receptor, a 12 transmembrane domain iron-exporting transporter, ferroportin. Binding of hepcidin to ferroportin causes internalization and degradation of the only known conduit by which iron can reach blood plasma and become bound to transferrin. Ferroportin is expressed on the basolateral surface of enterocytes, and the membranes of iron-recycling macrophages and hepatocytes. Thus, sustained increases in hepcidin concentrations will prevent iron absorption from the diet, slow the delivery of recycled iron from macrophages, inhibit iron mobilization from hepatic stores, and cause iron to be depleted from plasma and extracellular fluids (**Figure 2**, from (7)).

Homeostatic regulation of hepcidin

Hepcidin expression is homeostatically regulated by a complex signaling network consisting of stimulants and suppressants including iron, inflammation, erythropoietic activity and others (**Figure 2**). The predominant and the only documented hepcidin-regulating mechanism is transcriptional.

Physiologic Induction

Iron itself stimulates hepcidin production, but the nature of the signal and its sensors is not completely understood. Hepcidin regulation by iron involves the bone morphogenetic protein (BMP) cytokine family which activates the homologues of mothers against dodecapentaplegic (SMAD) signaling pathway. Though this pathway is involved in many developmental processes, it is adapted to iron homeostasis through its dependence on the iron-regulatory proteins hemochromatosis protein (HFE), transferrin receptor 2 (TFR2), hemojuvelin (HJV) and a specific iron-related bone morphogenetic protein, BMP6 (8). When this pathway is activated by iron, phosphorylated SMAD proteins are translocated into the nucleus where they bind to SMAD sites on the hepcidin promoter to increase hepcidin transcription. The work described in Chapter 1 of this dissertation provides evidence that plasma and tissue iron levels independently stimulate hepcidin production. Sensitivity of this pathway to plasma iron concentrations and tissue iron stores is enhanced by the HFE, TfR2 and HJV proteins which modulate the signal transduction by the BMP receptor and its BMP6 ligand.

Physiologic Suppression

Hepcidin is actively suppressed when there is an increased demand for iron during anemia and hypoxia, independently of the amount of iron stores present. The suppressive mechanism is not well understood, but is believed to be indirectly mediated by the hormone

erythropoietin (EPO) (9). EPO is secreted by the liver in the fetus and kidneys in the adult in response to hypoxia and initiates cellular signaling in developing erythroblasts that express the EPO receptor. Erythroblasts are thought to secrete an as-yet-unidentified factor to suppress hepcidin transcription in the liver.

Pathological regulation and dysregulation of hepcidin

Pathological induction

During inflammation or infection, stimulatory molecules including prominently interleukin-6 (IL-6) increase hepcidin production (**Figure 3, from** (7)**)**. This regulation is thought to have evolved as part of a protective mechanism to sequester plasma iron from pathogenic microbes to limit their growth. IL-6 is a cytokine that is highly produced by hepatocytes during the acute phase response. Binding of IL-6 to the IL-6 receptor initiates activation of Janus kinases (JAK) which phosphorylate the STAT3 transcription factors (signal transducers and activators of transcription (STAT))(10). The hepcidin promoter contains STAT3 binding sites which have been shown to be necessary and sufficient for transcriptional activation by IL-6 (11).

In inflammatory disorders, increased hepcidin production results in iron-restricted anemia caused by blockade of iron absorption and mobilization of iron stores for hemoglobin synthesis. Excess hepcidin has been measured in a group of diseases known collectively as anemias of inflammation (AI) (**Figure 4b,** from (12)**)**. Examples include IL-6 inducing cancers such as multiple myeloma, autoimmune diseases such as rheumatoid arthritis, inflammatory bowel disease, and about one third of patients with anemia of aging (6).

Apart from inflammation, increased hepcidin production with consequent iron-restricted anemia is also caused by hepcidin producing hepatic adenomas (13) and genetic

lesions in a hepcidin suppressor, protease TMPRSS6/MT-2 (14,15,16). Elevated plasma hepcidin concentrations may also result from defective hepcidin clearance as found in chronic kidney disease (17).

Pathologic Suppression

Hepcidin is physiologically suppressed during periods of increased red blood cell and hemoglobin production to increase iron flow to the bone marrow for the production of heme in developing red blood cells (**Figure 3**). In the iron-loading anemias, such as β-thalassemia, hepcidin transcription is pathologically suppressed by exuberant but ineffective erythropoiesis (**Figure 4c)**. In β-thalassemia, mutations in the beta chains of hemoglobin result in an imbalance in the number of alpha and beta globin chains, and premature red cell death. The body responds appropriately to the ensuing decrease in oxygen delivery and hypoxia by suppressing hepcidin, but continued ineffective red blood cell development results in chronic hepcidin deficiency and hyperabsorption of dietary iron. Hepcidin is suppressed in part by the cytokines GDF-15 and TWSG1 (18,19). Even in untransfused patients (β-thalassemia intermedia), iron overload is the main cause of morbidity and mortality. Transfusion treatment (β-thalassemia major patients) further exacerbates iron overload. Patients receive from 25-50 units of healthy red blood cells per year (each unit is about 500 ml of blood containing about 200 ml of red blood cells and about 200 mg of iron) delivering about 6-12 g of iron per year from early in life (20). As these red blood cells are phagocytosed, iron accumulates in the body and patients develop severe transfusional iron overload often despite cotreatment with iron chelators.

Other conditions such as hepatitis C and alcoholic liver disease where cycles of liver damage and repair are common are also associated with hepcidin deficiency and iron

loading (21,22). Chapter 4 of this dissertation describes contributions to a work that demonstrates new kinase signaling pathways that may mediate hepcidin suppression during liver repair. Hepatocyte growth factor (HGF) which is upregulated during liver regeneration and the related epidermal growth factor (EGF) both suppress hepcidin by inhibiting BMP signaling.

Hepcidin deficiency as a result of inadequate iron sensing and signaling

Hepcidin deficiency causes systemic iron overload. Hereditary hemochromatosis (HH) (types I-III) describes a group of autosomal recessive genetic diseases characterized by a reduced capacity to produce hepcidin (23). With increasing hepcidin deficiency, the resulting ferroportin excess enhances iron flow into plasma from the diet and iron release from macrophages. The iron buffering capacity of transferrin is exceeded, nontransferrin-bound iron (NTBI) consisting of iron complexes with acetate, citrate and albumin is taken up in the liver, heart and pancreas, and these organs become iron overloaded.

Type I hemochromatosis is the most common form of inherited iron overload and is caused by genetic lesions in the hemochromatosis (HFE) gene. HFE mutations are incompletely penetrant and cause clinically important disease in men much more often than women, suggesting that modifier genes, alcohol intake and dietary habits may also be important factors in the development of iron overload. The HFE protein resembles MHC class I proteins. HFE is expressed highly in hepatocytes, where it interacts with transferrin receptor 1 (TfR1). When diferric transferrin (holotransferrin) levels increase, HFE is displaced from its binding site on TfR1 by the binding of holotransferrin whose binding site of TfR1 overlaps that of HFE. Free HFE binds TfR2 and both molecules are thought to interact with the BMP receptor complex. The TfR2 protein is a homologue of TfR1, but binds iron transferrin with much lower affinity which

suggests that *in vivo* its primary function may not be iron uptake (24). Binding of iron-transferrin to TfR2 stabilizes the protein and, together with HFE interaction, this is an attractive candidate for the sensing mechanism for holotransferrin concentrations in plasma. TfR2 mutations cause type III HH, a more rapid onset of iron overload. Type II HH is caused by mutations in the hemojuvelin (HJV) gene which encodes a BMP coreceptor protein, or by mutations in the hepcidin (HAMP) gene itself. HJV and HAMP gene mutations are rare, but cause severe juvenile onset hemochromatosis (JH). Patients often die from severe cardiac and endocrine iron overload as early as the third decade of life. (**Figure 4C**)

Treatment of iron disorders

Hepcidin excess

The anemia of inflammation is typically treated with erythropoiesis-stimulating agents (ESAs), and supplemental iron (25). ESA treatment, however, is typically expensive, may have rare but serious side effects, and is not always effective in reversing the anemia. Assuming a central role of hepcidin in the development of anemia of inflammation, hepcidin antagonists present a promising alternative or complementary approach. Hepcidin antagonists in the form of neutralizing antibodies or engineered hepcidin-binding molecules are currently being studied as potential treatments for anemia of inflammation, as is soluble hemojuvelin, a known suppressor of hepcidin *in vitro*.

Hepcidin deficiency/suppression

The standard treatment for iron overload in hereditary hemochromatosis is phlebotomy which removes red blood cells (26). Red blood cells are extremely iron-rich compared to other cell types, containing about 1 mg of iron for each ml of packed cells, so that each unit of red

blood cells removes about 200 mg of iron from the body. Though phlebotomy is inexpensive and effective, patients often complain about venesection therapy (27). Non-anemic iron overloaded patients may require up to 100 weekly phlebotomies to restore body iron levels to a normal level and experience problems with venous access and lost employment time. Alternative approaches include erythrocytapherisis, which has been shown to remove up to 800 mg of iron, close to 4 times the amount removed by standard phlebotomy (28).

β-thalassemia intermedia patients do not receive blood transfusions to correct anemia, but, like transfused thalassemia major patients, undergo chelation therapy with deferoxamine, a siderophore produced by Streptomyces pilosus. Phlebotomy is contraindicated in β-thalassemia intermedia and other iron-loading anemias because it worsens anemia. Chelation regimens consist of 2 g of deferoxamine over a 10-12 hour period through an IV pump 5 nights per week. Nightly sessions result in the excretion of 20-50 mg iron in the urine and stool, which approximates the yearly iron input in highly transfused patients. Aggressive chelation therapy, however, can result in irreversible visual and auditory loss. More recently, oral iron chelators have been introduced, but they are also associated with significant side effects (29)

To improve patient quality of life and reduce the amount of phlebotomy and chelation required, alternative therapies are being explored. One approach is the use of hepcidin replacement therapy. Though hepcidin is only 25 amino acids long, it is difficult and expensive to synthesize. Chapters 2 and 3 of this dissertation describe the rationale for, and rational development of, synthetic hepcidin fragments and their treatment of iron overload caused by hepcidin deficiency.

Summary

The work in this dissertation provides new physiological insights into the pathogenesis of hepcidin insufficiency in HH (Chapter 1) and the novel signaling mechanisms underlying pathological hepcidin suppression (Chapter 4). Chapters 2 and 3 detail the development of hepcidin agonists and their successful use for the prevention of iron overload in mouse models of hereditary hemochromatosis.

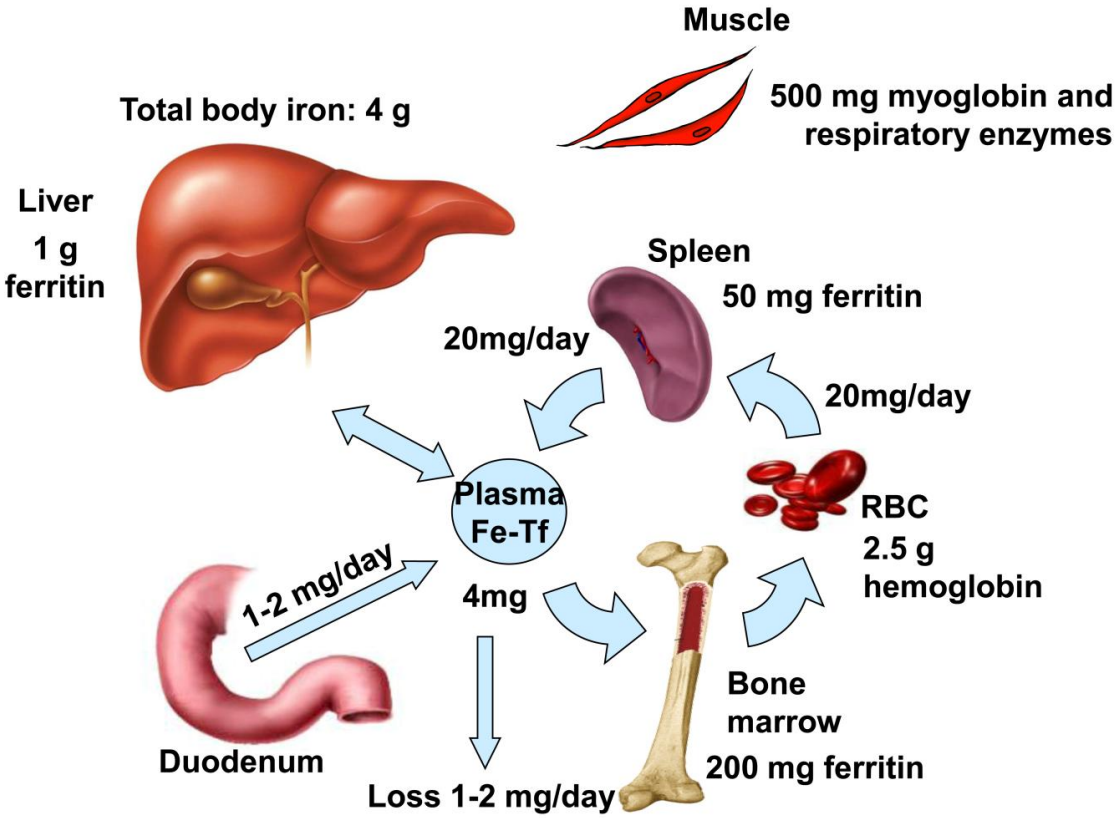


Figure 1: **Iron distribution in a typical adult male.** The total iron content of a 70 kg male approximates 4 g. 60% of the iron is found within mature red blood cells, but only 0.1% of the total iron content is in plasma transferrin destined for ferroprotein synthesis. 1-2 mg of iron is lost daily from cell sloughing and the equivalent amount of iron is absorbed from plant or animal based foods to replenish this loss. Approximately 20 mg of recycled iron is supplied by macrophages of the spleen to erythroblasts for hemoglobin synthesis and a small reserve (200 mg) of iron can be stored within the bone marrow as ferritin. During periods of prolonged iron deprivation or blood loss, the increased iron need can be sustained by hepatic ferritin stores which hold enough iron to make 1 liter of packed red blood cells or more than 2 liters of blood. Muscles and respiratory enzymes contain 10% of body iron as myoglobin and small amounts of iron distributed among the rest of the cells of the body.

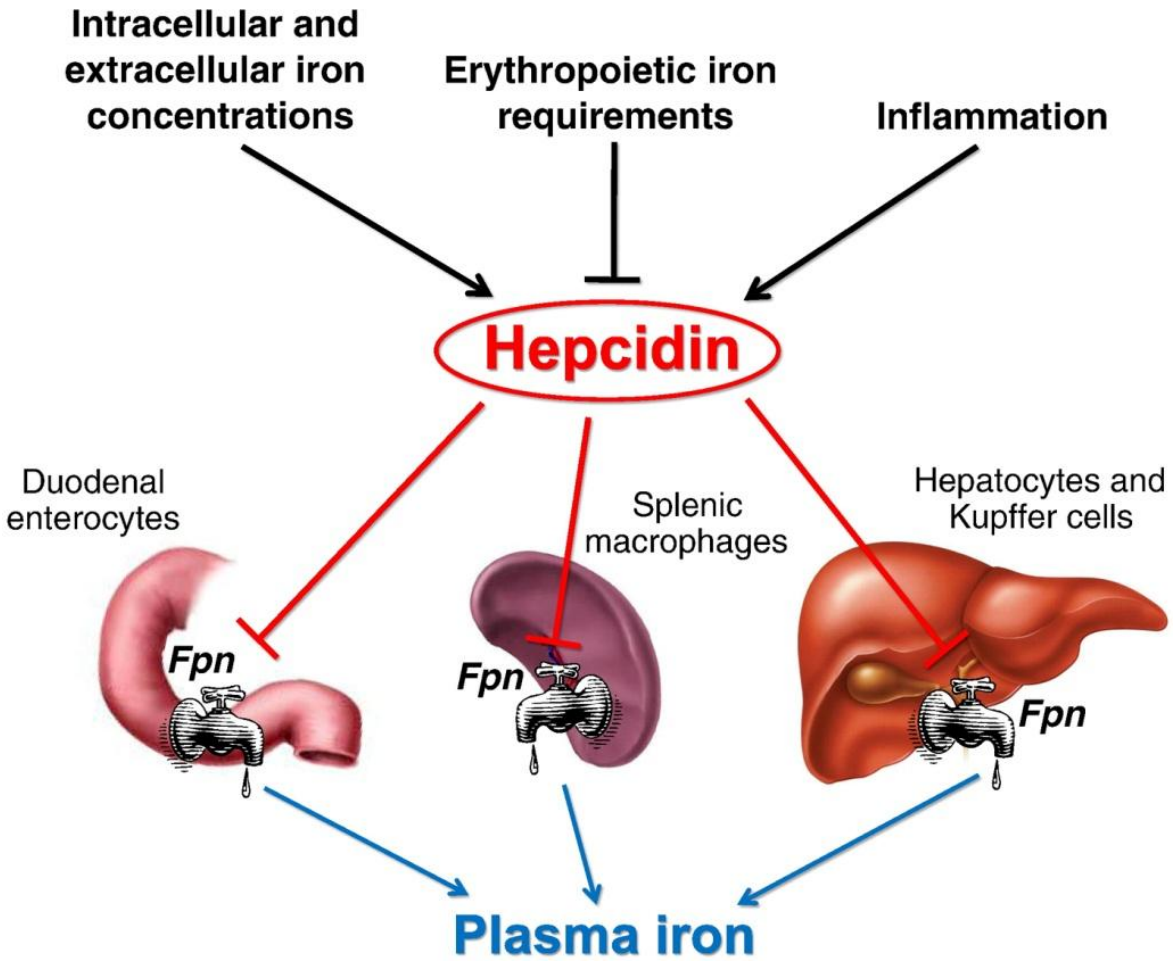


Figure 2 (from 7): **Regulation of iron balance.** Iron flows into plasma exclusively through the membrane channel, ferroportin. Enterocytes, macrophages, and to a lesser extent, hepatocytes, are the primary ferroportin expressing and, therefore, iron exporting cell types. The organs in which these cells are found (the duodenum, spleen and liver) are major sites for modulating iron flux (blue arrows). Ferroportin levels are controlled by a 25 amino acid hepatic hormone hepcidin. Hepcidin binding to ferroportin triggers endocytosis and proteolysis which halts iron flow (red arrows) into the plasma from ferroportin-expressing tissues. Hepcidin synthesis increases as iron stores increase, or during infection (black arrows) and decreases when there is a need for more iron during erythropoiesis.

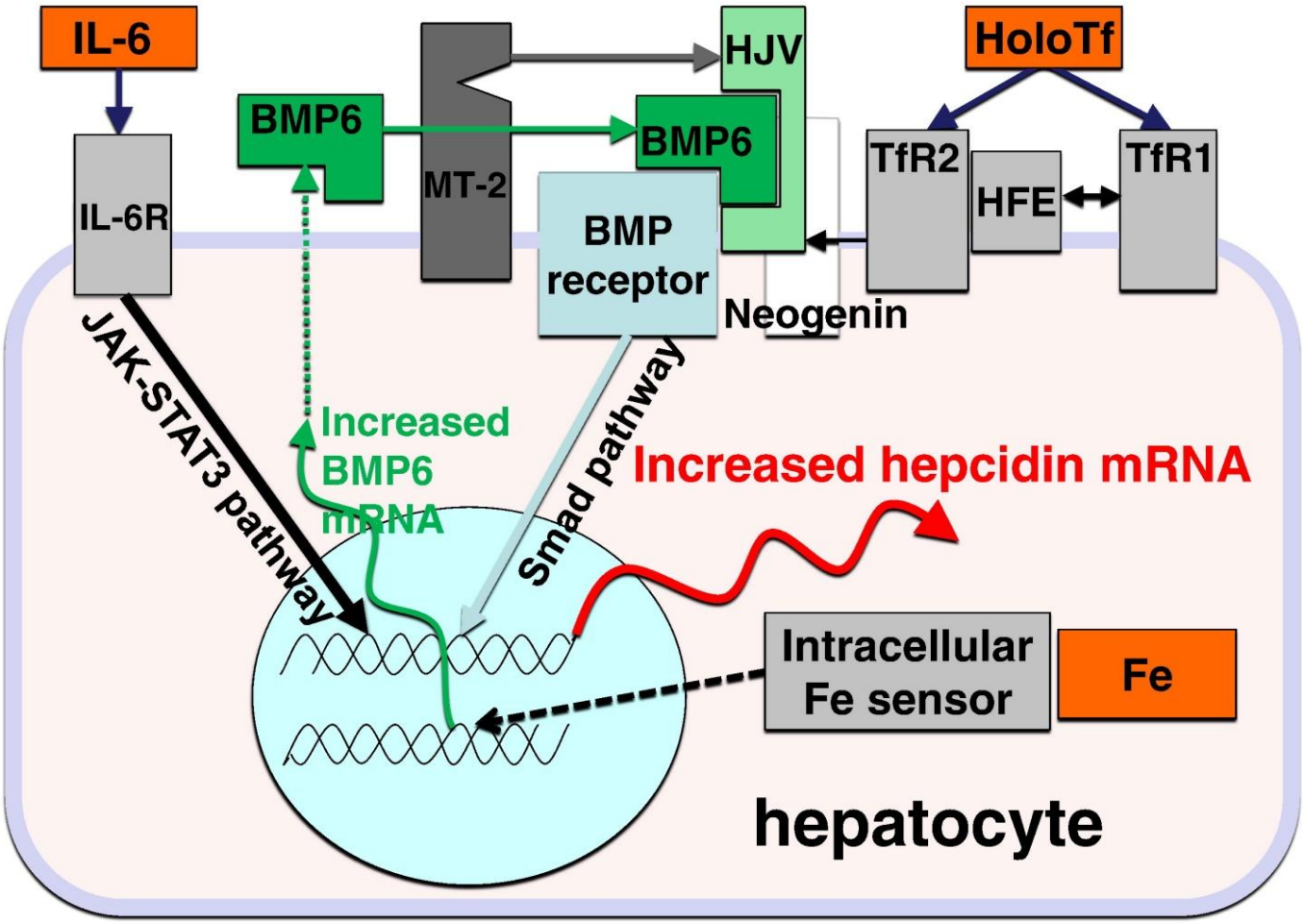


Figure 3 (from (7)): **Hepcidin-inducing signaling pathways.** Regulation of hepcidin production by liver cells occurs primarily through a transcriptional mechanism. The hepcidin promoter contains Bone Morphogenetic Protein (BMP) Responsive Elements (BRE's) which are recognized by transcription factors of the SMAD family. Binding strength of BMP to its receptor is modulated by several proteins including hemojuvelin (HJV), transferrin receptor 2 (TfR2), HFE, neogenin and matriptase-2 (MT-2). The absence of any one of these factors leads to defective downstream activation of the SMAD phosphorylation cascade (blue arrow) and hepcidin insufficiency. Chapter 1 presents evidence for independent intracellular and extracellular iron sensing mechanisms that regulate hepcidin transcription by increasing BMP6 transcription in the liver (green arrow). Inflammatory cytokines such as IL-6 also stimulate hepcidin production, but through the activation of the JAK-STAT3 pathway and STAT3 sites on the hepcidin promoter.

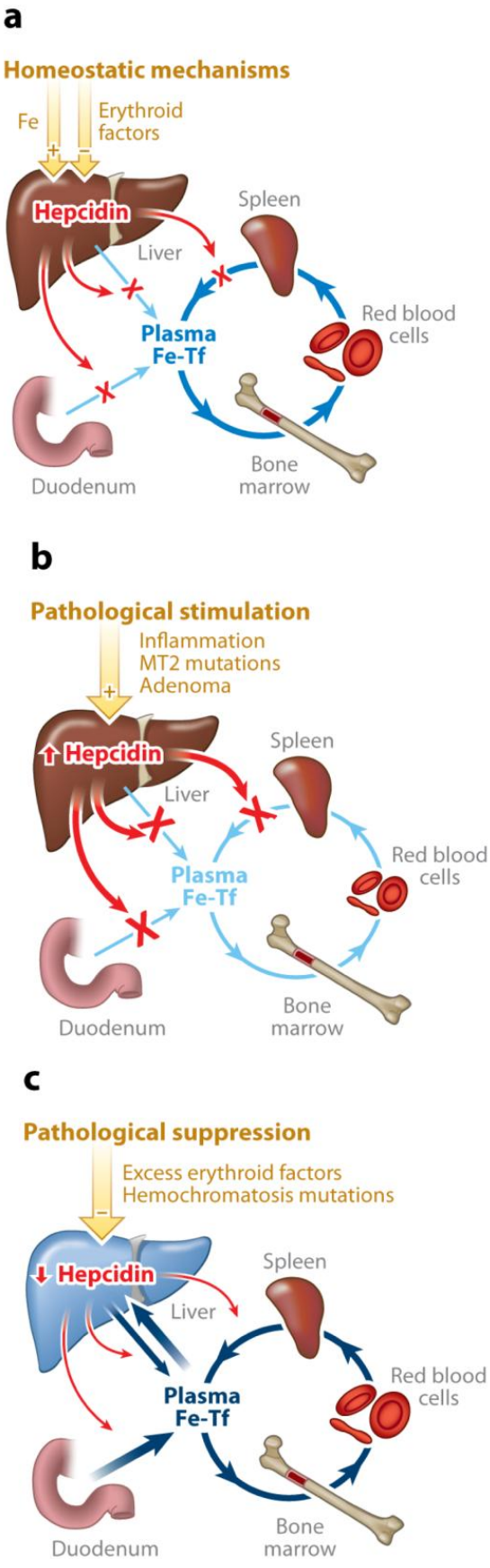


Figure 4: (from (12)) **Hepcidin homeostasis and dysregulation.** a) Hepcidin levels reflect a balance between stimulatory (iron, inflammation) and inhibitory stimuli (erythroid and growth factors). Hepcidin blocks iron flow from the duodenum, liver and spleen into the plasma (red X's). As plasma iron levels drop due to its use for continued red blood cell synthesis, the bone marrow secretes an unknown erythroid factor (yellow arrow) to decrease hepcidin production and enhance iron delivery to the plasma and developing red blood cells. b) Chronic inflammation, genetic lesions in hepcidin suppressing genes or hepcidin-producing tumors all lead to inappropriately high hepcidin levels (large red X's) which keeps plasma iron levels low despite the need to deliver iron to the bone marrow. Anemia develops which is refractory to iron treatment. c) Hepcidin deficiency arises from excessive production of erythropoietin (thalassemia) and other growth factors or from genetic lesions in hepcidin-producing genes (hereditary hemochromatosis). Low hepcidin levels, despite adequate iron supplies, results in the saturation of the body's iron carrying capacity. Non-transferrin bound iron circulates and can cause life-threatening organ damage.

Reference list

1. Wardman P, Candeias LP. Fenton chemistry: an introduction. Radiat. Res. 1996;145:523–531.

2. Ye H, Rouault TA. Human iron-sulfur cluster assembly, cellular iron homeostasis, and disease. Biochemistry. 2010;49:4945–4956.

3. Rouault TA, Tong W-H. Iron-sulphur cluster biogenesis and mitochondrial iron homeostasis. Nat. Rev. Mol. Cell Biol. 2005;6:345–351.

4. Ganz T. Macrophages and Systemic Iron Homeostasis. Journal of Innate Immunity [Internet]. 2012 [cited 2012 Apr 16];Available from: http://www.ncbi.nlm.nih.gov/pubmed/22441209

5. Syed BA, Sargent PJ, Farnaud S, Evans RW. An overview of molecular aspects of iron metabolism. Hemoglobin. 2006;30:69–80.

6. Ganz T. Hepcidin and iron regulation, 10 years later. Blood. 2011;117:4425–4433.

7. Ganz T, Nemeth E. Hepcidin and iron homeostasis. Biochimica Et Biophysica Acta [Internet]. 2012 [cited 2012 Mar 18];Available from: http://www.ncbi.nlm.nih.gov/pubmed/22306005

8. Babitt JL, Huang FW, Wrighting DM, Xia Y, Sidis Y, Samad TA, et al. Bone morphogenetic protein signaling by hemojuvelin regulates hepcidin expression. Nat.Genet. 2006;38:531–539.

9. Nicolas G, Viatte L, Bennoun M, Beaumont C, Kahn A, Vaulont S. Hepcidin, A New Iron Regulatory Peptide. Blood Cells, Molecules, and Diseases. 2002;29:327–335.

10. Carbia-Nagashima A, Arzt E. Intracellular proteins and mechanisms involved in the control of gp130/JAK/STAT cytokine signaling. IUBMB Life. 2004;56:83–88.

11. Wrighting DM, Andrews NC. Interleukin-6 induces hepcidin expression through STAT3. Blood. 2006;108:3204–3209.

12. Ganz T, Nemeth E. Hepcidin and disorders of iron metabolism. Annu. Rev. Med. 2011;62:347–360.

13. Weinstein DA, Roy CN, Fleming MD, Loda MF, Wolfsdorf JI, Andrews NC. Inappropriate expression of hepcidin is associated with iron refractory anemia: implications for the anemia of chronic disease. Blood. 2002;100:3776–3781.

14. Du X, She E, Gelbart T, Truksa J, Lee P, Xia Y, et al. The serine protease TMPRSS6 is required to sense iron deficiency. Science. 2008;320:1088–1092.

15. Finberg KE, Heeney MM, Campagna DR, Aydinok Y, Pearson HA, Hartman KR, et al. Mutations in TMPRSS6 cause iron-refractory iron deficiency anemia (IRIDA). Nat.Genet. 2008;40:569–571.

16. Silvestri L, Pagani A, Nai A, De Domenico I, Kaplan J, Camaschella C. The serine protease matriptase-2 (TMPRSS6) inhibits hepcidin activation by cleaving membrane hemojuvelin. Cell Metab. 2008;8:502–511.

17. Zaritsky J, Young B, Wang H-J, Westerman M, Olbina G, Nemeth E, et al. Hepcidin--a potential novel biomarker for iron status in chronic kidney disease. Clin J Am Soc Nephrol. 2009;4:1051–1056.

18. Tanno T, Bhanu NV, Oneal PA, Goh SH, Staker P, Lee YT, et al. High levels of GDF15 in thalassemia suppress expression of the iron regulatory protein hepcidin. Nat.Med. 2007;13:1096–1101.

19. Tanno T, Porayette P, Sripichai O, Noh S-J, Byrnes C, Bhupatiraju A, et al. Identification of TWSG1 as a second novel erythroid regulator of hepcidin expression in murine and human cells. Blood. 2009;114:181–186.

20. Rund D, Rachmilewitz E. Beta-thalassemia. N. Engl. J. Med. 2005;353:1135–1146.

21. Girelli D, Pasino M, Goodnough JB, Nemeth E, Guido M, Castagna A, et al. Reduced serum hepcidin levels in patients with chronic hepatitis C. J. Hepatol. 2009;51:845–852.

22. Ohtake T, Saito H, Hosoki Y, Inoue M, Miyoshi S, Suzuki Y, et al. Hepcidin is down-regulated in alcohol loading. Alcohol Clin.Exp.Res. 2007;31:S2–S8.

23. Brissot P, Ropert M, Le Lan C, Loréal O. Non-transferrin bound iron: A key role in iron overload and iron toxicity. Biochim. Biophys. Acta. 2012;1820:403–410.

24. Pietrangelo A. Hereditary hemochromatosis: pathogenesis, diagnosis, and treatment. Gastroenterology. 2010;139:393–408, 408.e1–2.

25. Bennett CL, Silver SM, Djulbegovic B, Samaras AT, Blau CA, Gleason KJ, et al. Venous Thromboembolism and Mortality Associated With Recombinant Erythropoietin and Darbepoetin Administration for the Treatment of Cancer-Associated Anemia. JAMA. 2008;299:914–924.

26. Brissot P, Troadec M-B, Bardou-Jacquet E, Le Lan C, Jouanolle A-M, Deugnier Y, et al. Current approach to hemochromatosis. Blood Rev. 2008;22:195–210.

27. Brissot P, Ball S, Rofail D, Cannon H, Jin VW. Hereditary hemochromatosis: patient experiences of the disease and phlebotomy treatment. Transfusion. 2011;51:1331–1338.

28. Rombout-Sestrienkova E, Nieman FHM, Essers BAB, van Noord PAH, Janssen MCH, van Deursen CTBM, et al. Erythrocytapheresis versus phlebotomy in the initial treatment of

HFE hemochromatosis patients: results from a randomized trial. Transfusion. 2012;52:470–477.

29. Galanello R, Campus S, Origa R. Deferasirox: pharmacokinetics and clinical experience. Expert Opin Drug Metab Toxicol. 2012;8:123–134.

Chapter 1

Chapter 1 is a published paper that provides new insights into the regulation of hepcidin by iron through the characterization of 4 mouse models of hereditary hemochromatosis.

Summary

The focus of this dissertation has been to understand the pathogenesis of hereditary hemochromatosis (HH) an inherited iron overload disease caused by deficiency of the peptide hormone, hepcidin. Discovery of hepcidin in 2001 marked the beginning of the molecular era of iron biology. Early studies showed that a knockout model of the USF2 gene, which fortuitously disrupted the then uncharacterized hepcidin gene, displayed iron overload (1). Subsequent studies showed that overexpression of hepcidin caused anemia (2) and that mice subjected to an iron rich diet increased liver hepcidin mRNA expression (3). Pathogenic hepcidin mutations confirmed the necessity of hepcidin in human iron homeostasis (4) and experiments showed that injection of synthetic hepcidin into mice caused rapid onset hypoferremia (5).

Understanding of hepcidin regulation by iron has been boosted by studies of mouse models harboring mutations in the hemochromatosis gene (HFE) (6), transferrin receptor 2 (TfR2) (7), and hemojuvelin (HJV) (8) genes which cause disease in humans, as well as the BMP6 (9) and BMPR (10) genes which are not yet associated with human iron overload. Collectively, the evidence shows that iron signals through the bone morphogenetic protein (BMP) pathway to increase hepcidin transcription (11). Our hypothesis was that HFE, TfR2, HJV and BMP mutant mice would show distinct defects in hepcidin production in response to dietary iron challenge. We found that in contrast to WT mice each of the 4 mouse models failed to respond to a short term iron challenge, but that HFE and TfR2 mice increased hepcidin levels

to normal after iron accumulated in the liver. This suggests that both short term increases in iron (plasma) and long-term (liver iron stores) independently increase hepcidin production.

We also observed a difference between the hepcidin response to iron *in vitro* and *in vivo*. Freshly isolated hepatocytes treated with iron transferrin increase hepcidin by less than 5 fold (Chapter 2, Figure 1B) while mice injected with iron transferrin increase hepcidin by 60 fold 24 hours after injection (Chapter 1 supplemental Figure 1, Chapter 2 Figure 3A). The data show that hepatocytes alone cannot replicate the *in vivo* hepcidin response to iron transferrin injection and suggests that other cell types may be involved in sensing iron. A recent study showed that epithelial cells lining liver sinusoids produce the most BMP6 relative to the other major cell types in the liver (12). Future work will be needed to establish the importance of non-hepatocyte cell types in the regulation of hepcidin by iron.

References

1. Nicolas G, Bennoun M, Devaux I, Beaumont C, Grandchamp B, Kahn A, et al. Lack of hepcidin gene expression and severe tissue iron overload in upstream stimulatory factor 2 (USF2) knockout mice. Proc. Natl. Acad. Sci. U.S.A. 2001;98:8780–8785.

2. Nicolas G, Bennoun M, Porteu A, Mativet S, Beaumont C, Grandchamp B, et al. Severe iron deficiency anemia in transgenic mice expressing liver hepcidin. Proceedings of the National Academy of Sciences. 2002;99:4596–4601.

3. Pigeon C, Ilyin G, Courselaud B, Leroyer P, Turlin B, Brissot P, et al. A new mouse liver-specific gene, encoding a protein homologous to human antimicrobial peptide hepcidin, is overexpressed during iron overload. J.Biol.Chem. 2001;276:7811–7819.

4. Roetto A, Papanikolaou G, Politou M, Alberti F, Girelli D, Christakis J, et al. Mutant antimicrobial peptide hepcidin is associated with severe juvenile hemochromatosis. Nat.Genet. 2003;33:21–22.

5. Rivera S, Nemeth E, Gabayan V, Lopez MA, Farshidi D, Ganz T. Synthetic hepcidin causes rapid dose-dependent hypoferremia and is concentrated in ferroportin-containing organs. Blood. 2005;106:2196–2199.

6. Ahmad KA, Ahmann JR, Migas MC, Waheed A, Britton RS, Bacon BR, et al. Decreased Liver Hepcidin Expression in the Hfe Knockout Mouse. Blood Cells, Molecules, and Diseases. 2002;29:361–366.

7. Wallace DF, Summerville L, Lusby PE, Subramaniam VN. First phenotypic description of transferrin receptor 2 knockout mouse, and the role of hepcidin. Gut. 2005;54:980–986.

8. Niederkofler V, Salie R, Arber S. Hemojuvelin is essential for dietary iron sensing, and its mutation leads to severe iron overload. J.Clin.Invest. 2005;115:2180–2186.

9. Meynard D, Kautz L, Darnaud V, Canonne-Hergaux F, Coppin H, Roth MP. Lack of the bone morphogenetic protein BMP6 induces massive iron overload. Nat.Genet. 2009;

10. Steinbicker AU, Bartnikas TB, Lohmeyer LK, Leyton P, Mayeur C, Kao SM, et al. Perturbation of hepcidin expression by BMP type I receptor deletion induces iron overload in mice. Blood. 2011;118:4224–4230.

11. Fleming RE, Feng Q, Britton RS. Knockout mouse models of iron homeostasis. Annu. Rev. Nutr. 2011;31:117–137.

12. Feng Q, Migas MC, Waheed A, Britton RS, Fleming RE. Ferritin Upregulates Hepatic Expression of Bone Morphogenetic Protein 6 and Hepcidin in Mice. American journal of physiology. Gastrointestinal and liver physiology [Internet]. 2012 [cited 2012 May 23];Available from: http://www.ncbi.nlm.nih.gov/pubmed/22517766

Evidence for Distinct Pathways of Hepcidin Regulation by Acute and Chronic Iron Loading in Mice

Emilio Ramos,[1] Léon Kautz,[4,5] Richard Rodriguez,[2] Michael Hansen,[2] Victoria Gabayan,[2] Yelena Ginzburg,[6] Marie-Paule Roth,[4,5] Elizabeta Nemeth,[2] and Tomas Ganz[2,3]

In response to iron loading, hepcidin synthesis is homeostatically increased to limit further absorption of dietary iron and its release from stores. Mutations in HFE, transferrin receptor 2 (Tfr2), hemojuvelin (HJV), or bone morphogenetic protein 6 (BMP6) prevent appropriate hepcidin response to iron, allowing increased absorption of dietary iron, and eventually iron overload. To understand the role each of these proteins plays in hepcidin regulation by iron, we analyzed hepcidin messenger RNA (mRNA) responsiveness to short and long-term iron challenge in iron-depleted *Hfe*, *Tfr2*, *Hjv*, and *Bmp6* mutant mice. After 1-day (acute) iron challenge, $Hfe^{-/-}$ mice showed a smaller hepcidin increase than their wild-type strain-matched controls, $Bmp6^{-/-}$ mice showed nearly no increase, and *Tfr2* and *Hjv* mutant mice showed no increase in hepcidin expression, indicating that all four proteins participate in hepcidin regulation by acute iron changes. After a 21-day (chronic) iron challenge, *Hfe* and *Tfr2* mutant mice increased hepcidin expression to nearly wild-type levels, but a blunted increase of hepcidin was seen in $Bmp6^{-/-}$ and $Hjv^{-/-}$ mice. BMP6, whose expression is also regulated by iron, may mediate hepcidin regulation by iron stores. None of the mutant strains (except $Bmp6^{-/-}$ mice) had impaired BMP6 mRNA response to chronic iron loading. *Conclusion:* TfR2, HJV, BMP6, and, to a lesser extent, HFE are required for the hepcidin response to acute iron loading, but are partially redundant for hepcidin regulation during chronic iron loading and are not involved in the regulation of BMP6 expression. Our findings support a model in which acute increases in holotransferrin concentrations transmitted through HFE, TfR2, and HJV augment BMP receptor sensitivity to BMPs. A distinct regulatory mechanism that senses hepatic iron may modulate hepcidin response to chronic iron loading. (HEPATOLOGY 2011;53:1333-1341)

Abbreviations: ANOVA, analysis of variance; apo-Tf, apotransferrin; BMP6, bone morphogenetic protein 6; HJV, hemojuvelin; holo-Tf, holotransferrin; MCV, mean corpuscular volume; mRNA, messenger RNA; qRT-PCR, quantitative reverse-transcription polymerase chain reaction; TfR1, transferrin receptor 1; TfR2, transferrin receptor 2; WT, wild-type.

From the Department of [1]Chemistry and Biochemistry, [2]Medicine, and [3]Pathology, David Geffen School of Medicine, University of California, Los Angeles, Los Angeles, CA; [4]University of Toulouse, UPS, Center of Pathophysiology of Toulouse Purpan and Biomedical Institute of Toulouse, France; [5]Université de Toulouse, UPS, Centre de Physiopathologie de Toulouse Purpan and Institut Biomédical de Toulouse, France; and the [6]New York Blood Center, New York, NY.

Received September 22, 2010; accepted December 25, 2010.

Supported by National Institutes of Health Grants R01 DK065029 (to T.G.) and R01 DK082717 (to E.N.); the Will Rogers Fund (to T.G.); the Ruth L. Kirschstein National Research Service Award GM007185 (to E.R.); and ANR-GENOPAT IRONREG (to M.P.R.).

Address reprint requests to: Tomas Ganz, M.D., Ph.D., Department of Medicine, David Geffen School of Medicine at UCLA, 10833 LeConte Avenue, CHS 37-055, Los Angeles, CA 90095-1690.
E-mail: tganz@mednet.ucla.edu; fax: 310-206-8766.

Copyright © 2011 by the American Association for the Study of Liver Diseases.

View this article online at wileyonlinelibrary.com.
DOI 10.1002/hep.24178
Potential conflict of interest: Nothing to report.
Additional Supporting Information may be found in the online version of this article.

Systemic iron homeostasis is dependent on the hepatic peptide hormone hepcidin, its receptor/iron channel ferroportin, and the feedback regulation of the two molecules by iron. Hepcidin controls the delivery of dietary and recycled iron to plasma by binding to the iron exporter ferroportin and inducing its endocytosis and degradation.[1] Increases in body iron levels stimulate hepcidin production in the liver, limiting further absorption of iron. The mechanism of hepcidin regulation by iron is not completely understood. Human studies have shown that blood hepcidin concentrations rapidly increase in response to oral iron challenge, are proportional to increases in diferric transferrin (holotransferrin) concentrations,[2,3] and strongly correlate with iron stores as reflected by serum ferritin.[3] In mice, hepcidin messenger RNA (mRNA) increase within 24 hours after the switch from a low-iron diet to a standard diet[4] and *in vivo* imaging of hepcidin promoter-reporter constructs in mice[5] confirmed high responsiveness of hepcidin promoter

activity to iron loading. Mouse primary hepatocytes treated with holotransferrin increase their hepcidin mRNA expression two-fold or more.[2,6] The aggregate evidence indicates that hepcidin regulation both *in vivo* and in cultured hepatocytes is predominantly transcriptional.

As indicated by mutations that cause hereditary hemochromatosis and inappropriately low hepcidin levels relative to the iron load, the genes encoding the proteins HFE, transferrin receptor 2 (TfR2), hemojuvelin (HJV), and bone morphogenetic protein 6 (BMP6) play fundamental roles in modulating hepcidin responses to iron.[7-10] The response of hepcidin to iron loading in the various mouse mutants has not been systemically compared. We hypothesized that the mutant mouse models would show distinct defects in hepcidin and BMP6 responses to short or long-term iron challenges.

Materials and Methods

Animals. *Hfe*$^{-/-}$ mice (The Jackson Laboratory, Bar Harbor, ME), *Tfr2*$^{Y245X/Y245X}$ mice (a gift from Robert Fleming, Saint Louis University, St. Louis, MO), and *Hjv*$^{-/-}$ mice (a gift from Paul Schmidt, Children's Hospital, Boston, MA) were maintained at UCLA, and *Bmp6*$^{-/-}$ mice were maintained at the University of Toulouse. All animal studies were approved by the animal research committees at the respective institutions. The wild-type (WT) mice used as controls were matched for the background strain of each mutant (C57BL/6 for *Hfe*$^{-/-}$, FVB for *Tfr2*^{Y245X}, 129S6/SvEvTac for *Hjv*$^{-/-}$, and CD1 for *Bmp6* $^{-/-}$). Both sexes were used for the experiments.

Dietary Iron Challenge. All mice were fed a standard diet (NIH 31 rodent diet, 336 ppm iron, Harlan Teklad, Indianapolis, IN) until 4 weeks of age and were then iron-depleted. Iron depletion in WT mice (C57BL/6, FVB, 129S6, and CD1) was achieved by placing animals on a diet containing <4 ppm iron for 14 days. The iron restriction did not cause a decrease in hemoglobin levels. Mutant mice (*Hfe*, *Tfr2*, *Hjv*, and *Bmp6*) and an additional group of C57BL/6 were iron-depleted through a combination of phlebotomy and a low-iron diet. After iron depletion, the mice were re-fed with a standard diet for 1 or 21 days. The number of mice used in each group of nonphlebotomized and phlebotomized mice is listed in Supporting Information Table 1.

Phlebotomy. Mutant mice were phlebotomized to reduce the baseline iron load to levels similar to those of WT mice. Before phlebotomy, iron-overloaded mutant mice had increased hemoglobin levels and mean corpuscular volume (MCV). Blood was removed from the retro-orbital sinus (300-500 μL/week) until the MCV was lowered to the WT range. Depending on the mutant strain, repeat phlebotomies were performed for 3-7 weeks. To control for the possible confounding effect of phlebotomy on hepcidin response to iron, we also phlebotomized WT controls. We only used the C57BL/6 strain because our earlier experiments indicated that FVB and 129S6 had a very similar hepcidin response to iron as C57BL/6 mice. Bondi et al.[11] showed in two WT strains that removal of 500 μL of blood resulted in transient suppression of hepcidin, with hepcidin mRNA returning to normal levels 2-3 days after phlebotomy. Our mice were therefore analyzed 1-2 weeks after the last phlebotomy.

Holotransferrin and Apotransferrin Administration. Six-week-old male mice (4-6 per treatment) were placed on a low-iron diet for 2 weeks and then received 10 mg human holotransferrin or apotransferrin (Sanquin, Amsterdam, The Netherlands)[12] in 200 μL saline intraperitoneally or saline alone, and were analyzed after 6 hours.

Analysis of Iron Parameters and mRNA Expression. Hematological parameters, serum iron, and tissue iron were measured as described.[4,13] Gene expression of *Hamp1*, *Bmp6*, and the reference gene *β-actin* were assessed by quantitative reverse-transcription polymerase chain reaction (qRT-PCR).[4,13] Primer sequences are listed in the Supporting Information. In every qRT-PCR run, an internal control sample was included to allow comparisons between different PCR plates. Results are expressed as $-\Delta$Ct (i.e., the cycle threshold differences between reference and target genes within each group of mice). The approximate fold induction between two conditions was calculated as $2^{-\Delta\Delta Ct}$. PCR efficiencies ranged between 90% and 100% for all transcripts.

Statistics. Statistics were calculated by SigmaStat (SyStat Software, Richmond, CA). Because some measurements were not normally distributed, the null hypotheses (no hepcidin increase after acute or chronic iron challenge, or no differences in hepcidin -ΔCt and iron loading between strains or between mutant versus WT) were tested by the nonparametric Mann-Whitney rank sum test. Data are reported as the median (interquartile range). Comparisons between all mouse strains were tested by one-way analysis of variance (ANOVA) and Dunn's method.

Mice of both sexes were used in the study. Each treatment group had a similar number of male and female mice, except for three acute iron challenge

groups (129S6 [4 male, 2 female], *Hjv* [4 male, 2 female], and *Bmp6* [2 male, 5 female]) and two chronic iron loading groups (*Hfe* [6 male, 4 female] and *Hjv* [6 male, 3 female]). Because female mice generally have higher hepcidin levels than male mice, for these particular groups we performed statistical analysis using sex as a covariable (two-way ANOVA). Sex had no significant effect on the outcome in any of the comparisons.

Results

Hepcidin Response to Acute Iron Challenge Is Blunted in Mouse Models of Hereditary Hemochromatosis

Iron Depletion. In WT mice (C57BL/6, FVB, 129S6, and CD1), iron depletion was achieved through a low-iron diet for 2 weeks, and liver iron content was lowered to <1 μmol/g wet weight (Supporting Information Table 1). However, *Hfe*, *Tfr2*, *Hjv*, and *Bmp6* mice had elevated liver iron concentrations and could not be iron-depleted by 2 weeks of a low-iron diet alone (data not shown). In order to make their iron stores comparable with those of WT mice, mutant mice were iron-depleted by weekly phlebotomy and a low-iron (4 ppm) diet until their elevated MCV, a convenient index of erythropoietic iron availability, was lowered to the WT range of ≈50 fL. A total of 1.5-3.5 mL blood (300-500 μL weekly) was removed from mutant mice, with *Hfe* requiring fewer and *Hjv* and *Bmp6* mice requiring more phlebotomies to reach the target MCV. Iron and erythropoietic activity have opposing effects on hepcidin expression, and to control for the potentially confounding effects of anemia, a group of WT mice (C57BL/6) was also subjected to the same phlebotomy protocol, with ≈1 mL of blood removed. At the last phlebotomy, the average hemoglobin concentration in C57BL/6 mice was 7.1 g/dL, and in *Hfe*, *Tfr2*, *Hjv*, and *Bmp6* mutants it was 9.7, 8.9, 6.8, and 9.9 g/dL, respectively. At the time of iron challenge (1-2 weeks after the last phlebotomy in phlebotomized mice; after 2 weeks of a low-iron diet in nonphlebotomized mice), the liver iron content in all WT and mutant mice had decreased to near 1 μmol/g wet weight (Fig. 1 and Supporting Information Table 1), with medians ranging from 0.2 (interquartile range, 0.1-0.2) μmol/g wet weight in 129S6 mice to 1.5 (interquartile range, 1.2-1.7) μmol/g wet weight in *Hjv* mutant mice showing effective depletion of liver iron stores.

Acute Iron Loading. After 1 day of standard iron diet (336 ppm iron), both WT and mutant mice significantly increased their serum iron concentration as well as their liver iron stores (Fig. 1, Supporting Information Table 1). The increase in liver iron content after only 1 day of a standard iron diet could be expected if mice absorbed as little as 10% of the iron from their food. The average daily consumption of food in mice is ≈4 g.[14] Thus, with standard chow containing 336 ppm iron, mice ingest up to 1.3 mg (≈25 μmol) per day, and would plausibly load the liver (approximate mass, 1 g) with 1-3 μmol of iron, as was observed.

Acute Hepcidin Response to Dietary Iron. After iron depletion, all mice had similarly low hepcidin mRNA, ranging from a median (interquartile range) −ΔCt of −12.0 (−12.7 to −11.9) in *Bmp6* mutant mice to −7.3 (−12.1 to −4.8) in FVB mice, with statistically insignificant differences except for the difference between *Hfe* and *Bmp6* mutants ($P < 0.05$; one-way ANOVA on rank sum test). After acute iron challenge, phlebotomized WT C57BL/6 mice increased their hepcidin mRNA −ΔCt by 12.9 or nearly 8,000-fold ($P < 0.001$) (Fig. 2). This response was similar to the hepcidin increase observed in diet-depleted C57BL/6 mice switched from a low-iron diet to a standard diet (Fig. 2), demonstrating that phlebotomy and anemia did not impair hepcidin regulation through acute iron loading. A similar magnitude of hepcidin mRNA increase was also observed in diet-depleted FVB, CD1, and 129S6 mice switched from a low-iron diet to a standard diet (Fig. 2). In contrast, *Tfr2* and *Hjv* mice failed to increase hepcidin in response to 1-day iron feeding, and *Bmp6* mice had a negligible response (Fig. 2), indicating that these proteins play essential roles in sensing acute changes in body iron levels. Among mutant mice, *Hfe* mice showed a partial increase in hepcidin expression (11-fold [$P = 0.027$]), a much smaller increase than in the matching WT strain C57BL/6 ($P < 0.001$), indicating that HFE plays a somewhat redundant role in sensing acute iron changes. Other proteins, possibly TfR2 or HJV, may partially compensate for the lack of HFE.

Hepcidin Response to Holotransferrin. Because 1-day feeding with a standard diet increased both serum and liver iron, we asked whether an increase in serum iron induced by a small dose of parenteral iron is sufficient for hepcidin induction. We injected C57BL/6 mice with saline, iron-free apotransferrin (apo-Tf), or holotransferrin (holo-Tf) at 10 mg/mouse (which for holo-Tf equals 14 μg or 0.25 μmol iron), a dose estimated to be 100 times smaller than the amount of iron ingested daily on a standard diet and 10 times smaller than the amount absorbed assuming a 10%

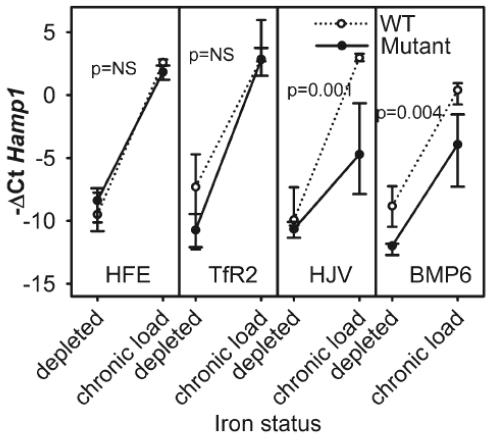


Fig. 3. Hepcidin response to chronic dietary iron challenge. The data are expressed as the median and interquartile range. Hepcidin mRNA expression was measured by qRT-PCR in iron-depleted and iron-loaded mutant mice and their respective WT strains.

Chronic Hepcidin Responses. At baseline, hepcidin levels were low in both WT and mutant mice (Fig. 3, Supporting Information Table 1) but were significantly lower only in *Bmp6* mutant mice compared with their WT counterparts ($P = 0.002$). In the chronically iron-loaded group, C57BL/6, FVB, and 129S6 WT mice showed a very similar increase in hepcidin mRNA (Fig. 3, Supporting Information Table 1), reaching a hepcidin mRNA expression at least 1,000-fold higher than that of the iron-depleted group, whereas the less iron-sensitive CD1 mice increased hepcidin ≈600-fold.

Chronically loaded *Hfe* and *Tfr2* mice also had at least 1,000-fold higher hepcidin mRNA than iron-depleted mice, reaching the level of hepcidin expression detected in chronically loaded WT mice (Fig. 3). *Hjv* and *Bmp6* had impaired hepcidin response to chronic iron loading (significantly different from all other mice [$P < 0.001$; one-way ANOVA]), but a partial response was still preserved in both types of mutants. In iron-loaded *Hjv* and *Bmp6* mice, hepcidin mRNA was ≈64-fold and 270-fold higher, respectively, than in iron-depleted mice. Importantly, both *Hjv* and *Bmp6* chronically loaded mice failed to reach hepcidin mRNA levels of the matching WT strain ($P = 0.001$ and $P = 0.004$, respectively). Although C57BL/6 mice had a similar hepcidin response to iron loading whether they were depleted by diet alone or diet and phlebotomy (Fig. 2), we reconsidered the possibility that hepcidin induction in *Hjv* and *Bmp6* mice may not be related to iron loading but rather to the difference in erythropoietic activity between the iron-depleted state when mice were anemic and iron-loaded state when mice were not anemic. To assess the potential effect of anemia apart from iron loading, we analyzed the correlation between hepcidin mRNA expression and hemoglobin levels in iron-depleted *Hjv* and *Bmp6* mice, which did not undergo any iron challenge (Supporting Information Fig. 3). Hepcidin expression changed very little with increasing hemoglobin values, suggesting that iron load rather than severity of anemia caused hepcidin increase in iron-fed *Hjv* and *Bmp6* mice.

Serum and Liver Iron in Chronic Versus Acute Iron Loading. Serum iron levels in WT mice and mutants after chronic iron loading were not significantly higher (and mostly were lower) than those measured after acute iron challenge (Fig. 4). In contrast, liver iron content in all mutants was higher after chronic loading when compared with acute iron challenge (Fig. 4, Supporting Information Table 1). The amount of liver iron in chronically loaded animals compared with acutely loaded animals was, respectively: *Hfe*, 5 and 2 μmol/g wet liver ($P = 0.004$); *Tfr2*, 16 and 4 μmol/g wet liver ($P = 0.001$); *Hjv*, 26 and 4 μmol/g wet liver ($P < 0.001$); and *Bmp6*, 26 and 1 μmol/g wet liver ($P = 0.001$). Therefore, any additional increase in hepcidin expression after chronic versus acute iron loading in chronically loaded mutant mice cannot be accounted for by changes in serum iron levels, but is related to increased iron stores.

Hepcidin Response Relative to Iron Load

Even though hepcidin levels in all mutant mice increased with chronic iron loading, the severity of iron overload relative to the WT strain of the same genetic background depended on the mutation. To assess the appropriateness of hepcidin response to iron loading, we correlated hepcidin expression with liver iron content of mutant mice and matching WT strains (Fig. 5). *Hfe* mice had the mildest impairment in hepcidin response, followed by *Tfr2* mice, whereas *Bmp6* and *Hjv* mice showed a more severe impairment. Although *Hjv* and *Bmp6* mice accumulated the most iron during chronic loading, their hepcidin expression did not reach the levels observed in the WT strains.

The Dependence of Hepcidin on Serum Iron and Hepatic Iron

To determine how serum iron and liver iron contribute to hepcidin regulation, we performed best-sets linear regression analysis of the dependence of hepcidin mRNA on serum and liver iron in each group of mice (Supporting Information Table 2). In WT strains, hepcidin showed mixed dependence of serum and liver

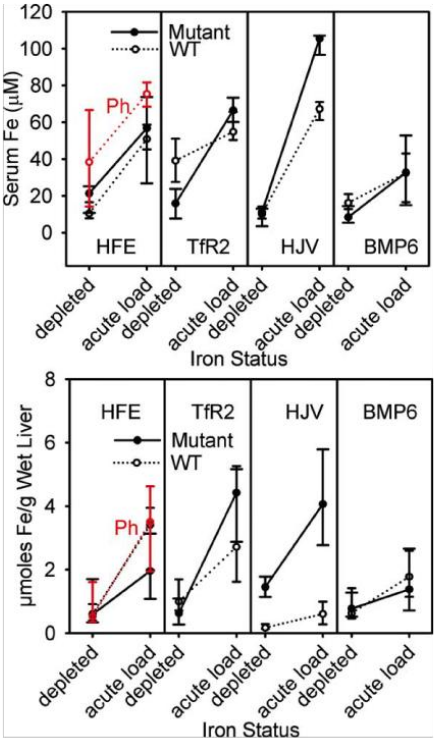


Fig. 1. Serum iron and nonheme liver iron increase after acute dietary iron challenge. To deplete iron stores (iron-depleted condition), mutant mice (*Hfe*, *Tfr2*, *Hjv*, and *Bmp6*) were placed on a low-iron diet and weekly phlebotomies, and strain-matched WT mice (C57BL/6, 129S6, FVB and CD1) were placed on a low-iron diet for 2 weeks. An additional control group of C57BL/6 mice (Ph) was subjected to a low-iron diet and phlebotomy. Acute iron challenge consisted of placing the mice on standard chow for 1 day. The data are expressed as the median and interquartile range. For comparison with chronic liver iron loading (Fig. 4, bottom panel), note that the scale for acute iron loading is five-fold smaller.

absorption rate. Injection of holo-Tf raised serum iron concentrations from 30 to 130 μM within 6 hours, and hepcidin mRNA increased to the maximal levels seen in this strain. Hepcidin mRNA levels in holo-Tf–treated mice were more than 100-fold or 16-fold higher than in saline or apo-Tf-treated mice, respectively ($P = 0.015$ and $P = 0.026$, respectively) (Supporting Information Fig. 1). Although $-\Delta$Ct in apo-Tf–injected animals was somewhat higher than in saline-injected animals, the difference was not statistically significant. Apo-Tf or holo-Tf injections had no significant effect on the expression of the inflammatory marker C-reactive protein (data not shown). Thus, an acute increase in holo-Tf concentrations is sufficient to induce maximal hepcidin expression even if the amount of iron delivered is quite small.

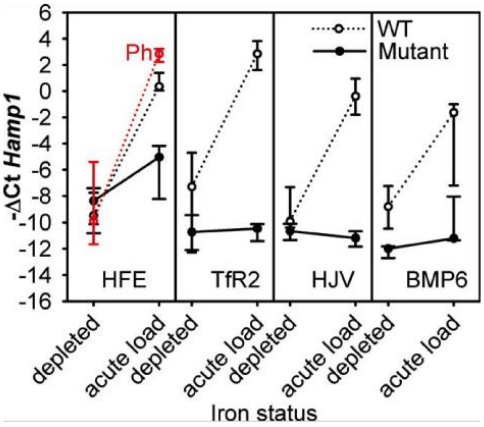


Fig. 2. Hepcidin response to acute dietary iron challenge is impaired in hemochromatotic mice. Animals were iron-depleted as described in Fig. 1. Hamp1 mRNA levels were measured either after iron depletion alone or after an additional 1-day dietary iron challenge (standard diet, 336 ppm iron). The data are expressed as the median and interquartile range.

Hepcidin Response to Chronic Iron Challenge Is Blunted in HJV *and* BMP6 *Knockout Mice, but Not in* HFE *and* Tfr2 *Mutants*

Chronic Iron Loading. For all four strains of WT mice, the iron-depleted condition was achieved by feeding mice a 4-ppm iron-restricted diet for 14 days, and the chronic iron challenge consisted of 21 days of a standard iron diet. For all hemochromatosis mutants, we phlebotomized the mice to iron-deplete them. The chronically iron-loaded condition was achieved by maintaining mice on a standard iron diet until they reached the same age as chronically loaded WT mice (9 weeks of age).

In WT mice, 21 days of a standard iron diet increased liver iron to 2-5 μmol/g wet weight (Supporting Information Table 1, Supporting Information Fig. 2). Iron loading in the mutant strains was more severe: *Hfe* had two-fold, *Tfr2* had four-fold, and *Hjv* and *Bmp6* had five- to six-fold the amount of liver iron of the WT mice (all differences statistically significant). As expected, the median spleen iron content was lower in all mutants than in the corresponding WT mice, despite more severe systemic iron overload in mutants (all differences statistically significant except 129S6 versus *Hjv*) (Supporting Information Fig. 2, Supporting Information Table 1).

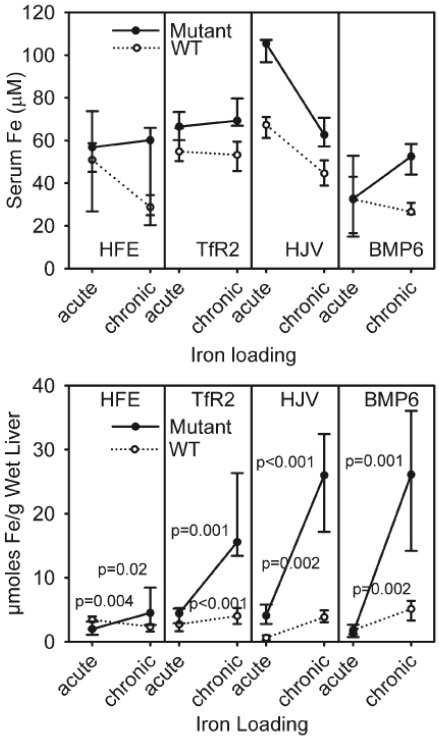


Fig. 4. Serum and liver iron after acute versus chronic dietary iron loading. Serum iron concentrations after chronic iron challenge were similar or lower than those reached after acute iron challenge, both in WT and mutant mice. Liver nonheme iron content in mutants increased after chronic iron loading when compared with acute challenge (*P* values for the difference of medians shown above the line connecting the acute and chronic loading values). The order of hepatic iron loading was Hjv = Bmp6 > Tfr2 > Hfe. The *P* values for the comparison of mutant and WT iron loading are shown near or between the corresponding points on the graph.

iron, ranging from predominant dependence on serum iron in C57BL/6 mice to predominant dependence on liver iron in CD1 mice. In all mutant strains, hepcidin mRNA was dependent on liver iron only.

Bmp6 *mRNA Increase in Response to Iron Loading Is Not Impaired in Mouse Models of Hereditary Hemochromatosis*

BMP6 plays an important role in the regulation of hepcidin by iron.[9,15] To understand whether BMP6 regulation by iron was altered in mutant mice, we measured *Bmp6* mRNA in our chronic iron-loading model. In all cases, *Bmp6* mRNA increased with iron loading (Fig. 6A), roughly proportionally to the liver iron content (Fig. 6B). There was a four-fold increase in *Bmp6* mRNA in WT and *Hfe* mice, which loaded the least iron; a six-fold increase in *Tfr2* mutants; and an eight-fold up-regulation in *Hjv* mice, which loaded the most iron. These results indicate that *Bmp6* expression is regulated independently of *Hfe*, *Tfr2*, and *Hjv*. Similar results were reported in other studies using *Hfe* or *Hjv* knockout mice.[16,17] In the acute iron-loading model, *Bmp6* mRNA levels tended to increase but did not reach statistical significance (data not shown).

Discussion

Mouse Models. We used four mouse models of hereditary hemochromatosis, $Hfe^{-/-}$, $Tfr2^{Y245X/Y245X}$, $Hjv^{-/-}$, and $Bmp6^{-/-}$, in order to examine the role of these proteins in hepcidin regulation by acute and chronic iron loading *in vivo*. Although $Tfr2^{Y245X/Y245X}$ is not a null mutant, truncated TfR2 is not detectable on the cell membrane both because of nonsense-mediated mRNA decay and defective subcellular transport of the truncated protein.[18] All four models were reported to have reduced hepcidin mRNA.[7-10,15,19] Importantly, to accurately assess hepcidin response to iron loading in mutant mice, we iron-depleted the mutant mice by phlebotomy so that the liver iron

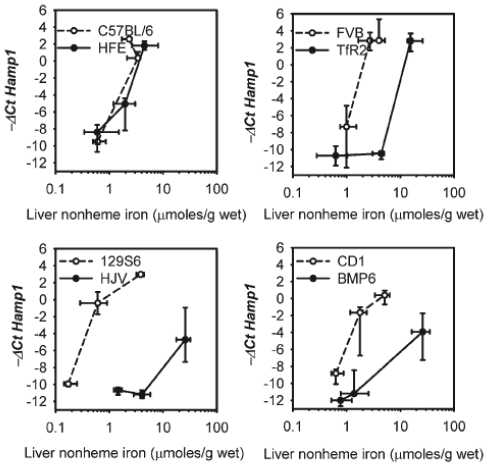


Fig. 5. HFE, Tfr2, HJV, and BMP6 mutations differentially alter the sensitivity of hepcidin response to iron. In the absence of HFE or TfR2, modestly higher liver concentrations were needed to reach the increase in hepcidin mRNA comparable to the WT strain. BMP6 and HJV loss decreased hepcidin responses to iron loading dramatically, and hepcidin mRNA remained low even at 10-fold higher liver iron concentrations. The data are expressed as the median and interquartile range.

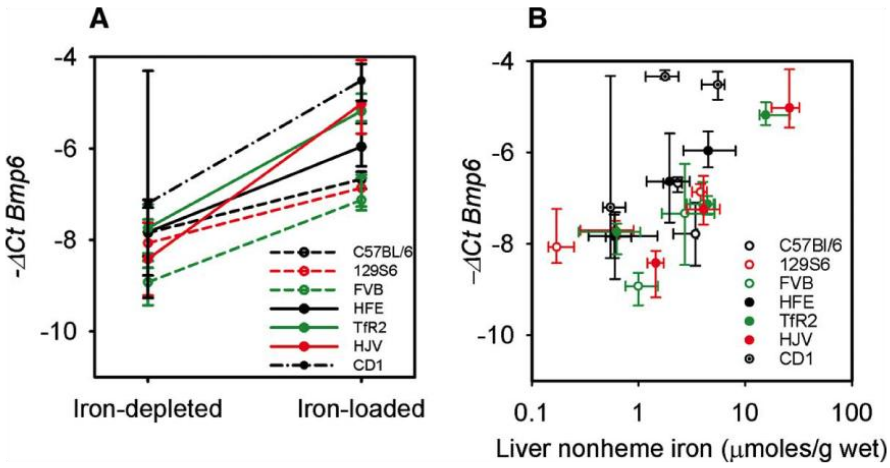


Fig. 6. BMP6 expression reflects iron load in WT and mutant strains. (A) BMP6 mRNA levels were measured by qRT-PCR in mutants and in their respective WT strains before and after chronic iron loading. Expression increased significantly in all the groups tested (C57BL/6, $P = 0.018$; 129S6, $P = 0.026$; FVB, $P < 0.001$; Hfe, $P = 0.037$; Tfr2, $P = 0.001$; Hjv, $P = 0.003$). The data are expressed as the median and interquartile range. BMP6 was also measured in mice before and after 1-day iron feeding, but the increase did not reach statistical significance. (B) BMP6 mRNA expression is proportional to the liver iron load (nonheme iron) in WT and mutant mice.

content in iron-depleted state was similar to that observed in WT mice.

Acute and Chronic Iron Loading. We found that chronic iron loading of WT and mutant mice did not raise serum iron more than 1 day iron-loading (Fig. 4). The iron stores in the liver of the mutant mice, however, substantially increased with chronic loading compared with 1-day challenge (Fig. 4). The chronic increase in iron stores was greatest in *Hjv* and *Bmp6* mice, intermediate in *Tfr2* mutant mice, and least in *Hfe* mice. The order of severity of iron loading is the same as reported in the human mutations involving HJV, TfR2, and HFE. On a standard iron diet, WT mice modestly increased their liver iron content compared with 1-day iron loading (Fig. 4, Supporting Information Table 1).

Hepcidin Response to Acute Iron Loading. After 1-day iron challenge, *Tfr2* and *Hjv* mice did not increase their hepcidin expression, *Bmp6* mice increased it minimally, and *Hfe* mice showed a significant but still blunted response. The result indicates that all four proteins participate in hepcidin regulation by acute iron changes (presumably by holo-Tf concentrations), but that TfR2, HJV, and BMP6 are required for this effect. Interestingly, not only serum iron but also the liver iron stores of WT and mutant mice increased significantly within 1 day of iron challenge, due to the large food consumption by mice relative to their body mass. To confirm that serum iron is a sufficient signal regulating hepcidin expression, we tested hepcidin responsiveness to a holo-Tf injection that contained much smaller amount of iron (14 μg) than was loaded into the liver by a 1-day diet (>100 μg). Hepcidin increased by ≈100-fold within 6 hours compared with solvent controls, and reached maximal hepcidin expression seen in the C57BL/6 mice, indicating that holo-Tf alone can modulate hepcidin mRNA levels.

Hepcidin Response to Chronic Iron Loading. Hepcidin expression after chronic iron loading of *Hfe* and *Tfr2* mice reached much higher levels than after acute loading and became similar to those of iron-loaded WT mice (Figs. 3 and 5). Although *Hjv* and *Bmp6* mutant mice accumulated the most iron after chronic loading with standard chow, their hepcidin expression rose only modestly and remained severely depressed when assessed relative to their total liver iron load (Fig. 5). The BMP6-deficient iron phenotype may be partially ameliorated if other BMPs associate with HJV to mediate signaling and increase hepcidin expression in response to iron loading. Current models of hepcidin regulation have focused on holo-Tf concentration as the key regulator of hepcidin, through the incompletely defined pathway centered on TfR1 and TfR2 as the likely holo-Tf sensors, interacting with HFE, HJV, and BMP6/BMPR. Increased hepcidin expression

after chronic compared with acute iron loading suggests that hepcidin is regulated not only by plasma iron, which is similar after acute and chronic iron loading, but also by intracellular iron stores, which are much higher after chronic than acute iron loading. Based on our findings, the pathway involved in hepcidin regulation by intracellular iron is mainly dependent on HJV and BMP6, with little if any nonredundant contribution from TfR2 or HFE. The greater severity of iron overload in the combined TfR2/HFE deficiency compared with the deficiency of either alone indicates that the two molecules may partially compensate for each other, both in mice and in humans.[20,21] Notably, both *Hjv* and *Bmp6* mice significantly increased hepcidin with chronic iron loading, albeit less than WT strains. Although the loss of either molecule may preserve sufficient BMP receptor activity to regulate hepcidin inefficiently, there is also evidence that alternative pathways are involved in iron regulation. Holo-Tf was reported to activate the extracellular signal-regulated kinase/mitogen-activated protein kinase pathway,[6] and it is possible that chronic stimulation of this pathway in *Hjv* and *Bmp6* mice results in hepcidin increase, unrelated to the rise in hepatic iron stores. Alternatively, another as yet unidentified pathway may play a role in sensing intracellular iron and signaling to hepcidin. We did not detect additional hepcidin suppression in diet iron-depleted C57BL/6 mice when they were subjected to phlebotomy (Fig. 2) or any dependence of hepcidin on the severity of post-phlebotomy anemia in *Hjv* and *Bmp6* mice (Supporting Information Fig. 3). Nevertheless, our studies cannot exclude that anemia-related erythropoietic factors contribute to the relative hepcidin suppression after phlebotomy and conversely, that the reversal of anemia contributes to the rise of hepcidin after iron loading.

Regulation of Hepcidin by Serum Iron Versus Liver Iron. Linear multivariate analysis of the dependence of hepcidin mRNA on serum iron versus liver iron revealed that in WT strains, both serum and liver iron contributed to hepcidin regulation. In mutants, only liver iron contributed to hepcidin regulation, and the effect of serum iron was lost. Thus, liver and serum iron may independently regulate hepcidin expression. However, we cannot exclude the possibility that the effects of serum iron are mediated by hepatocyte loading through potential nonlinear effects. For example, at low liver iron concentrations, changes in holo-Tf levels could cause small changes in liver iron content, to which hepcidin mRNA transcription could be highly sensitive. Nevertheless, strong support for the independent regulation of hepcidin by the extracellular effects of serum iron (probably sensed as holo-Tf) is provided by the low hepcidin levels in hypotransferrinemic humans and mice,[22,23] despite hepatic iron overload. Although some of hepcidin decrease could be attributed to the suppressive effects of ineffective erythropoiesis in hypotransferrinemic mice, hepcidin remained low even when the potential effect of erythropoiesis was negated by erythrocyte transfusion or cytotoxic therapy.

BMP6 Responses to Iron Loading. The expression of *Bmp6* mRNA is regulated by iron,[24] but the mechanism is not known. The continued rise of *Bmp6* mRNA during chronic iron loading parallels the rise in hepatic iron content (Fig. 6), suggesting that BMP6 production is predominantly responsive to intracellular iron stores. However, chronic iron loading of *Bmp6* mice resulted in a 270-fold increase in hepcidin mRNA, indicating that BMP6 is not the sole mediator of the intracellular iron signal. Interestingly, when compared with the matching WT strain, hepcidin response to chronic iron loading in *Hjv* mice appears even more impaired than in *Bmp6* mice, despite the significant increase in *Bmp6* expression in chronically iron-loaded *Hjv* mice. This supports the concept that HJV acts as an essential potentiator or coreceptor for BMP6 signaling, but that BMP6 may not be the only factor regulating hepcidin via HJV. Intracellular iron could also signal by altering the cell surface localization of HJV, as indicated by the ability of ferric ammonium citrate or holo-Tf to decrease the release of soluble HJV *in vitro*.[25] Because soluble HJV suppressed hepcidin, but membrane HJV stimulated it,[25] this effect of iron would be expected to stimulate hepcidin production. How iron affects the release of soluble HJV is unknown, but the regulation may involve neogenin, a receptor for repulsive guidance molecules,[26] or furin, a protease that cleaves HJV.[27]

In conclusion, our comparative studies of four hereditary hemochromatosis mouse models point to at least two distinct pathways of hepcidin regulation by iron, one sensing extracellular holo-Tf concentrations and the other sensing intracellular iron, presumably in hepatocytes. It is possible that intracellular iron, partially signaling through the HJV/BMP6 pathway, sets basal hepcidin expression, with membrane-bound HJV functioning to heighten the sensitivity of BMP receptors to BMP6 and possibly other ligands. Holo-Tf concentrations signaling through TfR2, HFE, and HJV further increase the sensitivity of BMP receptors to the BMP ligands through as yet unknown mechanisms. It is also possible that TfR2/HFE activate a parallel pathway to increase hepcidin expression. Although

not directly addressed in this study, the involvement of nonhepatocyte cell types in the regulation of hepatocyte hepcidin synthesis remains to be explored and could contribute to iron homeostasis.

References

1. Nemeth E, Tuttle MS, Powelson J, Vaughn MB, Donovan A, Ward DM, et al. Hepcidin regulates cellular iron efflux by binding to ferroportin and inducing its internalization. Science 2004;306:2090-2093.
2. Lin L, Valore EV, Nemeth E, Goodnough JB, Gabayan V, Ganz T. Iron transferrin regulates hepcidin synthesis in primary hepatocyte culture through hemojuvelin and BMP2/4. Blood 2007;110:2182-2189.
3. Ganz T, Olbina G, Girelli D, Nemeth E, Westerman M. Immunoassay for human serum hepcidin. Blood 2008;112:4292-4297.
4. Nemeth E, Rivera S, Gabayan V, Keller C, Taudorf S, Pedersen BK, et al. IL-6 mediates hypoferremia of inflammation by inducing the synthesis of the iron regulatory hormone hepcidin. J Clin Invest 2004; 113:1271-1276.
5. Flanagan JM, Truksa J, Peng H, Lee P, Beutler E. In vivo imaging of hepcidin promoter stimulation by iron and inflammation. Blood Cells Mol Dis 2007;38:253-257.
6. Ramey G, Deschemin JC, Vaulont S. Cross-talk between the mitogen activated protein kinase and bone morphogenetic protein/hemojuvelin pathways is required for the induction of hepcidin by holotransferrin in primary mouse hepatocytes. Haematologica 2009;94:765-772.
7. Kawabata H, Fleming RE, Gui D, Moon SY, Saitoh T, O'Kelly J, et al. Expression of hepcidin is down-regulated in TfR2 mutant mice manifesting a phenotype of hereditary hemochromatosis. Blood 2005;105:376-381.
8. Niederkofler V, Salie R, Arber S. Hemojuvelin is essential for dietary iron sensing, and its mutation leads to severe iron overload. J Clin Invest 2005;115:2180-2186.
9. Meynard D, Kautz L, Darnaud V, Canonne-Hergaux F, Coppin H, Roth MP. Lack of the bone morphogenetic protein BMP6 induces massive iron overload. Nat Genet 2009;41:478-481.
10. Vujic SM, Kiss J, Herrmann T, Galy B, Martinache S, Stolte J, et al. Hfe acts in hepatocytes to prevent hemochromatosis. Cell Metab 2008; 7:173-178.
11. Bondi A, Valentino P, Daraio F, Porporato P, Gramaglia E, Carturan S, et al. Hepatic expression of hemochromatosis genes in two mouse strains after phlebotomy and iron overload. Haematologica 2005;90: 1161-1167.
12. Li H, Rybicki AC, Suzuka SM, von BL, Breuer W, Hall CB, et al. Transferrin therapy ameliorates disease in beta-thalassemic mice. Nat Med 2010;16:177-182.
13. Pak M, Lopez MA, Gabayan V, Ganz T, Rivera S. Suppression of hepcidin during anemia requires erythropoietic activity. Blood 2006;108: 3730-3735.
14. Bachmanov AA, Reed DR, Beauchamp GK, Tordoff MG. Food intake, water intake, and drinking spout side preference of 28 mouse strains. Behav Genet 2002;32:435-443.
15. Andriopoulos B Jr, Corradini E, Xia Y, Faasse SA, Chen S, Grgurevic L, et al. BMP6 is a key endogenous regulator of hepcidin expression and iron metabolism. Nat Genet 2009;41:482-487.
16. Corradini E, Garuti C, Montosi G, Ventura P, Andriopoulos B Jr, Lin HY, et al. Bone morphogenetic protein signaling is impaired in an HFE knockout mouse model of hemochromatosis. Gastroenterology 2009;137:1489-1497.
17. Kautz L, Meynard D, Besson-Fournier C, Darnaud V, Al ST, Coppin H, et al. BMP/Smad signaling is not enhanced in Hfe-deficient mice despite increased Bmp6 expression. Blood 2009;114:2515-2520.
18. Fleming RE, Sly WS. Mechanisms of iron accumulation in hereditary hemochromatosis. Annu Rev Physiol 2002;64:663-680.
19. Huang FW, Babitt JL, Wrighting DM, Samad TA, Xia Y, Sidis Y, et al. Hemojuvelin acts as a bone morphogenetic protein co-receptor to regulate hepcidin expression. ASH Annual Meeting Abstracts 2005;106: 511.
20. Wallace DF, Summerville L, Crampton EM, Frazer DM, Anderson GJ, Subramaniam VN. Combined deletion of Hfe and transferrin receptor 2 in mice leads to marked dysregulation of hepcidin and iron overload. Hepatology 2009;50:1992-2000.
21. Pietrangelo A, Caleffi A, Henrion J, Ferrara F, Corradini E, Kulaksiz H, et al. Juvenile hemochromatosis associated with pathogenic mutations of adult hemochromatosis genes. Gastroenterology 2005;128: 470-479.
22. Trombini P, Coliva T, Nemeth E, Mariani R, Ganz T, Biondi A, et al. Effects of plasma transfusion on hepcidin production in human congenital hypotransferrinemia. Haematologica 2007;92:1407-1410.
23. Bartnikas TB, Andrews NC, Fleming MD. Transferrin is a major determinant of hepcidin expression in hypotransferrinemic mice. Blood 2010; doi:10.1182/blood-2010-05-287359.
24. Kautz L, Meynard D, Monnier A, Darnaud V, Bouvet R, Wang RH, et al. Iron regulates phosphorylation of Smad1/5/8 and gene expression of Bmp6, Smad7, Id1, and Atoh8 in the mouse liver. Blood 2008;112: 1503-1509.
25. Lin L, Goldberg YP, Ganz T. Competitive regulation of hepcidin mRNA by soluble and cell-associated hemojuvelin. Blood 2005;106: 2884-2889.
26. Zhang AS, Anderson SA, Meyers KR, Hernandez C, Eisenstein RS, Enns CA. Evidence that inhibition of hemojuvelin shedding in response to iron is mediated through neogenin. J Biol Chem 2007;282: 12547-12556.
27. Silvestri L, Pagani A, Nai A, De D, I, Kaplan J, Camaschella C. The serine protease matriptase-2 (TMPRSS6) inhibits hepcidin activation by cleaving membrane hemojuvelin. Cell Metab 2008;8:502-511.

Supplemental Table 1. Iron parameters in the experimental mouse groups. Medians and interquartile ranges are shown. Statistical comparisons (1d load compared to depleted, and chronic load compared to 1d) were evaluated using the Mann-Whitney rank sum test. D= low-iron diet; P=phlebotomy.

Liver iron (μmoles/g wet liver)

Strain	N	depleted	1 day load	chronic load
C57Bl6 (D)	5,6,5	0.6 (0.5,0.9)	3.4 (2.1,3.6)**	2.3 (1.7,2.6)
C57Bl6 (P +D)	4,4,ND	0.5 (0.4,1.3)	3.5 (2.1,4.6)$^{+}$	ND
HFE (P+D)	8,11,18	0.6 (0.3,1.5)	2.0 (1.2,3.0)*	4.5 (2.6,8.1)**
FVB (D)	8,12,8	1.0 (0.8,1.5)	2.7 (1.7,5.2)**	4.0 (2.8,5.2)
TfR2 (P+D)	6,6,7	0.6 (0.3,1.0)	4.4 (3.0,5.0)**	15.6 (13.6,26.1)***
129SV (D)	6,6,6	0.2 (0.1,0.2)	0.6 (0.3,0.9)*	3.8 (3.2,4.4)**
HJV (P+D)	8,8,11	1.5 (1.2,1.7)	4.1 (2.8,5.8)***	26.0 (17.7,32.1)***
CD1 (D)	6,6,6	0.6 (0.5,0.9)	1.8 (1.2,2.4)**	5.1 (3.4,6.3)**
BMP6 (P+D)	6,7,6	0.8 (0.5,1.3)	1.4 (0.8,2.6)	26.1 (16.3,35.5)***

$^{+}$p=0.057, *p<0.05, **p<0.01, ***p≤0.001 (1d to depleted, or chronic load to 1day)

Spleen iron (μmoles/g wet spleen)

Strain	N	depleted	1 day load	chronic load
C57Bl6 (D)	6,6,8	0.7 (0.7,0.9)	0.9 (0.6,1.4)	6.3 (4.6,8.2)
C57Bl6 (P +D)	4,4,ND	0.8 (0.7,1.9)	1.3 (1.0,1.5)	ND
HFE (P+D)	9,10,7	1.4 (0.4,2.7)	1.2 (0.9,1.5)	1.4 (1.3,1.7)
FVB (D)	5,9,5	1.5 (1.4,2.7)	2.0 (1.3,2.1)	12.7 (10.6,13.2)
TfR2 (P+D)	8,8,6	0.7 (0.6,0.9)	1.0 (0.8,1.4)	1.7 (1.2,2.0)
129SV (D)	6,6,6	0.6 (0.4,0.6)	0.4 (0.2,0.6)	2.1 (1.7,3.2)
HJV (P+D)	6,6,15	0.5 (0.2,1.5)	1.2 (0.8,1.5)	1.7 (0.9,2.2)
CD1 (D)	6,6,6	1.6 (1.2,1.8)	1.5 (1.4,1.8)	10.5 (8.8,12.8)
BMP6 (P+D)	6,7,6	0.6 (0.5,1.2)	1.1 (0.7,1.3)	4.5 (2.8,6.6)

Serum iron (μM)

Strain	N	depleted	1 day load	chronic load
C57Bl6 (D)	5,6,9	11 (8,14)	51 (49,58)***	29 (25,33)**
C57Bl6 (P +D)	4,4,ND	38 (15,64)	75 (70,80)$^{+}$	ND
HFE (P+D)	8,11,8	21 (12,25)	57 (29,72)**	60 (28,65)
FVB (D)	8,8,8	39 (28,50)	55 (51,63)*	53 (46,58)
TfR2 (P+D)	8,8,7	16 (8,22)	67 (62,72)**	69 (67,78)
129SV (D)	5,6,6	10 (9,14)	67 (64,69)***	45 (39,49)**
HJV (P+D)	6,6,10	11 (5,13)	105 (104,107)**	63 (60,69)**
CD1 (D)	6,6,5	16 (14,21)	32 (17,43)*	27 (26,29)
BMP6 (P+D)	6,6,6	8 (6,14)	33 (16,50)*	52 (45,58)

$^{+}$p=0.057, *p<0.05, **p<0.01, ***p<0.001 (1d to depleted, or chronic load to 1day)

Liver hepcidin mRNA (-ΔCt relative to actin mRNA)

Strain	N	depleted	1 day load	chronic load
C57Bl6 (D)	6,6,7	-9.5 (-9.8,-8.6)	0.4(0.3,1.1) **	2.6(2.4,2.8)**
C57Bl6 (P +D)	4,4,ND	-9.9(-11.3,-6.6)	2.8(2.4,3.1)*	
HFE (P+D)	9,10,9	-8.4(-10.7,-7.5)	-5.0(-8.1,-4.4)*	1.8(1.3,2.3)***
FVB (D)	8,8,7	-7.3(-12.1,-4.8)	2.9(1.7,3.8)***	2.9(2.7,5.4)
TfR2 (P+D)	8,8,7	-10.7(-11.9,-9.6)	-10.5(-11.1,-10.2)	2.8(1.6,3.7)***
129SV (D)	6,6,6	-9.9 (-10.2,-9.8)	-0.4(-1.7,0.9)*	3.0(2.9,3.1)**
HJV (P+D)	6,6,10	-10.7(-11.2,-10.3)	-11.2(-11.6,-10.7)	-4.7(-7.3,-0.9)***
CD1 (D)	6,6,6	-8.8(-10.1,-8.4)	-1.6 (-6.7,-1.0)*	0.4(-0.7,0.9)**
BMP6 (P+D)	6,7,6	-12.0(-12.7,-11.9)	-11.2(-11.3,-8.5)**	-3.9(-7.2,-1.7)**

*p<0.05, **p<0.01, ***p<0.001, 1d compared to depleted, or chronic load compared to 1d

Supplemental Table 2: Best subsets regression analysis of the dependence of hepcidin mRNA (expressed as –ΔCt, i.e. log_2 (hepcidin mRNA)) on serum and liver iron is shown. Abbreviations: R^2, regression coefficient, an indicator of fit; adj R^2, R^2 adjusted for the number of independent variables. R^2 (regression coefficient) is used as best criterion. The coefficient (Coef.) and its standard error (Std. Error) estimate the magnitude of the effect of the variable on hepcidin. The smaller the P value, the greater the probability that the variable helps predict hepcidin. The magnitude of increase in "adjusted" R^2 when the second variable is added to the model is indicative of the contribution that variable makes to improved fit.

C57BL/6

Model #	Variable	R^2	Adj R^2	Liver Fe	Serum Fe
1	1	0.462	0.424		*
2	2	0.555	0.487	*	*

Model # 1	R^2= 0.462		
Variable	**Coef.**	**Std. Error**	**P**
Constant	-8.545	2.161	0.001
Serum Fe	0.207	0.0596	0.004

Model # 2	R^2= 0.555		
Variable	**Coef.**	**Std. Error**	**P**
Constant	-9.522	2.123	<0.001
Liver Fe	1.569	0.951	0.123
Serum Fe	0.135	0.0711	0.080

HFE

Model #	Variable	R^2	Adj R^2	Liver Fe	Serum Fe
1	1	0.472	0.450	*	
2	2	0.502	0.458	*	*

Model # 1	R^2= 0.472		
Variable	**Coef.**	**Std. Error**	**P**
Constant	-8.111	1.051	<0.001
Liver Fe	1.317	0.284	<0.001

Model # 2	R^2= 0.502		
Variable	**Coef.**	**Std. Error**	**P**
Constant	-7.103	1.352	<0.001
Liver Fe	1.509	0.327	<0.001
Serum Fe	-0.0370	0.0316	0.254

FVB

Model #	Variable	R^2	Adj R^2	Liver Fe	Serum Fe
1	1	0.472	0.447		*
2	2	0.645	0.610	*	*

Model # 1	R^2= 0.472		
Variable	**Coef.**	**Std. Error**	**P**
Constant	-16.039	3.655	<0.001
Serum Fe	0.306	0.0705	<0.001

Model # 2	R^2= 0.645		
Variable	**Coef.**	**Std. Error**	**P**
Constant	-16.049	3.070	<0.001
Liver Fe	0.681	0.218	0.005
Serum Fe	0.222	0.0650	0.003

TfR2

Model #	Variable	R^2	Adj R^2	Liver Fe	Serum Fe
1	1	0.706	0.692	*	
2	2	0.714	0.685	*	*

Model # 1	R^2= 0.706		
Variable	**Coef.**	**Std. Error**	**P**
Constant	-11.056	0.995	<0.001
Liver Fe	0.576	0.0812	<0.001

Model # 2	R^2=0.714		
Variable	**Coef.**	**Std. Error**	**P**
Constant	-12.068	1.661	<0.001
Liver Fe	0.543	0.0930	<0.001
Serum Fe	0.0241	0.0315	0.453

129S6

Model #	Variable	R^2	Adj R^2	Liver Fe	Serum Fe
1	1	0.453	0.417	*	
2	2	0.724	0.685	*	*

Model # 1	R^2=0.453		
Variable	**Coef.**	**Std. Error**	**P**
Constant	-4.493	1.292	0.003
Liver Fe 129	1.785	0.506	0.003

Model # 2	R^2= 0.724		
Variable	**Coef.**	**Std. Error**	**P**
Constant	-8.929	1.526	<0.001
Liver Fe	1.520	0.379	0.001
Serum Fe	0.115	0.0310	0.002

HJV

Model #	Variable	R^2	Adj R^2	Liver Fe	Serum Fe
1	1	0.579	0.558	*	
2	2	0.589	0.546	*	*

Model # 1	R^2= 0.579		
Variable	**Coef.**	**Std. Error**	**P**
Constant	-10.869	0.864	<0.001
Liver Fe	0.239	0.0456	<0.001

Model # 2	R^2= 0.589		
Variable	**Coef.**	**Std. Error**	**P**
Constant	-10.180	1.339	<0.001
Liver Fe	0.242	0.0465	<0.001
Serum Fe	-0.0125	0.0184	0.504

CD1

Model #	**Variable**	**R^2**	**Adj R^2**	**Liver Fe**	**Serum Fe**
1	1	0.691	0.671	*	
2	2	0.764	0.730	*	*

Model # 1	R^2= 0.691		
Variable	**Coef.**	**Std. Error**	**P**
Constant	-8.697	0.987	<0.001
Liver Fe	1.755	0.303	<0.001

Model # 2	R^2= 0.764		
Variable	**Coef.**	**Std. Error**	**P**
Constant	-11.323	1.549	<0.001
Liver Fe	1.556	0.290	<0.001
Serum Fe	0.126	0.0609	0.057

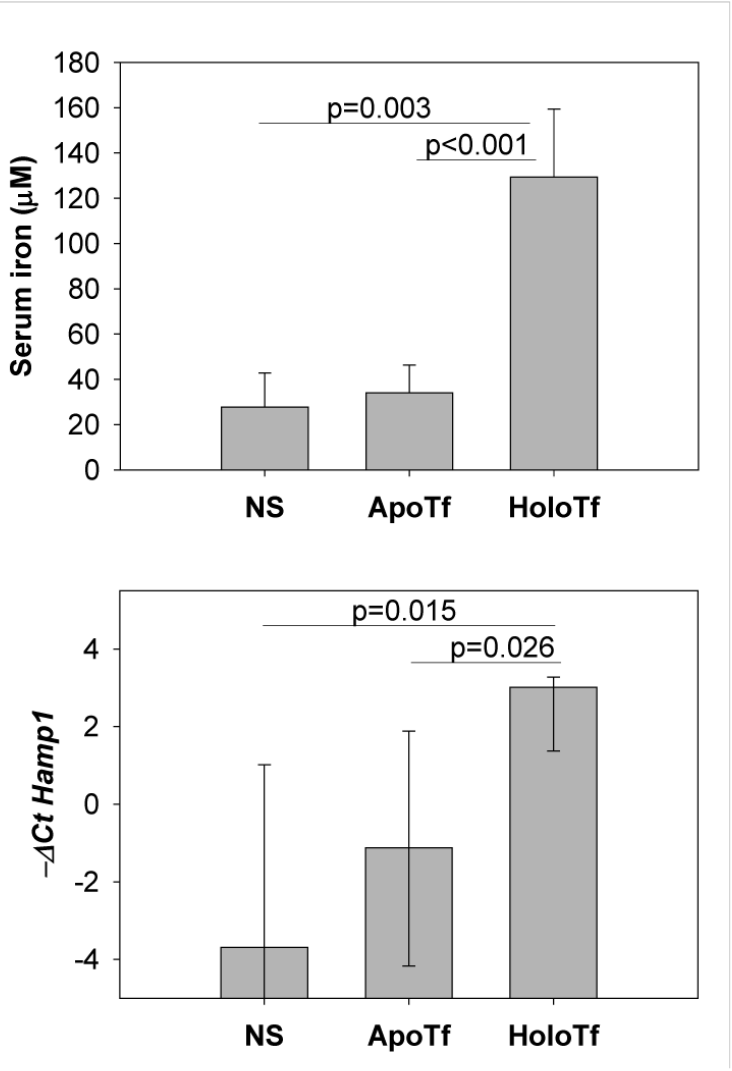
BMP6

Model #	**Variable**	**R^2**	**Adj R^2**	**Liver Fe**	**Serum Fe**
1	1	0.499	0.466	*	
2	2	0.549	0.484	*	*

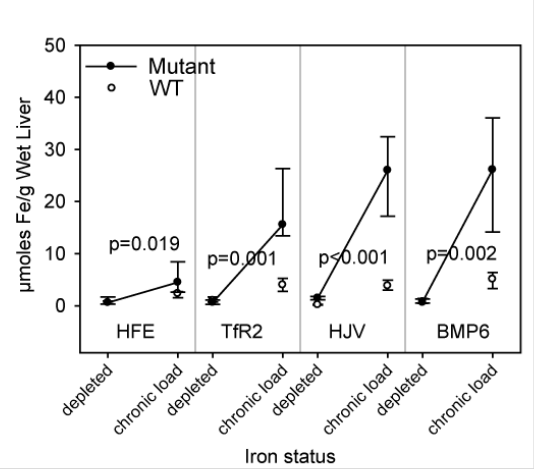
Model # 1	R^2= 0.499		
Variable	**Coef.**	**Std. Error**	**P**
Constant	-10.754	0.811	<0.001
Liver Fe	0.195	0.0504	0.002

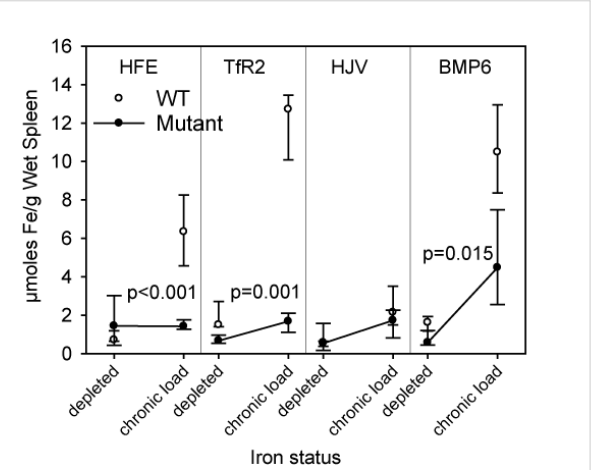
Model # 2	R^2= 0.549		
Variable	**Coef.**	**Std. Error**	**P**
Constant	-12.001	1.283	<0.001
Liver Fe	0.136	0.0686	0.068
Serum Fe	0.0546	0.0440	0.235

Supplemental Figure 1. Hepcidin mRNA expression in wild-type mice after an acute parenteral iron challenge. Four-week old mice were fed low iron diet for 14 days, after which they were injected with saline (NS, n=4) or 10 mg holo- or apotransferrin (Holo-Tf or Apo-Tf, n=6 each). Six hours after intraperitoneal injection, holo-Tf greatly increased serum iron concentration (mean and standard deviation) and hepcidin expression (median and interquartile range) as compared to NS or apo-Tf. As previously shown, intraperitoneal administration effectively delivers both transferrin forms into the blood circulation (1-3). The duration of the stimulus was chosen based on our human studies which showed that the increase in serum hepcidin after a single iron pill was detected after 8-12 hours (4).

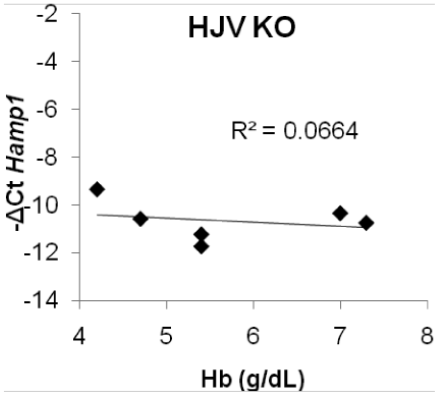


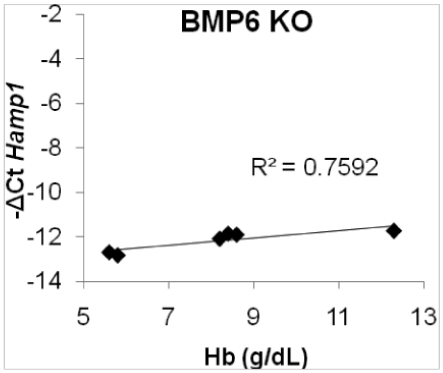
Supplemental Figure 2. Chronic iron loading in different strains and mutants. Graphs show medians and interquartile range of non-heme iron content in the liver (top panel) and the spleen (bottom panel). Each mutant strain is shown with its corresponding WT strain, and p-values refer to comparisons of WT to mutant strains after iron-loading.





Supplemental Figure 3. Correlation between hepcidin mRNA expression and Hb levels in phlebotomized *Hjv* and *Bmp6* KO mice.





qRT-PCR primer sequences:
HAMP 1:
forward 5'TTGCGATACCAATGCAGAAGA3'; reverse 5'GATGTGGCTCTAGGCTATGTT3'
Bmp6:
forward 5'AGAAGGGCACTCTTTCAGGTTCCA3'; reverse 5'TCACACCGAGAGTCAACACAA3'
ß-actin:
forward 5'ACCCACACTGTGCCCATCTA3'; reverse 5'-CACGCTCGGTCAGGATCTTC3'

Supplemental Reference List

1. Bartnikas TB, Andrews NC, Fleming MD. Transferrin is a major determinant of hepcidin expression in hypotransferrinemic mice. Blood 2010. Oct 18. [Epub ahead of print]

2. Li H, Rybicki AC, Suzuka SM, von BL, Breuer W, Hall CB, et al. Transferrin therapy ameliorates disease in beta-thalassemic mice. Nat Med 2010;16:177-182.

3. Regoeczi E, Zaimi O, Chindemi PA, Charlwood PA. Absorption of plasma proteins from peritoneal cavity of normal rats. Am J Physiol 1989;256:E447-E452.

4. Ganz T, Olbina G, Girelli D, Nemeth E, Westerman M. Immunoassay for human serum hepcidin. Blood 2008;112:4292-4297.

Chapter 2

Chapter 2 is a published paper that defines a novel signaling mechanism underlying pathological hepcidin suppression by growth factors associated with liver repair.

Summary

The work in this thesis centered on investigating the molecular basis of iron overload caused by inadequate hepcidin production. Hepcidin deficiency can be caused by mutations in genes necessary for hepcidin production as in hereditary hemochromatosis types I-III (see Chapter 1). In all cases, iron overload stems from the loss of function of the hepcidin-stimulating bone morphogenetic protein (BMP) pathway and decreased phosphorylation of SMAD transcriptional activators which bind the hepcidin promoter. Conversely, hyperactivity of hepcidin suppressing genes (TWSG1 and GDF-15) due to ineffective erythropoiesis also leads to iron overload even in non-transfused β-thalassemia intermedia patients (1,2). Iron overload has also been demonstrated in people who suffer from chronic hepatitis C and the mild to moderate increase in iron status is associated with worsened disease prognosis (3). Studies have shown that hepcidin levels are decreased during chronic hepatitis C infection (4) and we hypothesized that decreased hepcidin production was a side effect of continuous damage and repair that occurs during chronic liver disease. Importantly, little was known about the intracellular hepcidin suppressing pathways.

In this study we aimed to define the ligands and downstream machinery of a hepcidin suppressing pathway. We showed that both hepatocyte growth factor (HGF) and epidermal growth factor (EGF) suppress hepcidin transcription by disrupting signals from the BMP pathway. By inhibiting kinase pathways commonly upregulated by HGF and EGF in primary cell lines, we identified the PI3 kinase and MEK/ERK pathways as candidates that mediate hepcidin

suppression. Additionally, we showed that the HGF and EGF increase levels of TGIF, a known repressor of the SMAD transcription factors which activate hepcidin production. I made contributions to *in vitro* kinase inhibition experiments as well as *in vivo* studies of the hepcidin-suppressive effect of EGF in mice. This is the first work to show how hepcidin is suppressed at the molecular level and provides new drug targets for reversing hepcidin suppression during chronic liver disease.

References

1. Tanno T, Porayette P, Sripichai O, Noh S-J, Byrnes C, Bhupatiraju A, et al. Identification of TWSG1 as a second novel erythroid regulator of hepcidin expression in murine and human cells. Blood. 2009;114:181–186.

2. Tanno T, Bhanu NV, Oneal PA, Goh SH, Staker P, Lee YT, et al. High levels of GDF15 in thalassemia suppress expression of the iron regulatory protein hepcidin. Nat.Med. 2007;13:1096–1101.

3. Metwally MA, Zein CO, Zein NN. Clinical significance of hepatic iron deposition and serum iron values in patients with chronic hepatitis C infection. Am. J. Gastroenterol. 2004;99:286–291.

4. Girelli D, Pasino M, Goodnough JB, Nemeth E, Guido M, Castagna A, et al. Reduced serum hepcidin levels in patients with chronic hepatitis C. J. Hepatol. 2009;51:845–852.

Inhibition of Hepcidin Transcription by Growth Factors

Julia B. Goodnough,[1] Emilio Ramos,[2] Elizabeta Nemeth,[3]* and Tomas Ganz[1,3]*

The hepatic peptide hormone hepcidin controls the duodenal absorption of iron, its storage, and its systemic distribution. Hepcidin production is often insufficient in chronic hepatitis C and alcoholic liver disease, leading to hyperabsorption of iron and its accumulation in the liver. Hepatocyte growth factor (HGF) and epidermal growth factor (EGF) mediate the hepatic regeneration after liver injury. We examined the effect of the growth factors on hepcidin synthesis by hepatocytes. HGF and EGF treatment of primary mouse hepatocytes, as well as EGF administration in mice, suppressed hepcidin messenger RNA (mRNA) synthesis. The suppression of hepcidin by these growth factors was transcriptional, and was mediated by a direct effect of HGF and EGF on the bone morphogenetic protein (BMP) pathway regulating hepcidin synthesis. We further show that growth factors interfered with nuclear localization of activated sons of mothers against decapentaplegic (Smad) and increased the nuclear pool of the BMP transcriptional corepressor TG-interacting factor (TGIF). In a kinase screen with small-molecule kinase inhibitors, inhibitors in the PI3 kinase pathway and in the mitogen-activated ERK kinase/extracellular signal-regulated kinase (MEK/ERK) pathway prevented HGF suppression of hepcidin in primary mouse hepatocytes. *Conclusion:* HGF and EGF suppress hepatic hepcidin synthesis, in part through PI3 kinase MEK/ERK kinase pathways which may be modulating the nuclear localization of BMP pathway transcriptional regulators including activated Smads1/5/8 and the corepressor TGIF. EGF, HGF, and possibly other growth factors that activate similar pathways may contribute to hepcidin suppression in chronic liver diseases, promote iron accumulation in the liver, and exacerbate the destructive disease processes. (HEPATOLOGY 2012;00:000–000)

The hepatic hormone hepcidin controls the flow of iron from dietary absorption, storage, and recycling into blood plasma, and thereby regulates plasma iron concentrations and stores.[1] In turn, plasma iron concentrations and hepatic iron stores transcriptionally modulate hepcidin synthesis,[2,3] completing a homeostatic feedback loop. The bone morphogenetic protein (BMP) pathway is essential for iron and hepcidin regulation.[4] The BMP receptor complex and a range of BMP ligands, including BMP6, induce hepcidin expression by activating sons of mothers against decapentaplegic (Smad)4 and Smad1/5/8.[5-7] Human mutations that cause hereditary hemochromatosis either ablate the hepcidin gene (rare) or affect iron-specific hepcidin regulatory proteins that are thought to interact with the BMP pathway.[1]

Hepcidin insufficiency and hepatic iron loading are seen in chronic hepatitis of multiple etiologies, including alcoholic hepatitis and viral hepatitis[8-10] and the resulting chronic iron loading in the liver worsens disease prognosis.[11] The mechanism of hepcidin suppression in chronic hepatitis is not known.

Chronic hepatitis is characterized by repeated liver injury and repair. Growth factors mitogenic for hepatocytes are important mediators of liver repair and regeneration. Hepatocyte growth factor (HGF) and epidermal growth factor (EGF) are well-

Abbreviations: BMP, bone morphogenetic protein; EGF, epidermal growth factor; ERK, extracellular signal-regulated kinase; HGF, hepatocyte growth factor; IGF, insulin-like growth factor; MAPK, mitogen activated protein kinase; MEK, mitogen-activated ERK kinase; Met, HGF receptor (Met protooncogene); PDGF, platelet-derived growth factor; PI3-kinase, phosphoinositide 3-kinase; Smad, sons of mothers against decapentaplegic; TGIF, TG-interacting factor.

From the [1]Department of Pathology; [2]Department of Chemistry and Biochemistry; [3]Department of Medicine, David Geffen School of Medicine, University of California, Los Angeles, CA.

Received July 14, 2011; accepted January 15, 2012.

Supported by Roche Foundation for Anemia Research (RoFAR) (to T.G.); National Institutes of Health grants R01 DK065029 (to T.G.), R01 DK082717 (to E.N.); the Will Rogers Fund (to T.G.); Ruth L. Kirschstein National Research Service Award (NRSA) F30 DK082151 (to J.G.); Ruth L. Kirschstein NRSA GM007185 (to E.R.).

**These authors contributed equally to this study.*

Address reprint requests to: Tomas Ganz, M.D., Ph.,D., Department of Medicine, David Geffen School of Medicine at UCLA, 10833 LeConte Avenue, CHS 37-055, Los Angeles, CA 90095-1690. E-mail: tganz@mednet.ucla.edu; fax: 310-206-8766.

Copyright © 2012 by the American Association for the Study of Liver Diseases.

View this article online at wileyonlinelibrary.com.

DOI 10.1002/hep.25615

Potential conflict of interest: Nothing to report.

Additional Supporting Information may be found in the online version of this article.

characterized mediators of hepatic regeneration following experimental injury.[12-14] We explored the modulation of hepcidin synthesis by these growth factors.

Materials and Methods

Detailed methods are provided in the Supporting material.

Reagents. Murine EGF, HGF, insulin-like growth factor (IGF)-1, and IGF-2, rat platelet-derived growth factor (PDGF)-BB, and human BMP6 were from R&D Systems (Minneapolis, MN). Recombinant mouse interleukin (IL)-6 and recombinant human EGF were from Millipore (Billerica, MA). Kinase inhibitors EHT1864, PHA665752, NSC23766, 10-DEBC hydrochloride were from Tocris Bioscience (St. Louis, MO), and U73112, LY294002, Calphostin, JNK Inhibitor II, STAT3 inhibitor VII, U0126, ERK inhibitor peptide II FR180204, Akt inhibitor II, and Akt inhibitor X from Millipore.

Cell Culture and Transient Transfections. Hepatocytes were isolated from 6- to 8-week old wildtype (WT) C57BL/6 mice by a two-step portal vein collagenase perfusion method and used within hours or after 18-hour incubation with serum-free William's E Medium (serum-starved). Transfection of hepatocytes and HepG2 cells was done with Nucleofector (Lonza Group, Basel, Switzerland) according to the manufacturer's instructions. The hepcidin-luciferase reporter included human hepcidin promoter spanning −1 to −2997,[15] and the BRE-luciferase reporter was obtained from H.Y. Lin.[16] Luciferase activity was measured by a Veritas Microplate Luminometer (Turner Biosystems, now Promega, Sunnyvale, CA).

RNA Isolation and Real-Time Quantitative Polymerase Chain Reaction (PCR). Quantitative real-time reverse-transcription (RT)-PCR data are presented as either fold-change relative to control or using the ΔΔCt method which naturally yields a logarithmic scale. Fold-change was calculated by the method of Pfaffl,[17] where the target gene (Hepc1 or ID1) was referenced to a housekeeping gene (β-actin) and the data presented as a ratio to the control treatment within each experiment. The average relative expression value of the triplicate control treatments was assigned as 1 in each experiment. Relative quantification was performed using the comparative Ct, or ddCt method.[18] The target gene (Hepc1 or ID1) was first normalized to a reference housekeeping gene (β-actin) and then presented as the difference from the control treatment within each experiment. The average ddCt value of the triplicate control treatments was zero in each experiment.

Cell Fractionation and Western Blots. Cells for whole-cell lysates were plated in 60-mm collagen-coated dishes (BD Biocoat, Franklin Lakes, NJ) and cells for fractionated lysates (nuclear and cytosolic) were plated in 10-cm collagen-coated dishes. After treatment, whole-cell lysates were collected in ice-cold NETT buffer (150 mM NaCl, 10 mM EDTA, 10 mM Tris, 1% Triton X-100) containing HALT protease/phosphatase inhibitor cocktail (ThermoScientific/Pierce, Rockford, IL). Fractioned lysates were separated into nuclear and cytosolic fractions using the NE-PER kit (Pierce) according to the manufacturer's instructions. Lysates (30 μg of fractionated lysates, 50 μg of whole-cell lysates) were electrophoresed on 4%-20% LongLife iGels (NuSep, Lawrenceville, GA) and transferred to Immobilon-P PVDF membrane (EMD Millipore) for western blotting, visualization by chemiluminescence, and quantification with the ChemiDoc XRS+ System with Image Lab software (BioRad, Hercules, CA).

Kinase Inhibitor Screen. Twenty-four hours after isolation, serum-starved hepatocytes were pretreated with kinase inhibitors in a 0.5 μL volume of dimethyl sulfoxide (DMSO). Each kinase inhibitor was added to duplicate or triplicate wells and after 1 hour 20 ng/mL HGF was added, then 1 hour later 10 ng/mL BMP6 was added. Depending on the kinase inhibitor, cultures were incubated for a minimum of 8 hours or overnight prior to sample collection.

Injection of Mice with Recombinant Human EGF. WT 6-week-old C57BL/6 mice were mildly iron-depleted by being placed on a diet with less than 4 ppm iron (Harlan Teklad) for 7 days prior to the experiment. On the day of injection, mice received a series of three intraperitoneal injections (spaced 6 hours apart) of 50 μg human EGF (Millipore) or saline. Some mice were injected with 5 mg holotransferrin (Sanquin, Amsterdam, The Netherlands) with the third dose of EGF or saline. Liver samples were collected 24 hours after the first dose of EGF was administered.

Results

HGF and EGF Suppress Hepcidin Messenger RNA (mRNA) In Vitro and In Vivo

HGF dose-dependently suppressed hepcidin mRNA in hepatocytes (Fig. 1A). When hepcidin was induced F1
by its physiological stimuli, holotransferrin or BMP, HGF significantly lowered both baseline hepcidin expression and the maximal induction of hepcidin by holotransferrin (Fig. 1B) or by a range of BMP6

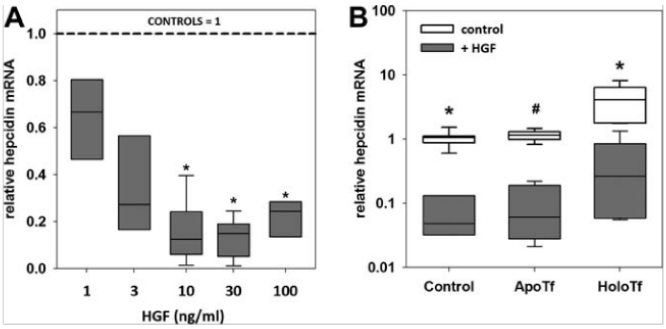


Fig. 1. HGF suppresses hepcidin mRNA expression. Fresh primary mouse hepatocytes were treated with HGF for 18 hours in William's E Medium with 5% fetal bovine serum (FBS). The boxplot represents the 25th and 75th percentile, the band the 50th percentile, and whiskers the minimum and maximum of the data. (A) Hepcidin mRNA was dose-dependently suppressed by HGF. *$P < 0.05$ by one-way analysis of variance (ANOVA) on ranks as compared with untreated control. (B) Hepatocytes were treated with HGF (20 ng/mL) and apo- or holo-transferrin (30 μM). *$P < 0.001$ by Mann-Whitney rank sum test, #$P < 0.001$ by t test.

concentrations (Fig. 2A). At each concentration of BMP6, HGF addition caused 10- to 20-fold suppression of hepcidin mRNA. In experiments where IL-6 was used as the inducing cytokine, HGF suppression of hepcidin mRNA was overcome by increasing concentrations of IL-6, even though it is a less potent hepcidin inducer than BMP6 (Supporting Fig. S1). Among other growth factors tested, only EGF suppressed hepcidin mRNA similarly to HGF (Fig. 2B). PDGF (Fig. 2C) and IGFs-1 and -2 (Supporting Fig. S2) had no effect on BMP induction of hepcidin mRNA.

To test whether the suppressive effect of growth factors could be relevant *in vivo*, we injected mice with EGF, holotransferrin, or their combination (Fig. 3), using recombinant human EGF because of much lower cost. Increased expression of the known EGF target transcript osteopontin confirmed that EGF had a detectable effect in the liver (Fig. 3B). EGF significantly suppressed hepcidin responses to holotransferrin (Fig. 3A), with hepcidin mRNA approximately 20-fold lower than in mice that received holotransferrin alone.

HGF Represses Transcription from the Hepcidin Promoter and Other BMP-Responsive Promoters

In primary mouse hepatocytes transfected with hepcidin promoter-luciferase reporter, HGF strongly suppressed the induction of the hepcidin promoter by BMP2 (Fig. 4A). We tested a broader range of BMPs in HepG2 cells transfected with hepcidin-luciferase reporter and found that HGF suppressed the induction of the hepcidin reporter by BMP-2, 4, 6, and 9) (Fig. 4C; Supporting Fig. S3A). Thus, HGF is a broadly

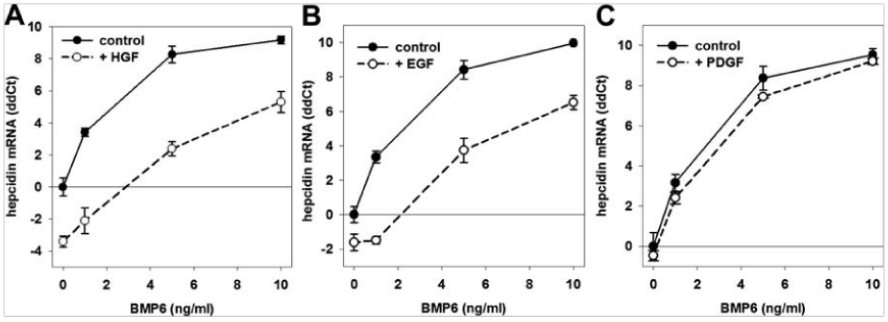


Fig. 2. HGF and EGF suppress hepcidin mRNA induction by BMP-6. Hepatocytes were serum-starved for 18 hours prior to treatment with increasing concentrations of BMP6 and (A) 20 ng/mL HGF, (B) 20 ng/mL EGF, and (C) 20 ng/mL PDGF-BB. The plots represent hepcidin mRNA concentration relative to untreated controls. ($P < 0.001$, paired t test comparing controls versus HGF or EGF treatment).

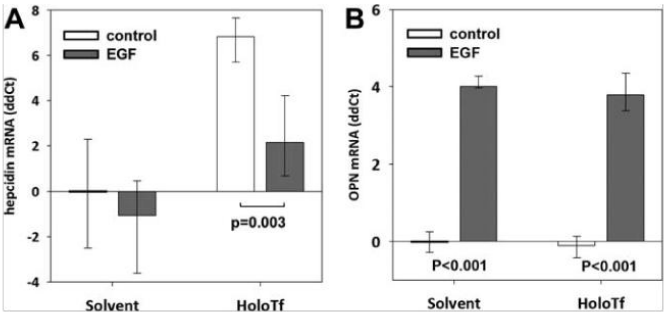


Fig. 3. *In vivo*, EGF suppresses hepatic hepcidin mRNA induction by holotransferrin. Six-week-old C57BL/6 male mice received three EGF or saline intraperitoneal injections over 12 hours, with and without 5 mg holotransferrin coadministration at the last injection. The upper and lower limits of the boxplots represent the 25th and 75th percentile, respectively; the band represents the median, n = 8 per treatment group. Hepatic hepcidin (A) or osteopontin (B) mRNA expression was analyzed 24 hours after the first EGF injection.

active transcriptional suppressor of the BMP response of the hepcidin promoter.

We also tested the effect of HGF on another BMP-sensitive luciferase reporter containing the BMP-responsive element (BRE) from the promoter of the gene for ID1 (inhibitor of DNA binding 1), a known direct target gene for BMP.[16] In transfected mouse hepatocytes and HepG2s, HGF suppressed the induction of the BRE-luciferase reporter by BMP-2, -4, -6, and -9 (Fig. 4B,D; Supporting Fig. S3B). Further, in primary mouse hepatocytes HGF and EGF similarly modulated the BMP-dependent induction of ID1 mRNA (Supporting Fig. S4). Taken together, these data indicate that HGF and EGF inhibit transcription

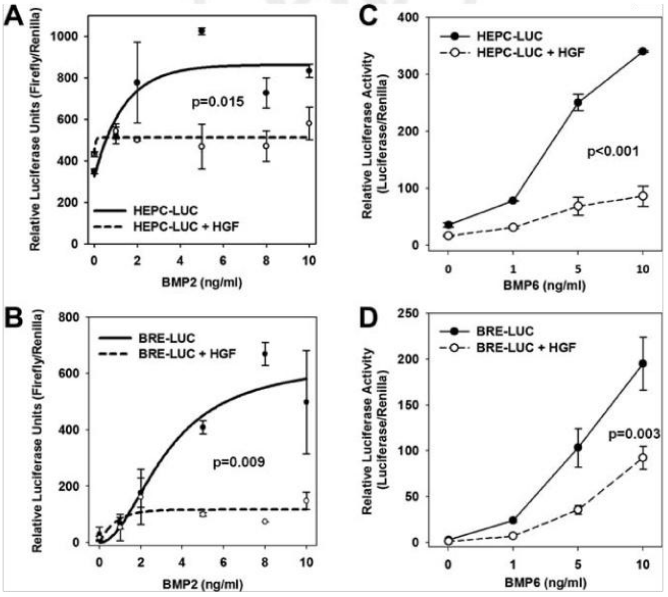


Fig. 4. HGF suppresses hepcidin transcription. (A,B) Hepatocytes were transiently transfected with a hepcidin-luciferase reporter (HEPC-LUC) or BMP-responsive luciferase reporter (BRE_LUC) and thymidine-kinase Renilla transfection control reporter. Cells were treated with human BMP2, with and without HGF and incubated for 24 hours. (C,D) HepG2 cells were transiently transfected with the hepcidin-luciferase reporter (HEPC-LUC) or BMP-responsive luciferase reporter (BRE_LUC) and Renilla transfection control. Statistical significance was tested with *paired *t* test or #Wilcoxon signed rank test.

of BMP-sensitive genes including hepcidin, likely by modulating BMP pathway signaling or BMP-dependent assembly of transcriptional machinery.

Effect of HGF and EGF on Signaling in the BMP Pathway

When BMPs bind to their receptor (BMP-R), the receptor phosphorylates and activates cytosolic signaling proteins R-Smads 1, 5, and/or 8, which form complexes with the common mediator Smad4. These complexes translocate into the nucleus where they transactivate BMP-dependent transcription.[19] The induction of hepcidin mRNA by BMP6 occurred within 4 hours, and costimulation with HGF or EGF suppressed the maximal induction of hepcidin mRNA within the same timeframe (Supporting Fig. S5). The short timeframe favored a mechanism based on rapid, covalent modifications of signaling mediators rather than the synthesis of new transcriptional regulators. We hypothesized that HGF and EGF were initiating kinase signaling that resulted in decreased activation of Smad1/5/8, or in inhibitory modification of Smad1/5/8, through prevention or removal of the activating C-terminal phosphorylation[20] or by targeting Smads 1/5/8 for degradation.

HGF and EGF Do Not Decrease Smad1/5/8 Activation. BMP-dependent activating phosphorylation of Smad 1/5/8 was equal in the growth factor-treated and BMP-only series (Fig. 5A,B), indicating that despite the presence of HGF or EGF the BMP signal was still fully transduced to the R-Smads. This makes it unlikely that BMP ligand-trap proteins, modification or degradation of BMP-Rs, or R-Smad deactivation play an important role in the modulation of the BMP effect by HGF or EGF. Further, total nuclear Smad1/5/8 is not decreased by HGF treatment (Fig. 5A).

HGF and EGF Do Not Induce Inhibitory Smads. Additional modulation at the ligand-receptor level is provided by BMP pathway inhibitors including BAMBI,[21] Smad 6,[22,23] and Smad7, the latter already known to play a role in hepcidin regulation.[7,24] The concentrations of BAMBI and inhibitory Smads determine their effect on signaling.[23] We used whole-cell lysates of primary mouse hepatocyte cultures treated with BMP and HGF or EGF to examine the protein levels of the three inhibitors. After overnight incubation, neither Smads 6 or 7 (Supporting Fig. S6A,B) nor BAMBI (data not shown) were induced by growth factor treatments.

HGF or EGF Do Not Decrease Protein Levels of R-Smads1 and 5 or Common Mediator Smad4. Growth factors have been reported to decrease the total Smad1 pool by proteasomal degradation.[25] Treatment with HGF had no effect on total Smad1 or Smad5 (Supporting Fig. S6C,D) in the 2 hours following HGF treatment or overnight (data not shown). Treatment with EGF also did not cause a change in total Smad 1/5/8 in whole cell lysates (Fig. 5B).

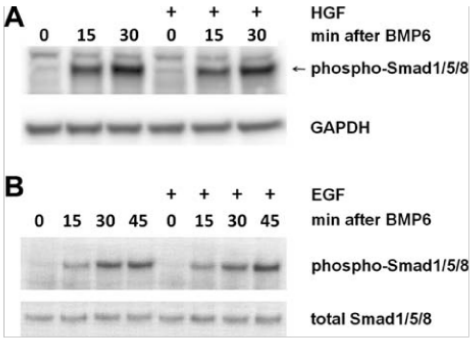


Fig. 5. HGF and EGF do not inhibit BMP activation of signaling mediators Smad1/5/8. Serum-starved hepatocytes were treated with 20 ng/mL murine HGF (A) or EGF (B) 1 hour before addition of human BMP6 (10 ng/mL). Western blots of whole-cell lysate were probed with anti-pSmad1/5/8. As loading controls, blots were probed with anti-GAPDH or total Smad1/5/8.

The common mediator Smad4 is also a target for regulatory input and its ubiquitination leads to its degradation in the proteasome.[26] Decreased Smad4 in the context of hepcidin reporter suppression by hypoxia was recently described.[27] From hepatocytes treated with BMP6 with and without HGF, we blotted nuclear lysates for Smad4. Smad4 levels in the nucleus were unaffected by HGF, indicating that the BMP signal had adequate access to co-Smad for formation of transcription complexes (Supporting Fig. S6E). Thus, the mechanism for growth factor suppression of hepcidin does not include overall degradation of the receptor-activated Smad pool or Smad4.

BMP-Dependent Nuclear Localization of Smad1/5/8 Is Modestly Suppressed by HGF and EGF. The linker region between the two globular domains of Smad1 can be phosphorylated by several kinases, including the mitogen-activated protein kinase (MAPK) ERK2, cyclin-dependent kinases (CDK), and glycogen synthase kinase-3β (GSK3β)[25] and the modification inhibits nuclear translocation of Smads. Growth factors including HGF and EGF induce linker phosphorylation[28] acting to limit BMP signaling during development.

After growth factor treatment of BMP6-stimulated hepatocytes, immunoblots for phospho-Smad1/5/8

Author Proof

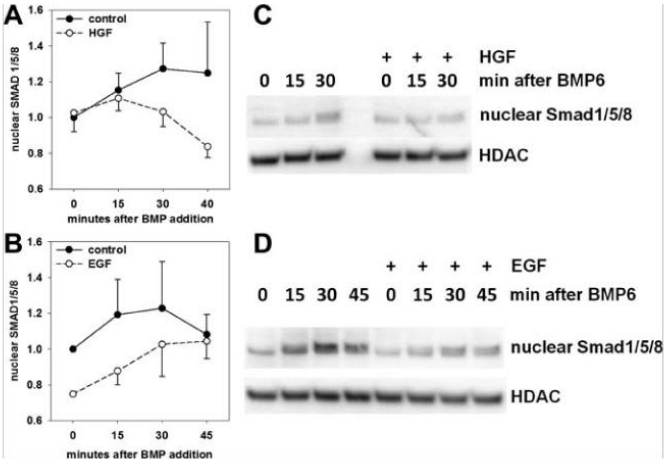


Fig. 6. HGF and EGF modestly decrease BMP-stimulated nuclear import of SMADs. Serum-starved hepatocytes were pretreated with 20 ng/mL murine HGF (A,C) or 20 ng/mL murine EGF (B,D) 1 hour before treatment with human BMP6 (40 ng/mL). Nuclear lysates were analyzed by western blotting and digital imaging. Histone deacetylase was used as a loading control. Four independent experiments were performed for A and B. Pairwise *t* test: $P = 0.04$ for HGF; $P = 0.004$ for EGF.

showed moderately decreased nuclear localization of phospho-Smad/1/5/8 (Fig. 6). The difference between the growth-factor treated nuclear lysates and the control lysates was statistically significant for both growth factors by pairwise *t* test when four repeated experiments were analyzed together for each growth factor.

Nuclear Levels of the Transcriptional Corepressor TG-Interacting Factor (TGIF) Are Increased After Treatment with HGF

We next considered modes of BMP pathway suppression that target the Smad transcriptional complex. The Smad transcriptional complex is nucleated by R-Smad/Smad4, but the binding affinity is regulated by DNA-binding coactivators or corepressors such as TGIF.[29] Figure 7 demonstrates increased protein levels of TGIF in nuclear lysates of cells treated with HGF, suggesting a mechanism for HGF interference with Smad transcriptional complexes.

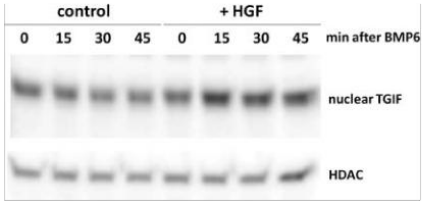


Fig. 7. HGF increases the nuclear protein levels of BMP-corepressor TGIF. Serum-starved hepatocytes were treated with murine HGF 40 ng/mL 1 hour prior to the addition of 25 ng/mL BMP6. The nuclear fraction of the cell lysate was blotted and probed for the BMP corepressor TGIF, with histone deacetylase as a loading control.

Taken together, these data indicate that the mechanism for HGF suppression is downstream of the multiple levels of Smad regulation and may involve a combination of decreased nuclear localization of activated Smad1/5/8 as well as induction of transcriptional corepressors such as TGIF.

Which of the Kinase Pathways Downstream of HGF/Met Are Suppressing Hepcidin?

HGF activates signaling pathways through its receptor, tyrosine kinase Met. Met signaling is complex, branching into multiple distinct but interacting signaling modules, so that HGF suppression of BMP signaling to hepcidin may be the product of more than one downstream signal from HGF/Met (Supporting Fig. S7). Using primary hepatocytes treated with BMP6, we performed a limited screen with small-molecule kinase inhibitors against individual kinase pathways known to be activated by HGF.

The proof of principle experiment tested for inhibition of HGF signaling by a kinase inhibitor for the Met receptor itself (PHA665752). Inhibition of the Met receptor abrogated HGF suppression of both hepcidin mRNA and ID1 mRNA (Fig. 8A,B). Interestingly, the dose required to inhibit HGF (1 μM) was 20 times the median inhibitory concentration (IC_{50}) (25-50 nM) for inhibition of receptor activation in

Author Proof

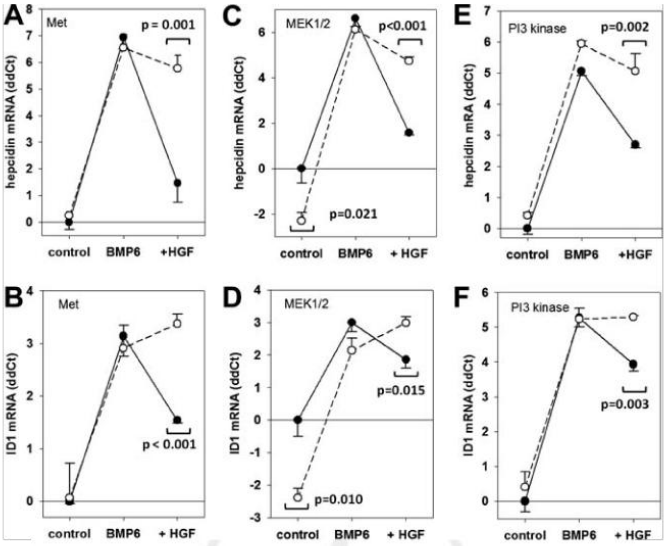


Fig. 8. Reversal of HGF effect by PI3 kinase or MEK1/2 inhibition. Serum-starved hepatocytes were pretreated for 1 hour with one of the following kinase inhibitors: 1 μM Met inhibitor PHA665752, 8 μM PI3 kinase inhibitor LY294002, or 25 μM U0126 MEK1/2 inhibitor, then treated with BMP6 with or without HGF for 18 hours. Inhibition of the HGF receptor Met blocked the suppressive effect of HGF on hepcidin (A) ($P = 0.001$, t test), and on the unrelated BMP-responsive gene ID1 (B) ($P < 0.001$, t test). (C) Inhibition of MEK1/2 also appears to reverse hepcidin suppression by HGF; however, the inhibitor also suppressed baseline hepcidin ($P = 0.021$). (D) The MEK1/2 inhibitor also reversed the HGF suppression of ID1 ($P = 0.015$, t test) and suppressed ID1 at baseline ($P = 0.010$, t test). Inhibition of PI3 kinase fully reversed the suppression of (E) hepcidin ($P = 0.002$, t test) as well as (F) ID1 ($P = 0.003$, t test).

epithelial cell lines (kidney, lung, and mammary cells). The requirement for high doses of inhibitor may be due to the hepatocyte cell membrane resistance to permeation of small molecule kinase inhibitors, akin to difficulties with the transfection of primary hepatocyte using liposomal methods. Alternatively, the known catabolic activity of hepatocytes toward small organic molecules may cause rapid degradation of many of our inhibitors. Bearing this in mind, we examined a higher range of inhibitor concentrations.

MAPK/ERK Signaling Plays Only a Partial Role in HGF Crosstalk with Hepcidin. Two MAPK pathways are known to be activated by HGF: Rac1/JNK and Ras/MEK/ERK. Two Rac1 inhibitors (5 μM EHT1864, 94 μM NSC23766) did not inhibit HGF suppression of hepcidin mRNA, nor did JNK inhibition (1 μM, JNK Inhibitor II). With MEK1/2 inhibitor U0126, we observed partial reversal of HGF suppression of hepcidin mRNA (Fig. 8C) as well as ID1 mRNA (Fig. 8D). The ERK inhibitor peptide II (5 μM) recapitulated these data (data not shown). The high dose of U0126 (25 μM) reversed HGF suppression of hepcidin and ID1, but it also affected the baseline hepcidin and ID1 mRNA, indicating that the activity of the inhibitor at 25 μM may have effects not specific to HGF. These data indicate at most a partial role for HGF/MEK signaling to hepcidin; alternatively, inhibition of MEK1/2 may result in mild hepcidin increase by mechanisms independent of HGF.

Major Pathways Not Involved: PKC, PLC, and STAT3. Broadening our focus, we sought to rule out other major pathways downstream of the Met receptor (Supporting Fig. S7). Small-molecule inhibitors of protein kinase C (1.25 μM Calphostin), phospholipase C (5 μM U73112), or STAT3 (1 μM inhibitor VII) affected neither BMP induction of hepcidin, nor did they reverse suppression of hepcidin by HGF. We conclude that none of these major pathways plays a role in the regulation of hepcidin by HGF.

PI3 Kinase Inhibition Reverses Hepcidin Suppression by HGF. Treatment of primary mouse hepatocytes with PI3K inhibitor LY294002 at a moderate concentration (8 μM, 5× IC_{50}) significantly reversed HGF suppression of hepcidin ($P = 0.04$, t test compared with controls) (Fig. 8E) without affecting baseline hepcidin mRNA in the controls or maximal hepcidin induction by BMP6. ID1 suppression was similarly reversed (Fig. 8F). Increased phosphorylation

of AKT confirmed activation of PI3K by HGF, and loss of AKT phosphorylation confirmed the effectiveness of the PI3K inhibitor (Supporting Fig. 8). Pretreatment with the Met inhibitor also prevented AKT activation (Supporting Fig. S9A). In agreement with hepcidin mRNA suppression in primary hepatocytes, only HGF and EGF, but not PDGF, IGF-1, or IGF-2 caused activation of AKT (Supporting Fig. S9B).

Discussion

We report the growth factors HGF and EGF as a new category of hepcidin suppressors that robustly block hepcidin transcriptional regulation by the known physiologic inducers, iron and BMPs. The ability of EGF to suppress iron-induced hepcidin mRNA was also confirmed in mice. Our data also indicate that HGF and EGF regulate hepcidin by suppressing BMP signaling upstream of the hepcidin promoter, a suppressive effect that extends to the unrelated BMP-sensitive promoter and mRNA transcript of ID1. The rapid onset of suppression suggests direct molecular crosstalk between BMP and growth factor signaling mediators. The crosstalk does not extend to the IL-6 pathway, as HGF does not significantly suppress hepcidin mRNA at higher IL-6 concentrations.

Growth factor regulation of BMP signaling through MAPK-mediated nuclear exclusion of R-Smads has been extensively reported in culture systems using transfected, highly overexpressed tagged Smad constructs. The data from such studies suggest that Smad linker phosphorylation by growth factor-activated MAPK/ERK nearly entirely abrogates BMP-dependent nuclear localization of activated Smads.[25] Our findings indicate that in hepatocytes the endogenous R-Smad pool is less strictly regulated. The trend we observed for nuclear exclusion of activated Smads and the increased regulatory phosphorylation at MAPK motifs on the Smad linker is modest at best and seems unlikely to account for the dramatic inhibition of hepcidin induction by HGF and EGF. Furthermore, the activation of the R-Smads was not suppressed by the growth factors, nor was the cellular pool of Smads1 and 5 and co-Smad4 degraded. We also detected no evidence of transcriptional induction of BMP negative regulators such as inhibitory Smads.

R-Smad by itself interacts weakly with its cognate promoter element and its association with other transcription factors is thought to be required for optimal activity. The increased protein levels of a transcriptional corepressor, TGIF, in the nuclei of hepatocytes treated with HGF suggests a likely mechanism for HGF crosstalk with BMP signaling. Phosphorylation of the corepressor TGIF by EGF-activated Ras/MEK signaling has been reported; TGIF phosphorylation resulted in stabilization of the repressor and formation of R-Smad/TGIF transcriptionally suppressive complexes.[30] We surmise that HGF may suppress hepcidin induction by BMP through MAPK stabilization of TGIF.

HGF is a pleiotropic growth factor that activates a multitude of downstream signaling pathways; many of the mitogenic, morphogenic, and motogenic effects of Met are regulated by more than one of these downstream signals. Our kinase inhibitor screen in primary hepatocytes identified at least two signaling pathways (MEK and PI3K) that appear to regulate hepcidin. The activity of the MEK1/2 inhibitor U0126 in our studies suggested a role for MEK in HGF suppression. It was previously reported that Ras/MEK activation by EGF results in phosphorylation and stabilization of the Smad transcriptional corepressor TGIF.[30] HGF may cause a similar stabilization of TGIF by way of MEK activation. A more detailed exploration of the similarities and differences between HGF and EGF pathways will be undertaken in a future study.

In view of the role of growth factors HGF, EGF, and transforming growth factor alpha (TGF-α), which also binds to the EGF receptor, as mediators of the hepatic regenerative response,[14] the suppression of hepcidin by growth factors may be relevant to hepcidin deficiency and hepatic iron loading in chronic liver diseases. Elevated liver tissue concentrations of growth factors in chronic viral and alcoholic hepatitis could be repressing maximal hepcidin response to iron, thereby increasing dietary iron absorption and worsening the liver injury. As in hereditary hemochromatosis, the relative lack of hepcidin induction by iron in chronic hepatitis results in chronic hyperabsorption of dietary iron. Excess iron accumulates particularly in the liver due to the avid uptake of non-transferrin-bound iron (NTBI) by hepatocytes, as well as the first-pass effect of portal circulation from the gut. The iron deposition is often parenchymal and compounds preexisting liver injury from hepatitis, worsening disease prognosis. In chronic hepatitis C (CHC), iron correlates with development of cirrhosis and hepatocellular carcinoma (HCC).[11] The role of iron in disease progression has been supported by studies in which phlebotomy improved disease indices in nonalcoholic steatohepatitis and CHC.[31,32] However, the effects of iron on hepatitis C may be complex; excess iron promotes tissue damage but it also suppresses viral replication, perhaps accounting for the divergent outcomes of phlebotomy interventions.[33]

Regulation of hepcidin by growth factors may be important for normal iron homeostasis as well. Hepcidin must be physiologically suppressed during early years of life, when continuing growth and development require greater iron absorption than in the mature adult.[34] Although few studies exist of hepcidin levels in children and adolescents, a recent study in children and adult patients undergoing hemodialysis found that the pediatric control group had serum hepcidin concentrations that were only a third as high as the adult control group.[35] Interestingly, hepatic hepcidin mRNA is not detectable by northern blot in mice from embryonic day 15.5 to postnatal day 56 apart from a transient induction at birth extending to postnatal day 2.[36] Hepcidin expression, therefore, only reaches a high level in the adult mouse liver, concordant with the human studies suggesting that hepcidin is repressed during early growth and maturation.

Finally, better understanding of the pathways that mediate hepcidin suppression may help identify useful targets for new treatments for iron restrictive disorders (anemia of inflammation, anemia of chronic kidney disease) in which hepcidin excess contributes to the pathogenesis of anemia and to erythropoietin resistance.

Acknowledgment: We thank Victoria Gabayan for excellent technical assistance with all the mouse studies.

References

1. Ganz T, Nemeth E. Hepcidin and disorders of iron metabolism. Annu Rev Med 2011;62:347-360.
2. Ramos E, Kautz L, Rodriguez R, Hansen M, Gabayan V, Ginzburg Y, et al. Evidence for distinct pathways of hepcidin regulation by acute and chronic iron loading in mice. HEPATOLOGY 2011;53:1333-1341.
3. Corradini E, Meynard D, Wu Q, Chen S, Ventura P, Pietrangelo A, et al. Serum and liver iron differently regulate the bone morphogenetic protein 6 (BMP6)-SMAD signaling pathway in mice. HEPATOLOGY 2011;54:273-284.
4. Babitt JL, Huang FW, Xia Y, Sidis Y, Andrews NC, Lin HY. Modulation of bone morphogenetic protein signaling in vivo regulates systemic iron balance. J Clin Invest 2007;117:1933-1939.
5. Meynard D, Kautz L, Darnaud V, Canonne-Hergaux F, Coppin H, Roth MP. Lack of the bone morphogenetic protein BMP6 induces massive iron overload. Nat Genet 2009;41:478-481.
6. Andriopoulos B Jr, Corradini E, Xia Y, Faasse SA, Chen S, Grgurevic L, et al. BMP6 is a key endogenous regulator of hepcidin expression and iron metabolism. Nat Genet 2009;41:482-487.
7. Kautz L, Meynard D, Monnier A, Darnaud V, Bouvet R, Wang RH, et al. Iron regulates phosphorylation of Smad1/5/8 and gene expression of Bmp6, Smad7, Id1, and Atoh8 in the mouse liver. Blood 2008;112:1503-1509.
8. Girelli D, Pasino M, Goodnough JB, Nemeth E, Guido M, Castagna A, et al. Reduced serum hepcidin levels in patients with chronic hepatitis C. J Hepatol 2009;51:845-852.
9. Fujita N, Sugimoto R, Takeo M, Urawa N, Mifuji R, Tanaka H, et al. Hepcidin expression in the liver: relatively low level in patients with chronic hepatitis C. Mol Med 2007;13:97-104.
10. Nishina S, Hino K, Korenaga M, Vecchi C, Pietrangelo A, Mizukami Y, et al. Hepatitis C virus-induced reactive oxygen species raise hepatic iron level in mice by reducing hepcidin transcription. Gastroenterology 2008;134:226-238.
11. Lambrecht RW, Sterling RK, Naishadham D, Stoddard AM, Rogers T, Morishima C, et al. Iron levels in hepatocytes and portal tract cells predict progression and outcomes of patients with advanced chronic hepatitis C. Gastroenterology 2011;140:1490-1500.
12. Bhave VS, Paranjpe S, Bowen WC, Donthamsetty S, Bell AW, Khillan JS, et al. Genes inducing iPS phenotype play a role in hepatocyte survival and proliferation in vitro and liver regeneration in vivo. HEPATOLOGY 2011;54:1360-1370.
13. Factor VM, Seo D, Ishikawa T, Kaposi-Novak P, Marquardt JU, Andersen JB, et al. Loss of c-Met disrupts gene expression program required for G2/M progression during liver regeneration in mice. PLoS ONE 2010;5.
14. Fausto N. Liver regeneration. J Hepatol 2000;32:19-31.
15. Maes K, Nemeth E, Roodman GD, Huston A, Esteve F, Freytes C, et al. In anemia of multiple myeloma, hepcidin is induced by increased bone morphogenetic protein 2. Blood 2010;116:3635-3644.
16. Korchynskyi O, ten Dijke P. Identification and functional characterization of distinct critically important bone morphogenetic protein-specific response elements in the Id1 promoter. J Biol Chem 2002;277:4883-4891.
17. Pfaffl MW. A new mathematical model for relative quantification in real-time RT-PCR. Nucleic Acids Res 2001;29:e45.
18. Livak KJ, Schmittgen TD. Analysis of relative gene expression data using real-time quantitative PCR and the 2(-Delta Delta C(T)) method. Methods 2001;25:402-408.
19. Kawabata M, Miyazono K. Signal transduction of the TGF-beta superfamily by Smad proteins. J Biochem 1999;125:9-16.
20. Knockaert M, Sapkota G, Alarcon C, Massague J, Brivanlou AH. Unique players in the BMP pathway: small C-terminal domain phosphatases dephosphorylate Smad1 to attenuate BMP signaling. Proc Natl Acad Sci U S A 2006;103:11940-11945.
21. Onichtchouk D, Chen YG, Dosch R, Gawantka V, Delius H, Massague J, et al. Silencing of TGF-beta signalling by the pseudoreceptor BAMBI. Nature 1999;401:480-485.
22. Hata A, Lagna G, Massague J, Hemmati-Brivanlou A. Smad6 inhibits BMP/Smad1 signaling by specifically competing with the Smad4 tumor suppressor. Genes Dev 1998;12:186-197.
23. Imamura T, Takase M, Nishihara A, Oeda E, Hanai J, Kawabata M, et al. Smad6 inhibits signalling by the TGF-beta superfamily. Nature 1997;389:622-626.
24. Mleczko-Sanecka K, Casanovas G, Ragab A, Breitkopf K, Muller A, Boutros M, et al. SMAD7 controls iron metabolism as a potent inhibitor of hepcidin expression. Blood 2010;115:2657-2665.
25. Sapkota G, Alarcon C, Spagnoli FM, Brivanlou AH, Massague J. Balancing BMP signaling through integrated inputs into the Smad1 linker. Mol Cell 2007;25:441-454.
26. Moren A, Imamura T, Miyazono K, Heldin CH, Moustakas A. Degradation of the tumor suppressor Smad4 by WW and HECT domain ubiquitin ligases. J Biol Chem 2005;280:22115-22123.
27. Chaston TB, Matak P, Pourvali K, Srai SK, McKie AT, Sharp PA. Hypoxia inhibits hepcidin expression in HuH7 hepatoma cells via decreased SMAD4 signaling. Am J Physiol Cell Physiol 2011;300:C888-C895.
28. Kretzschmar M, Doody J, Massague J. Opposing BMP and EGF signalling pathways converge on the TGF-beta family mediator Smad1. Nature 1997;389:618-622.
29. Wotton D, Massague J. Smad transcriptional corepressors in TGF beta family signaling. Curr Top Microbiol Immunol 2001;254:145-164.

Author

30. Lo RS, Wotton D, Massague J. Epidermal growth factor signaling via Ras controls the Smad transcriptional co-repressor TGIF. EMBO J 2001;20:128-136.
31. Kato J, Miyanishi K, Kobune M, Nakamura T, Takada K, Takimoto R, et al. Long-term phlebotomy with low-iron diet therapy lowers risk of development of hepatocellular carcinoma from chronic hepatitis C. J Gastroenterol 2007;42:830-836.
32. Fargion S, Valenti L, Fracanzani AL. Beyond hereditary hemochromatosis: new insights into the relationship between iron overload and chronic liver diseases. Dig Liver Dis 2011;43:89-95.
33. Mueller S. Increased iron in HCV infection: collateral damage or antiviral defense? J Hepatol 2010;53:990-992.
34. Lonnerdal B, Kelleher SL. Iron metabolism in infants and children. Food Nutr Bull 2007;28:S491-S499.
35. Zaritsky J, Young B, Gales B, Wang HJ, Rastogi A, Westerman M, et al. Reduction of serum hepcidin by hemodialysis in pediatric and adult patients. Clin J Am Soc Nephrol 2010;5:1010-1014.
36. Nicolas G, Bennoun M, Porteu A, Mativet S, Beaumont C, Grandchamp B, et al. Severe iron deficiency anemia in transgenic mice expressing liver hepcidin. Proc Natl Acad Sci U S A 2002;99:4596-4601.

Chapter 3

Chapter 3 is a published paper that describes *in vitro* studies of the hepcidin-ferroportin interaction and the initial tests of early hepcidin mimetics *in vivo*.

Summary

Chapter 3 details the structure-function analysis of the hepcidin-ferroportin interaction and the deduction of the minihepcidin scaffold that laid the foundation for the development of more potent minihepcidins described in Chapter 2. The rational design of hepcidin mimetics was made possible by studies that identified the amino acid residues necessary for hepcidin and ferroportin to interact.

Deletion of ferroportin is embryonic lethal in zebrafish and mice (1,2), but the study of disease-causing ferroportin mutations was crucial to indentifying important ferroportin functional domains. Loss of function mutations in which iron export through ferroportin is reduced or gain of function due to hepcidin insensitivity have been observed (3). In particular, mutation of ferroportin cysteine 326 mild elevation of plasma iron and iron deposition in the liver (4) due to its inability to bind hepcidin (5).

We aimed to identify other important ferroportin residues within the vicinity of C326 as well as the hepcidin residues that bind to this region. Important ferroportin residues were identified by creating a series of ferroportin constructs containing sequential alanine or conservative amino acid substitutions from residues 324-343 and measuring radioactive hepcidin binding. Hepcidin residues were identified by synthesizing fragments of the N-terminus with alanine substitutions and measuring their ability to degrade ferroportin in cell lines. We found that aromatic and hydrophobic residues, as well as cysteine, conferred the hepcidin ferroportin interaction.

Certain synthetic hepcidin fragments displayed *in vitro* activity and were modified to increase potency and stability *in vivo*. My contribution to this work was to characterize the *in vivo* potency of hepcidin and minihepcidin peptides in WT and hemochromatotic mice.

References

1. Donovan A, Brownlie A, Zhou Y, Shepard J, Pratt SJ, Moynihan J, et al. Positional cloning of zebrafish ferroportin1 identifies a conserved vertebrate iron exporter. Nature. 2000;403:776–781.

2. Donovan A, Lima CA, Pinkus JL, Pinkus GS, Zon LI, Robine S, et al. The iron exporter ferroportin/Slc40a1 is essential for iron homeostasis. Cell Metab. 2005;1:191–200.

3. Drakesmith H, Schimanski LM, Ormerod E, Merryweather-Clarke AT, Viprakasit V, Edwards JP, et al. Resistance to hepcidin is conferred by hemochromatosis-associated mutations of ferroportin. Blood. 2005;106:1092–1097.

4. Sham RL, Phatak PD, West C, Lee P, Andrews C, Beutler E. Autosomal dominant hereditary hemochromatosis associated with a novel ferroportin mutation and unique clinical features. Blood Cells, Molecules, and Diseases. 2005;34:157–161.

5. Fernandes A, Preza GC, Phung Y, De Domenico I, Kaplan J, Ganz T, et al. The molecular basis of hepcidin-resistant hereditary hemochromatosis. Blood. 2009;114:437–443.

Research article

Minihepcidins are rationally designed small peptides that mimic hepcidin activity in mice and may be useful for the treatment of iron overload

Gloria C. Preza,[1] Piotr Ruchala,[2] Rogelio Pinon,[2] Emilio Ramos,[3] Bo Qiao,[2] Michael A. Peralta,[4] Shantanu Sharma,[5] Alan Waring,[2,6] Tomas Ganz,[1,2] and Elizabeta Nemeth[2]

[1]Department of Pathology, [2]Department of Medicine, and [3]Department of Chemistry and Biochemistry, UCLA, Los Angeles, California, USA. [4]Department of Chemistry, Columbia University, New York, New York, USA. [5]Materials and Process Simulation Center, California Institute of Technology, Pasadena, California, USA. [6]Department of Physiology and Biophysics, School of Medicine at the University of California, Irvine, Irvine, California, USA.

Iron overload is the hallmark of hereditary hemochromatosis and a complication of iron-loading anemias such as β-thalassemia. Treatment can be burdensome and have significant side effects, and new therapeutic options are needed. Iron overload in hereditary hemochromatosis and β-thalassemia intermedia is caused by hepcidin deficiency. Although transgenic hepcidin replacement in mouse models of these diseases prevents iron overload or decreases its potential toxicity, natural hepcidin is prohibitively expensive for human application and has unfavorable pharmacologic properties. Here, we report the rational design of hepcidin agonists based on the mutagenesis of hepcidin and the hepcidin-binding region of ferroportin and computer modeling of their docking. We identified specific hydrophobic/aromatic residues required for hepcidin-ferroportin binding and obtained evidence in vitro that a thiol-disulfide interaction between ferroportin C326 and the hepcidin disulfide cage may stabilize binding. Guided by this model, we showed that 7–9 N-terminal amino acids of hepcidin, including a single thiol cysteine, comprised the minimal structure that retained hepcidin activity, as shown by the induction of ferroportin degradation in reporter cells. Further modifications to increase resistance to proteolysis and oral bioavailability yielded minihepcidins that, after parenteral or oral administration to mice, lowered serum iron levels comparably to those after parenteral native hepcidin. Moreover, liver iron concentrations were lower in mice chronically treated with minihepcidins than those in mice treated with solvent alone. Minihepcidins may be useful for the treatment of iron overload disorders.

Introduction

Hepcidin is a peptide hormone that mediates systemic iron homeostasis in vertebrates (1). Hepcidin controls plasma iron concentrations by inhibiting dietary iron absorption and release of recycled iron from macrophages. The hormone acts by inducing the endocytosis of its receptor ferroportin, the sole known cellular exporter of iron. Hepcidin deficiency causes or contributes to iron overload in several diseases, including hereditary hemochromatosis (2, 3), β-thalassemia (4, 5), and chronic hepatitis C (6, 7).

Current treatment modalities for iron overload include phlebotomy and iron chelation. Phlebotomy is a relatively inexpensive and effective treatment for hereditary hemochromatosis but is not satisfactory for all patients. Some patients do not tolerate phlebotomy because of concurrent anemia, poor vascular access, adverse physiological responses to phlebotomy, fears, religious beliefs, and the lack of long-term convenient access to phlebotomy centers (8). Even the patients who are compliant with phlebotomy treatment may prefer oral therapy if it were available.

In β-thalassemia, phlebotomy is generally not feasible because it worsens anemia, and iron overload is treated by regular chelation (9). Iron chelators have side effects ranging from mild to very serious, and compliance is often suboptimal. Iron overload remains a major cause of morbidity and mortality in β-thalassemia.

Additional therapeutic options are clearly desirable. Given the causal role of hepcidin deficiency in the development of iron overload, replacement of hepcidin would be a rational approach to the prevention and treatment of iron overload in these disorders (10). However, the use of natural hepcidin as a potential replacement therapy in hepcidin-deficient conditions has major limitations. Bioactive hepcidin is 25–amino acids long and has 4 disulfide bonds, rendering the production of a correctly folded full-length hepcidin expensive. The half-life of natural hepcidin is very short (11) due to its rapid renal excretion. Furthermore, peroral absorption of hepcidin would be low due to its large size (~2.7 kDa). In search of alternatives to full-length hepcidin, we carried out a structure-function analysis of the hepcidin-ferroportin interface. Based on this information, we developed a series of 7– to 9–amino acid peptides, "minihepcidins," that mimic the activity of hepcidin in cell-based bioassays and in mice. Our findings establish the feasibility of small, drug-like hepcidin agonists for the treatment of iron overload disorders due to hepcidin deficiency.

Conflict of interest: Tomas Ganz and Elizabeta Nemeth are officers and shareholders in Intrinsic LifeSciences, a company engaged in the development of iron-related diagnostic products.

Citation for this article: *J Clin Invest.* 2011;121(12):4880–4888. doi:10.1172/JCI57693.

Results

Definition of the extracellular loop of ferroportin involved in hepcidin binding

We previously showed that an extracellular ferroportin residue, C326, is essential for hepcidin binding (12), but the extent of the extracellular loop surrounding C326 was not known. In the 2 published models of ferroportin topology, the extracellular loop containing C326 spans the region from D325 to S342 (13) or F316 to T334 (14). We subjected the proposed ends of the extracellular loop to cysteine-scanning mutagenesis. In WT ferroportin, C326 and possibly C205 have extracellular location (13). Because of that, a double mutant (C205S/C326S) of human ferroportin-GFP was used as a template for site-directed mutagenesis to introduce cysteines in multiple positions between M312 and L345. To determine which of the newly introduced cysteines were located on the cell surface, HEK293T cells were transfected with plasmids encoding control or mutant ferroportin-GFP and biotinylated using nonpermeable, sulfhydryl (SH)-reactive biotin-maleimide. Streptavidin-peroxidase probing of SDS-PAGE blots of immunoprecipitated ferroportin-GFP showed that, as expected, WT ferroportin-GFP but not the C205S/C326S double mutant was biotinylated (Figure 1A). Ferroportin mutants with cysteine substitutions in the region between M312 and L322 and between I344-L345 were expressed on the plasma membrane (Figure 1B) but were not biotinylated, suggesting that these residues are located in a transmembrane (or intracellular) region. In contrast, G323, F324, T334C, S338C, S340C, and S343C mutant ferroportins were all biotinylated, demonstrating their extracellular location and indicating that the extracellular loop containing C326 likely extends from G323 to S343.

A previous study (15) described the F324-S343 ferroportin region as the hepcidin-binding domain (HBD) and reported that a synthetic peptide corresponding to the HBD interacts with hepcidin in a manner similar to that of the membrane-associated cellular ferroportin. However, in our studies, the synthetic HBD peptide (RR-FDCITTGYAYTQGLSGSILS-RR) did not bind hepcidin specifically. As analyzed by surface plasmon resonance, synthetic human hepcidin interacted equally with the WT and C326S HBD peptide (Supplemental Figure 1A; supplemental material available online with this article; doi:10.1172/JCI57693DS1) or with unalkylated and alkylated HBD (data not shown). In contrast, similar modifications to ferroportin have dramatic effects on hepcidin binding (12). Any interactions that were observed between human hepcidin and HBD were nonspecific and probably due to hepcidin aggregating readily on a variety of surfaces (Supplemental Figure 1B). The reverse configuration, in which hepcidin was coated on the chip and HBD was in fluid phase, did not result in any binding (Supplemental Figure 1C). The results indicate that the synthetic F324-S343 peptide does not bind hepcidin specifically and that the segment does not function as an autonomous HBD.

Ferroportin residues in the vicinity of C326 also participate in hepcidin binding

To determine whether ferroportin residues other than C326 contribute to hepcidin binding, we mutagenized to alanine each residue in the C326 extracellular loop of WT human ferroportin (Fpn)-GFP except for A332, which was substituted with D (aspartate). HEK293T cells were transfected with the ferroportin mutants, and the uptake of radiolabeled hepcidin was measured. To account for the variability of transfection efficiency, radioactive counts were normalized to the expression of ferroportin-GFP as determined by Western blotting. D325A protein was expressed at very low levels, and we therefore tested the mutant D325N, which had a normal level of expression. Remarkably, substitutions in the first half of the extracellular loop markedly reduced hepcidin binding, whereas mutations in the second half did not interfere with hepcidin binding (Figure 1C). However, a reduction in hepcidin binding by a specific mutation may occur not only because the residue is involved in contacting hepcidin but because of mistrafficking of the mutant protein or because of a conformational change, leading to reduced accessibility of the binding site containing C326. To address these possibilities, we used SH-reactive biotin-maleimide to biotinylate cells transfected with the ferroportin-GFP mutants from Figure 1C. The mutations that reduced hepcidin binding without affecting the accessibility of C326 were F324A and Y333A but not D325N, I327A, and A332D (Figure 1D). Thus, F324 and Y333 likely make direct contact with hepcidin. The fluorescence microscopy images of the mutants' cellular localization are shown in Supplemental Figure 2.

Identification of hepcidin residues critical for binding to ferroportin

We showed previously that deletion of the 5 N-terminal residues of hepcidin ablated the ability of the peptide to cause ferroportin degradation (16). By substituting individual N-terminal residues (residues 1–6 and 8), we also showed that H3, F4, and I6 were important for the peptide activity and that those positions required hydrophobic side chains for interaction with ferroportin (17). Here, we mutagenized the next large hydrophobic residue, F9. Substitutions of F9 with alanine or cyclohexylalanine (a nonaromatic hydrophobic residue) resulted in 100- and 10-fold reduced activity respectively, suggesting that position 9 requires an aromatic side chain (Figure 2A).

Because our previous study on the ferroportin thiol residue C326-SH (12) indicated that disulfide bond formation may occur during hepcidin-ferroportin interaction, we next focused on the effect of individual disulfide bond substitutions on hepcidin peptide activity. Although we previously partially explored this question (16), the hepcidin structure has since been revised (18), and we generated synthetic hepcidin mutants in which we substituted pairs of cysteines with alanines according to the revised connectivity (C7A/C23A, C10A/C13A, C11A/C19A, C14A/C22A). A dose-response analysis of the mutant peptide activity (Figure 2B) showed that all these mutants had a similar decrease in activity (up to 100 fold). Circular dichroism spectroscopy indicated that the mutant peptides had slightly more disordered structure than the native peptide (Supplemental Figure 3), perhaps partially accounting for the diminished activity. Given that none of the mutants displayed a complete loss of activity, the result suggests that if disulfide exchange is involved in hepcidin binding, more than one disulfide bond could participate in exchange with C326-SH on ferroportin.

RosettaDock computer modeling

To gain further insight into the hepcidin-ferroportin interaction, we performed computer modeling. The input structures were the full-length hepcidin (PDB 2KEF), with the most recent disulfide bond assignment (18), and a region of ferroportin (residues 306–362) encompassing the C326 extracellular loop and flanking transmembrane helices, with structure based on a recently developed theoretical model of ferroportin molecule (19). Ferroportin and hepcidin structures were refined using HyperChem 7.5 and GROMACS

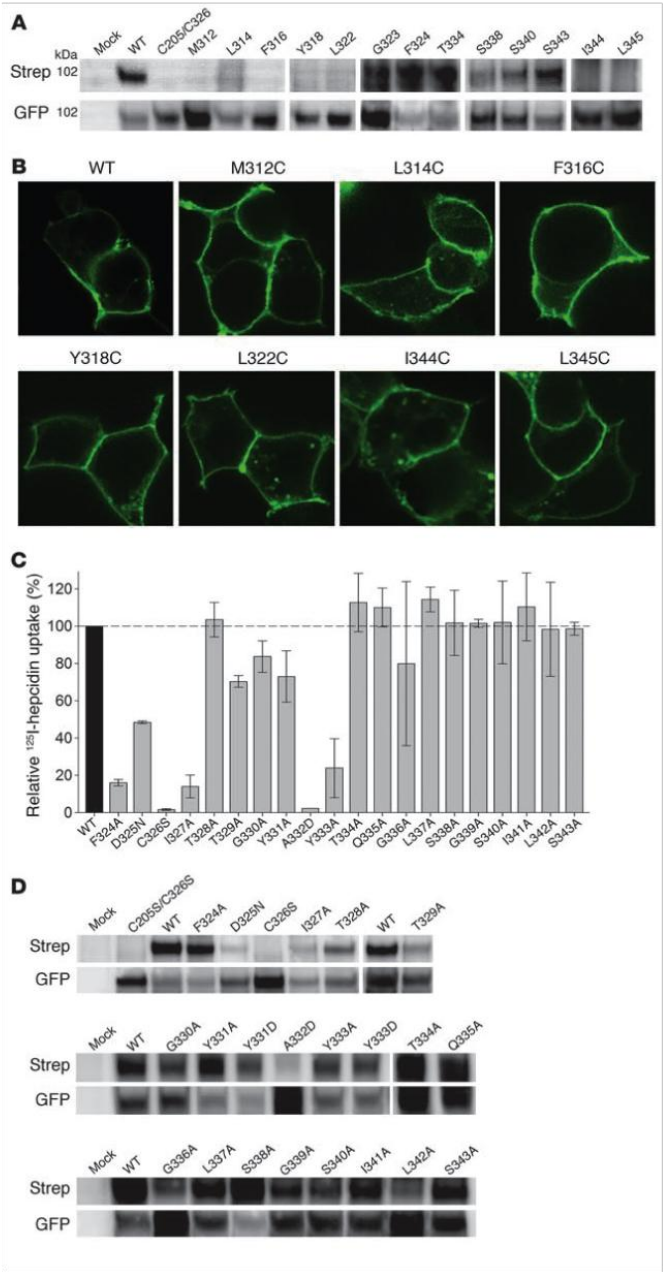


Figure 1
Defining the hepcidin-binding loop on ferroportin. (**A**) To detect the boundaries of the C326-containing extracellular loop, certain residues between M312 and L345 on the human Fpn-GFP C205S/C326S mutant were substituted with cysteine. Mutant constructs were transfected into HEK293T cells, and cell-surface biotinylation was performed using a nonpermeable, SH-reactive biotin-maleimide. Protein lysates were immunoprecipitated with anti-GFP antibody, analyzed by SDS-PAGE, blotted, and probed with streptavidin-peroxidase to determine which mutated residues had extracellular localization. The bottom row indicates the amount of Fpn-GFP that was immunoprecipitated. Each mutant was tested in at least 3 separate experiments. (**B**) Confocal microscopy of HEK293 cells transfected with cysteine substitution mutants. Mutant proteins M312C, L314C, F316C, Y318C, L322C, I344, and L345 were all displayed on the cell surface similar to WT ferroportin-GFP, indicating that mistrafficking was not the reason for the absence of cell-surface biotinylation in **A**. Original magnification, ×63. (**C**) To define the contribution of residues in the C326 extracellular loop to hepcidin binding, alanine-scanning mutagenesis and other substitutions were performed as indicated. After transfection of HEK293T cells, cellular uptake of ^{125}I-hepcidin was determined and normalized to the Fpn-GFP levels in each sample, determined by Western blotting. Each bar represents the average of 3 to 4 separate experiments, and error bars indicate standard deviation. (**D**) Cell-surface biotinylation of constructs from **C**. Of the mutants that showed decreased hepcidin uptake, only F324A and Y333A mutants had thiol-specific biotinylation similar to that of WT Fpn-GFP, whereas others (D325N, I327A, A332D) had decreased cell-surface thiol-biotinylation, suggesting that these mutants may be mistrafficked or that a conformational change may be blocking the C326-SH accessibility.

before docking studies. The initial stage docking program ZDOCK (20) was first used to identify the lowest energy conformer set, and this ensemble was optimized using the RosettaDock program (21). The RosettaDock refinement run generated 1,000 structures whose energy scores were plotted versus the root mean square distance from the starting input conformation (Figure 3A). The plot showed the optimal energetic "funnel" of low-energy structures. The 10 best-scoring low-energy structures all had the N terminus of hepcidin as the part forming the interface with ferroportin. Of those 10 structures, the conformation most compat-

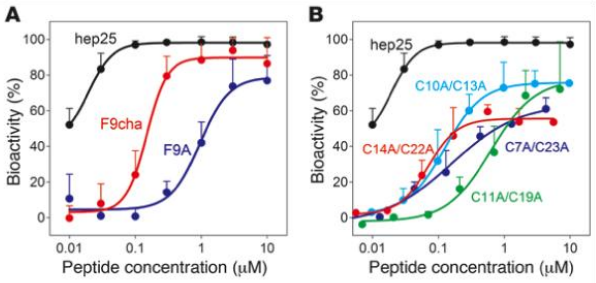


Figure 2
Hepcidin amino acid residues important for binding to ferroportin. Full-length 25–amino acid hepcidin variants were prepared by chemical synthesis and oxidatively refolded. The peptide activity was measured by a flow cytometry–based assay detecting ferroportin-GFP degradation. (**A**) F9 substitution with nonaromatic cyclohexylalanine (cha) or alanine caused a 10- and 100-fold decrease in peptide activity. (**B**) Pairwise substitutions of cysteines with alanines to remove individual disulfide bonds reduced bioactivity to a similar extent. Each data point is the average of 3 to 4 individual experiments and error bars indicate SD.

ible with our mutagenesis data (second-lowest energy structure) was used as the final hypothetical model of the ferroportin-hepcidin complex (Figure 3B and Supplemental Figure 4).

The model highlighted that aromatic and hydrophobic side chain interactions can drive the hepcidin-ferroportin interaction (Supplemental Table 1). In the model, H3, F4, and I6 of hepcidin formed a hydrophobic pocket for the interaction with Y333 of ferroportin, and F9 of hepcidin interacted with F324 of ferroportin through pi-stacking, in agreement with our mutagenesis data. The model also positioned the C326 residue in close proximity to the hepcidin disulfide framework.

Minihepcidins display agonist activity

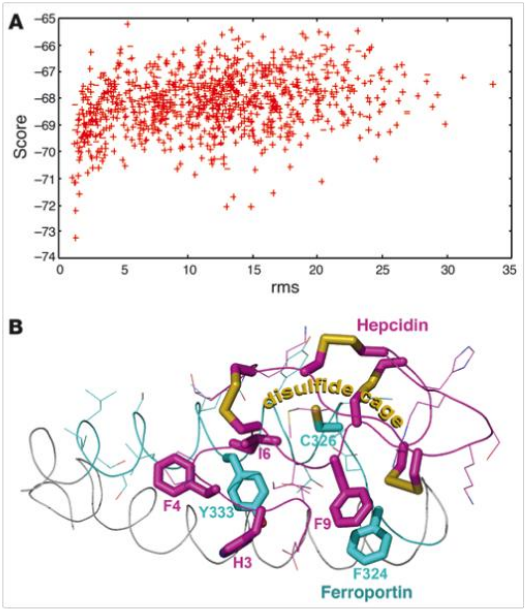
The mutagenesis approach as well as RosettaDock modeling suggested that hepcidin residues important for binding to ferroportin are located at the highly conserved N terminus of the peptide and prominently include residues H3, F4, I6, and F9. We thus synthesized short peptides (minihepcidins), consisting of up to 9 N-terminal amino acids of hepcidin (Supplemental Table 2), and tested their ability to cause ferroportin-GFP degradation in the cellular bioassay. These first generation minihepcidins showed substantial agonist activity (Figure 4), although they were less potent than the full-length hepcidin (EC_{50} = 9 nM). The minihepcidin containing 9 N-terminal residues (hep9, DTHFPICIF; EC_{50} = 76 nM; Supplemental Figure 5) was more active than shorter minihepcidins.

Figure 3
A RosettaDock model of the interaction between hepcidin and the ferroportin loop surrounding C326. (**A**) Plot of the full set of 1,000 structures generated in the RosettaDock refinement run. The energy score versus the root mean square (rms) distance from the starting structure shows the optimal energetic funnel of low-energy structures clustered around a single position. The plot indicates that the docking algorithm has reached a good local minimum and that the lowest scoring (lowest free energy) structures are the most stable. The second-lowest energy structure was most compatible with our mutagenesis data and is presented in **B**. (**B**) Hepcidin sequence is shown in pink, with yellow disulfide connectivities. Ferroportin extracellular loop is shown in cyan, transmembrane helices are shown in gray, and the sulfur of C326 is shown in yellow. The strongly interacting side chain pairs are displayed in thicker lines. Hydrogens are not shown. The model identified hydrophobic interactions between H3, F4, and I6 on hepcidin and Y333 on ferroportin and pi-stacking interaction between F9 and F324. The interaction of aromatic residues on the hepcidin and ferroportin surfaces brings C326 close to the disulfide network of hepcidin (disulfide cage), raising the possibility of transient disulfide exchange.

Thiol cysteine is required for minihepcidin activity

Because our previous study showed that a thiol form of the C326 residue on ferroportin was necessary for hepcidin binding and that the mutant with isosteric substitution C326S did not bind hepcidin in vitro (12) and caused hepcidin resistance in vivo (22), we hypothesized that a disulfide exchange between C326 and the disulfide framework of hepcidin may occur upon hepcidin binding to ferroportin. To determine whether disulfide bonding could also be involved in minihepcidin binding to ferroportin, we tested the requirement for cysteine on minihepcidin by mutating the C7 residue of hep9. We found that the activity of hep9 depended on its ability to participate in disulfide exchange. Isosteric substitution with serine (C7S) or blocking of C7 thiol with a t-butyl group (C7-S-t-but), which prevents disulfide exchange, ablated the agonist activity of hep9 (Figure 5A). However, the activity was considerably preserved when the blocking group was disulfide linked to C7 (C7-SS-t-but) and was therefore capable of disulfide exchange.

These results strongly suggest that the minihepcidin-ferroportin interaction is dependent on the thiol-thiol interaction or



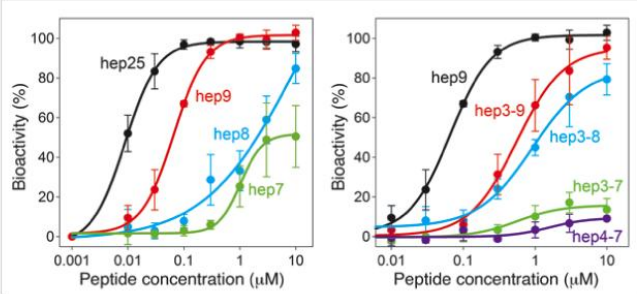


Figure 4
Minihepcidins are effective hepcidin agonists. The activity of synthetic minihepcidins was determined by flow cytometric quantitation of ferroportin-GFP degradation in stably transfected HEK293 cells. Each point is an average of 5 to 6 experiments and error bars indicate SD. hep8, DTHFPICI; hep7, DTHFPIC; hep3-9, HFPICIF; hep3-8, HFPICI; Hep3-7, HFPIC; Hep4-7, FPIC.

disulfide formation and that the hepcidin-ferroportin interaction could involve disulfide exchange. To further examine this, we tested whether the hepcidin-ferroportin complex is affected by reducing agents. In our previous experiments, we noted that ^{125}I-hepcidin forms a complex with ferroportin that does not dissociate during protein extraction, immunoprecipitation, and SDS-PAGE. However, this complex readily dissociated in the presence of DTT (Figure 5B), supporting the possibility of hepcidin-ferroportin disulfide exchange.

Design and in vitro bioassay of minihepcidins

In order to optimize the agonist activity, we designed additional minihepcidins of varying lengths and structural modifications (Supplemental Table 2). All peptides were synthesized as carboxyamides (-$CONH_2$) to make their C terminus similar to the corresponding intact hepcidin segment. The peptide activity was tested in a cellular bioassay in vitro, measuring their ability to cause degradation of ferroportin-GFP (16).

Substitution or stabilization of the C7 thiol group in hep9 decreases bioactivity. To increase the stability of minihepcidins, we synthesized circular peptides by introducing an internal disulfide bond with C7. We also modified the size and reactivity of the amino acid corresponding to C7 by introducing various cysteine analogs at that position. All of these cysteine analogs showed decreased bioactivity relative to that of hep9.

Retro-inverso minihepcidins are bioactive. To increase the resistance of minihepcidins to proteolysis in vivo, we introduced unnatural amino acids (chemical structures shown in Supplemental Table 3) or synthesized retro-inverso analogs. Retro-inverso peptides are composed of D-amino acids assembled in the reverse order from that of the parent L-peptide sequence, making them sterically similar to the original but much more resistant to proteolysis. Retro-inverso hep9 analog (ri-hep9, FICIPFHTD) and retro-inverso hep3-9 (ri-hep3-9, FICIPFH) caused ferroportin degradation in vitro, although with several fold lower activity than that of hep9.

Effects of other peptide modifications. Additional peptide variants were pegylated in order to increase solubility, reduce immunogenicity, and increase circulatory time by reducing renal clearance. To increase the intestinal uptake of minihepcidins via enterohepatic circulation of bile acids, the pegylated retro-inverso hep9 was conjugated with chenodeoxycholic or ursodeoxycholic bile acids (cheno-ri-hep9 and urso-ri-hep9). Cheno-ri-hep9 had similar activity in vitro to that of unmodified hep9, while urso-ri-hep9 had 10-fold lower activity. We also synthesized retro-inverso hep9 conjugated to palmitoyl groups because palmitoylation of peptides could increase intestinal absorption, reduce renal excretion through increased binding to albumin, and potentially increase affinity for cell membranes (23). Singly palmitoylated retro-inverso hep9 (palmitoyl-ri-hep9) was as active as hep9, but the peptide with 2 palmitoyl groups had no activity. Beta-propeller and collagen domain modifications, designed to multimerize minihepcidins and thereby reduce their renal excretion, resulted in inactive minihepcidins.

Minihepcidins induce hypoferremia in mice

Several of the peptides that were most active in vitro were selected for testing in mice. Although our minihepcidins were derived from the human sequence, the human hepcidin is active in the mouse presumably because of the high degree of identity between mouse and human sequences of hepcidin and ferroportin. Selected ana-

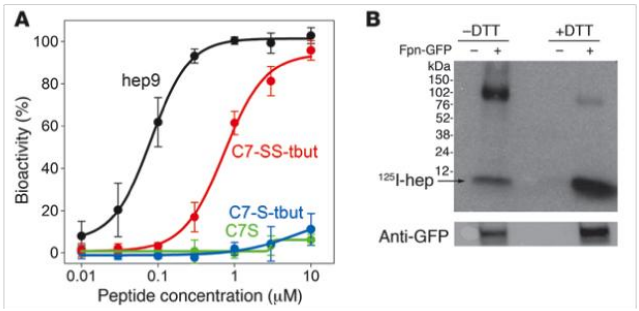


Figure 5
Evidence for the role of disulfide exchange in the hepcidin-ferroportin interaction. (**A**) The agonist activity of minihepcidin depends on its thiol reactivity. Hep9 was modified at residue C7; C7-SS-tbut contains an exchangeable tert-butyl group disulfide-linked to C7; C7-S-tbut contains a tert-butyl group in a thioether linkage to C7, which prevents disulfide exchange; and C7S contains a serine in position 7 instead of a cysteine. Each data point is the average of 3 to 4 individual experiments and error bars indicate SD. (**B**) Reducing agents disrupt ^{125}I-hepcidin association with Fpn-GFP. ^{125}I-hepcidin (^{125}I-hep) was added to cells expressing ferroportin-GFP for 15 minutes, and total cellular protein was immunoprecipitated using anti-GFP antibody. The sample was split into 2 identical aliquots, and DTT was added to 1 of the aliquots (final concentration 100 mM). The amount of immunoprecipitated Fpn-GFP was determined by Western blotting. Similar experiments were performed at least 5 times.

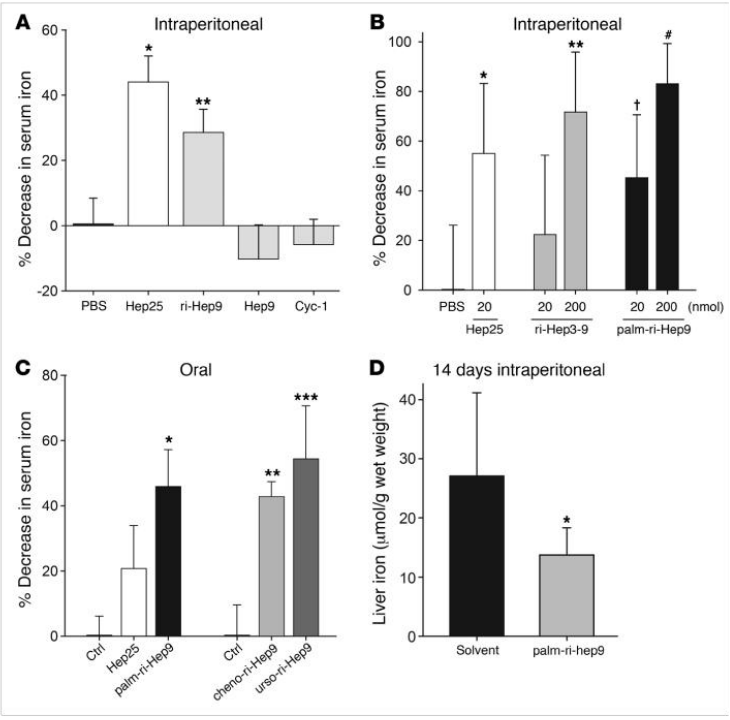


Figure 6
Bioactivity of parenteral and oral minihepcidins in mice. (**A**) Full-length hepcidin (20 nmoles), minihepcidins (200 nmoles), or diluent were injected intraperitoneally (n = 6 animals per treatment), mice were euthanized after 4 hours, and nonheme iron levels were determined in serum. ri-hep9, retro-inverso hep9; Cyc-1, minihepcidin with a disulfide bond (CDTHFPICIF). *P = 0.003 and **P = 0.035 in comparison with control mice. (**B**) Full-length hepcidin (20 nmoles), minihepcidins (20 and 200 nmoles), or diluent were injected intraperitoneally into mice (n = 5–7 per treatment), and their serum iron was measured after 4 hours. ri-hep3-9, retro-inverso HFPICIF. *P = 0.02; **P = 0.002; †P = 0.015; #P < 0.001. (**C**) Peptides (200 nmoles) or diluent were administered orally by gavage, and serum iron measured was after 4 hours. The results are expressed as the percentage of decrease in serum iron as compared with the serum iron levels in PBS-treated mice to normalize for the variations in absolute serum iron levels between experiments. *P = 0.006; **P = 0.003; ***P = 0.01. (**D**) Hepcidin-1 knockout mice were injected intraperitoneally with palm-ri-hep9 (100 nmoles per mouse; n = 7) or diluent (n = 6) daily for 2 weeks. Liver iron content was measured on day 15. *P = 0.03. Error bars represent SD.

logs were injected intraperitoneally into mice, and a decrease in serum iron was measured 4 hours after injection. Control mice were treated with the diluent or with 20 nmoles human hep25 (~50 μg per mouse). Even at 10-times higher concentrations, minihepcidin hep9 had no effect on serum iron levels, presumably because it was rapidly degraded, but a more stable retro-inverso hep9 showed significant activity (P = 0.028; Figure 6A). Minihepcidins conjugated to fatty or bile acids were even more active. Injection of 20 nmoles palmitoyl-ri-hep9 caused almost as large a decrease in serum iron levels as the equivalent dose of hep25 (Figure 6B). Importantly, when the cysteine residue in palmitoyl-ri-hep9 was substituted with serine, no serum iron decrease was observed (Supplemental Figure 6). Injection of a higher dose of palmitoyl-ri-hep9 (200 nmoles) caused more profound hypoferremia than did injection of hep25, with an 80% drop in serum iron (Figure 6B). Even a 7–amino acid retro-inverso peptide (ri-hep3-9; Figure 6B) was bioactive after parenteral injection, causing a 70% decrease in serum iron at 200 nmoles. The decrease in serum iron was not a consequence of the induction of endogenous hepcidin, as murine hepatic hepcidin-1 mRNA levels measured by qRT-PCR were not increased in agonist-treated mice compared with those in controls (Supplemental Figure 7).

Selected minihepcidins are bioactive when administered by gavage

In many situations, the most desirable method of drug delivery is by the peroral route. To test whether minihepcidins administered orally would exert a hypoferremic effect, we gavaged mice with 200 nmoles retro-inverso hep9 that was palmitoylated or conjugated to bile acids (chenodeoxycholic or ursodeoxycholic acid). All 3 minihepcidins caused a significant decrease in serum iron compared with that in controls gavaged with diluent or with Hep25 (Figure 6C).

Minihepcidins prevent liver iron overload in hepcidin-1 knockout mice

In a proof-of-principle experiment, we examined the chronic effect of minihepcidin injections on liver iron accumulation in a mouse model of hereditary hemochromatosis. We chose hepcidin-1 knockout mice to eliminate any possibility of endogenous hepcidin contributing to the regulation of iron loading. *Hepc1*$^{-/-}$ animals were injected parenterally with palmitoyl-ri-hep9 (100 nmoles; n = 7) or diluent (n = 6) daily for 2 weeks. The end point hemoglobin (15 ± 2 g/dl and 15.9 ± 1.5 g/dl in palmitoyl-ri-hep9 and control group, respectively) and other hematological parameters were similar between the 2 groups of mice, indicating that minihepcidin injections did not cause iron-restricted erythropoiesis. However, the nonheme iron concentration of the liver was significantly lower in animals treated with the minihepcidin (13.7 ± 4 μmoles/g wet weight) than that in those treated with diluent only (27.1 ± 13.7 μmoles/g wet weight) (P = 0.03; Figure 6D).

Discussion

In hereditary hemochromatosis, hepcidin deficiency is a consequence of destructive mutations in the genes encoding hepcidin (24) or one of its regulators, HFE (3) (most common), transferrin receptor 2 (25), or hemojuvelin (26). Hepcidin deficiency results

in excessive intestinal iron absorption and maldistribution of tissue iron. If severe and untreated, the disease can progress to cirrhosis, hepatocellular carcinoma, and endocrine and cardiac problems. In the US, about 0.4% of people of mixed European descent have hereditary hemochromatosis mutations that put them at risk for iron overload (27).

Iron overload also occurs in β-thalassemia, a disease that affects millions of patients whose origins are in the Mediterranean basin and Asia, regions historically affected by endemic malaria (28). In β-thalassemia, hepcidin is suppressed by increased erythropoietic activity through mechanisms that are still incompletely defined. In the absence of transfusions (β-thalassemia intermedia), hepcidin levels are very low (4, 5), and patients develop iron overload similar to that of severe hereditary hemochromatosis and may succumb to iron overload if untreated (29). In β-thalassemia major, transfusions rather than dietary iron absorption are the predominant cause of iron overload. Here, hepcidin levels are higher, because ineffective erythropoiesis is suppressed by transfusions and also because the additional iron load stimulates hepcidin production. However, in the intervals between transfusions, hepcidin concentrations progressively decrease toward the end of the interval (4, 5, 30), and this recurrent lowering of hepcidin may also contribute to iron overload in β-thalassemia major.

Milder hepcidin insufficiency is seen in chronic liver disease, including viral hepatitis (6, 7, 31). The cause of hepcidin suppression in these diseases is not yet clear, but the resulting chronic iron loading in the liver worsens the prognosis (32).

Therapeutic augmentation of hepcidin levels would be expected to curb hyperabsorption of dietary iron in these patients. The proof of this concept was achieved in mouse model of HFE hereditary hemochromatosis, in which the introduction of a hepcidin transgene into *Hfe*$^{-/-}$ mice prevented the development of iron overload (33). Hepcidin also causes redistribution of iron when iron overload is already established. Hepcidin induction in HFE-null mice carrying a Tet-inducible hepcidin construct did not acutely reverse the iron overload but did shift the excess iron from hepatocytes and other parenchymal cells to macrophages (34). Macrophages are relatively resistant to the toxic effects of iron (35), as demonstrated by the relatively benign course of "ferroportin disease," in which iron accumulates in macrophages. Most affected patients have no clinical manifestations, despite often severe iron overload (36). Thus, hepcidin-mediated redistribution of iron from parenchyma to macrophages in iron-overloaded patients could potentially limit iron toxicity in the heart, the pancreas, and the liver.

In addition to the beneficial effect of hepcidin on iron balance and distribution, recent studies suggest that hepcidin may also improve disordered erythropoiesis in β-thalassemia. Although the mechanism is still not understood, transgenic expression of hepcidin in a mouse model of β-thalassemia intermedia increased hemoglobin and decreased extramedullary erythropoiesis (37).

Using full-length hepcidin for the treatment of iron overload conditions would be expected to be expensive, not only because the synthesis and refolding of hepcidin with 4 disulfide bonds allows for a large number of alternative folds but also because of the relatively high dose required for its biological effect. Even assuming that hepcidin could be produced at a cost comparable to that of recombinant insulin, a typical dose of hepcidin would likely be many fold higher than that of insulin. In human patients with type 1 diabetes mellitus (and mouse models), a typical dose of insulin is 0.2–0.7 U/kg/d or 9–32 μg/kg/d (1 U is the biological equivalent of 45.5 μg pure crystalline insulin). A typical dose of hepcidin, on the other hand, is 50 μg/mouse/d or 2 mg/kg/d, which is nearly 100-times higher than the typical dose of insulin. Given the current limitations of peptide synthetic technology, designing more potent and less expensive hepcidin analogs would be advantageous.

In this study, we developed small peptides, minihepcidins, that act as hepcidin agonists. Their rational design was facilitated by the identification of the region on hepcidin and ferroportin molecules that is critical for their binding. Together with our previous structure-function studies (16, 17), we showed that hydrophobic contacts dominate the ligand-receptor interaction and that several N-terminal amino acids of hepcidin, up to residue 9, are critical for its activity. We therefore used the first 9 residues as the scaffold for minihepcidin design. We also found that the ability to participate in thiol-thiol interactions is essential for minihepcidin activity. Blocking the only cysteine (C7) with a protective group abrogated the peptide activity unless the protective group was added in such a way that disulfide exchange was possible. Furthermore, in contrast to its Cys-containing counterpart, minihepcidin bearing the Cys to Ser substitution did not cause serum iron decrease in mice after intraperitoneal injection.

To improve agonist activity, we developed the minihepcidins with structural modifications that addressed some undesirable physicochemical properties of the minihepcidin scaffold, such as thiol instability, hydrophobicity, poor gastrointestinal absorption, susceptibility to proteolysis, and instability in the bloodstream. We succeeded in designing minihepcidins of 7– or 9–amino acids in length that were active in mice in vivo. Intraperitoneal injection of proteolysis-resistant retro-inverso minihepcidins caused hypoferremia similar to that caused by native hepcidin. In a proof-of-principle experiment, chronic administration of minihepcidins significantly decreased iron loading in a mouse model of hereditary hemochromatosis. Hepcidin-1 knockout mice, which received intraperitoneal injections of a retro-inverso minihepcidin daily for 2 weeks, had significantly lower liver iron content that hepcidin-1 knockout mice injected with solvent.

Importantly, minihepcidin conjugated to fatty or bile acids caused hypoferremia after oral administration by gavage also. Given the number and rich variety of peptides involved in biological processes, relatively few have been FDA approved as therapeutics, and their efficient delivery by the oral route is still an unmet goal. Development of oral hepcidin analogs would represent a major advance in peptide pharmacology.

The mainstay of treatment for patients with iron overload is phlebotomy if they are not anemic and iron chelation if they have anemia. Although these measures are effective at reducing excess iron, they are frequently not well tolerated by patients, and compliance with iron-depleting therapy is suboptimal. If hepcidin therapy proves to be effective and relatively free of side effects, it could represent a major improvement over existing therapies, either alone or in combination with current approaches to allow modifications that would make the treatment less burdensome and better accepted by patients.

Methods

Site-directed mutagenesis. For cysteine scanning of the ferroportin region M312-L345, the human ferroportin-GFP C205S/C326S mutant (12) was used as a template for site-directed mutagenesis. For alanine scanning of the region F324-S343, WT human ferroportin-GFP was used as a template. Primers were selected using the QuikChange Primer Design (https://www.

genomics.agilent.com/), and mutagenesis was performed using QuikChange II XL Mutagenesis Kit (Agilent Technologies). Mutant plasmids were sequenced to verify the presence of the mutations.

Transient transfection and microscopy. WT and mutant ferroportin-GFP plasmids were transiently transfected into HEK293T cells using either Lipofectamine 2000 (Invitrogen) or Amaxa nucleofection (Lonza) (12). Cells were visualized with an epifluorescence microscope (Nikon Eclipse), and images were acquired with a SPOT camera and SPOT Advanced Imaging Software (Diagnostic Instruments). Confocal microscopy was performed at the UCLA CNSI Advanced Light Microscopy Facility, using a Leica TCS-SP MP Confocal and Multiphoton Inverted Microscope equipped with an argon laser (488 nm blue excitation, JDS Uniphase). The images were acquired using a ×63 oil-immersion objective lens and LCS Lite Software (Leica Confocal Software, Leica Microsystems).

Cell-surface biotinylation. Cells were treated with a nonpermeable SH-reactive, maleimide-PEG_2-biotin (12) (0.5 mM final concentration) according to the manufacturer's instructions (Pierce). Each ferroportin-GFP construct was analyzed in at least 3 independent experiments.

^{125}I-hepcidin internalization assay. The assay was performed as described previously (12, 38). Cells were treated with ^{125}I-hepcidin for 1 hour at 37°C. The radioactivity of untransfected cells was subtracted as background for each point. The counts were then normalized to the ferroportin-GFP expression of each sample as determined by quantitation of Western blots using Image Lab Software (Bio-Rad).

Immunoprecipitation and Western blotting. Cell lysis, immunoprecipitation, and Western blotting were performed as previously described (12). Polyclonal ab290 anti-GFP antibody (Abcam) was used for immunoprecipitation, biotinylated proteins were detected with streptavidin-HRPO (Pierce), and a monoclonal anti-GFP antibody (clones 7.1 and 13.1, Roche) was used to determine the amount of ferroportin-GFP that was immunoprecipitated.

Surface plasmon resonance. Surface plasmon resonance was performed on a BIAcore 3000 System (BiaCore AB) as previously described (39). Peptides were immobilized on a CM5 sensor chip by the amine-coupling protocol at a range of response units (1,100–6,000 response units). Analyte solutions were prepared at concentrations of 1–10 μg/ml in HBS-EP buffer (10 mM HEPES, pH 7.4, 150 mM NaCl, 3 mM EDTA, and 0.005% surfactant P20). Analytes were introduced into the flow cells at 50 μl/min for 3 minutes at 37°C. Resonance signals were corrected for nonspecific binding by subtracting the signal of the control flow cell and analyzed using BIAevaluation 4.1 software (Biacore).

Peptide synthesis and purification. All peptides were synthesized using the standard solid-phase fmoc chemistry (16) and were purified using reverse-phase HPLC. Minihepcidins were synthesized as carboxyamides (-$CONH_2$), which created a charge-neutral end more similar to a peptide bond than the negatively charged –COOH. The list of minihepcidins with their sequences is shown in Supplemental Table 2, and the structures of unnatural amino acids are displayed in Supplemental Table 3.

Circular dichroism spectroscopy. Circular dichroism spectra (185–260 nm) of the hepcidin peptides were recorded on a JASCO 720 Spectropolarimeter (Easton) as previously described (16). Estimates of the secondary structure contributions were made using the SELCON algorithm (40) and spectral basis set SP43 in the Olis Global Works software suite (Olis).

Modeling of hepcidin-ferroportin interaction. The structure for hepcidin (NP_066998, http://www.ncbi.nlm.nih.gov/protein/NP_066998) was modeled by the coordinate set for the lowest energy conformer from the Protein Data Bank (PDB 2KEF) (18). The structure for ferroportin (NP_055400.1, http://www.ncbi.nlm.nih.gov/protein/NP_055400.1) was approximated using the coordinate set provided by Nathan Subramaniam (19). The ferroportin region spanning residues 306–362 and the hepcidin structure were individually minimized in the HyperChem environment to obtain the lowest energy conformer.

Hepcidin was first docked into the ferroportin segment using the initial-stage docking program ZDOCK (http://zdock.bu.edu/). The lowest energy conformer set was then used as starting ensemble for a more refined docking using RosettaDock (http://rosettadock.graylab.jhu.edu/), which generated a low-energy structure used as a final hypothetical model for the ferroportin-hepcidin complex.

In vitro bioassay for measuring the activity of hepcidin derivatives. ECR293-Fpn (38), a cell line stably transfected with the mouse ferroportin-GFP construct under the control of the ponasterone-inducible promoter, was used for flow cytometry measurements of GFP fluorescence as previously described (16). For each peptide, the treatment with the full range of peptide concentrations was repeated independently 3 to 7 times.

In vivo bioassay for measuring activity of hepcidin derivatives. Animal studies were approved by the Animal Research Committee at UCLA. Six-week-old C57BL/6 mice were obtained from The Jackson Laboratory. Mice were placed on an iron-deficient diet (~4 ppm iron, Harlan Teklad) for 2 weeks to suppress endogenous hepcidin and to decrease its mouse-to-mouse variability (16, 41). Mice were subjected to the following treatments: (a) intraperitoneal injection with 0, 20, or 200 nmoles peptide solubilized in 100 μl SL220 solubilization agent (NOF) and (b) gavage with 0 or 200 nmoles peptide in 250 μl 1× solvent (Cremophor EL [Sigma-Aldrich]/ethanol/PBS = 12.5:12.5:75) (42). Mice were sacrificed 4 hours later, and serum iron was determined using a colorimetric assay (Diagnostic Chemicals) (16). To normalize for the variations in absolute serum iron levels among experiments, the results were expressed as the percentage of decrease in serum iron as compared with the serum iron levels in PBS-treated mice. Each peptide concentration was tested in 5 to 7 animals.

For the study of chronic minihepcidin effects, we used hepcidin-1 knockout mice, originally provided to our laboratory by Sophie Vaulont (43). *Hamp1*$^{-/-}$ mice (5–6 weeks of age, 6 males, and 7 females) were placed on low-iron diet for 2 weeks (4 ppm iron) to slow down the development of iron overload prior to injections with minihepcidins. The mice were then switched to the standard mouse chow (336 ppm iron) and given 100 μl intraperitoneal injections daily of either 100 nmoles palmitoyl-ri-hep9 solubilized in SL220 or the solvent only. After 2 weeks, the mice were euthanized, and their nonheme liver iron concentration was measured. Nonheme iron concentration was determined as described (44), using acid-based protein precipitation followed by a colorimetric assay for iron quantitation (Diagnostic Chemicals).

Quantitative real-time PCR. Liver RNA was extracted using TRIzol reagent (Invitrogen). Gene expression of *Hamp1* and the reference gene β-actin (*Actb*) was assessed by qRT-PCR using the iScript cDNA Synthesis Kit and iQ SYBR Green Supermix (Bio-Rad) (45). HAMP1 primer sequences are as follows: 5′-TTGCGATACCAATGCAGAAGA-3′ and 5′-GATGTGGCTCTAGGCTATGTT-3′. β-Actin primer sequences are as follows: 5′-ACCCACACTGTGCCCATCTA-3′ and 5′-CACGCTCGGTCAGGATCTTC-3′.

Statistics. SigmaPlot version 11.0 (Systat Software) was used for statistical analyses. A *P* value of less of 0.05 was considered significant.

Acknowledgments

We would like to acknowledge the Office of Information Technology at the University of California, Irvine, and Broadcom Corp. for providing the Broadcom Distributed/Unified Cluster used for the molecular dynamics simulation and docking of the protein complex. The UCLA Jonsson Comprehensive Cancer Center and Center for AIDS Research Flow Cytometry Core Facility was instrumental for flow cytometry measurements. Matthew Schibler at the UCLA CNSI Advanced Light Microscopy Facility provided help with confocal microscopy. We thank Grace Jung for assistance with Biacore analysis and Nathan Subramaniam for providing the PDB file of

his ferroportin model. The work was funded by NIH grants R01 DK 082717 (to E. Nemeth) and R01 DK 065029 (to T. Ganz).

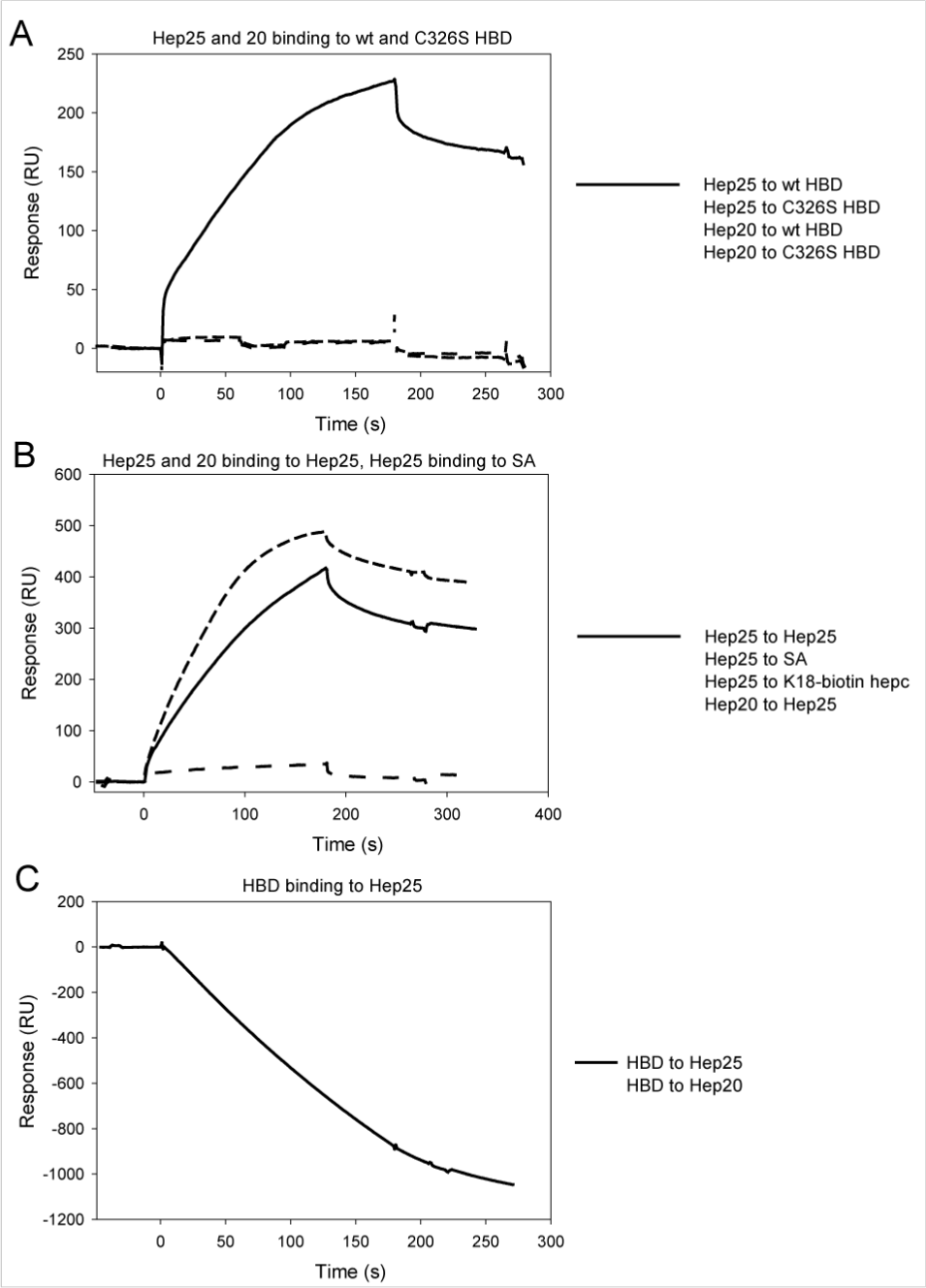
Received for publication February 21, 2011, and accepted in revised form September 21, 2011.

Address correspondence to: Elizabeta Nemeth, CHS 37-055, Department of Medicine, David Geffen School of Medicine at UCLA, 10833 Le Conte Ave., Los Angeles, California 90095-1690, USA. Phone: 310.825.7499; Fax: 310.206.8766; E-mail: enemeth@mednet.ucla.edu.

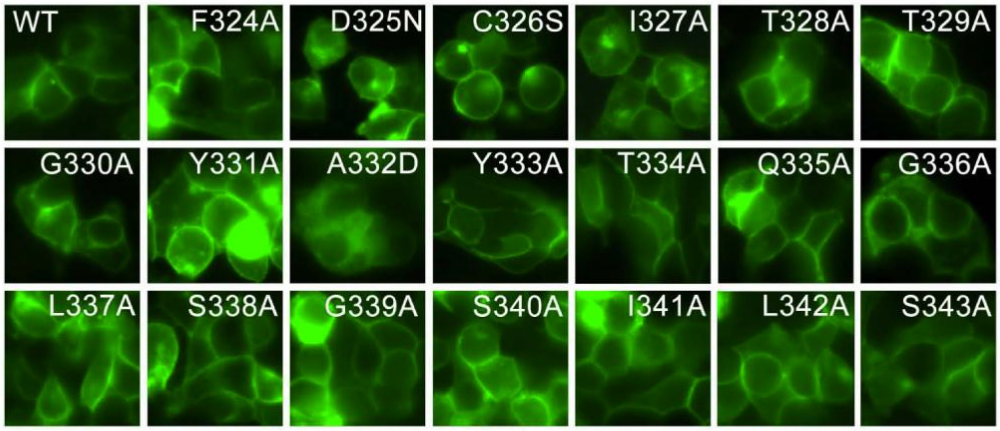
1. Ganz T, Nemeth E. Hepcidin and disorders of iron metabolism. *Annu Rev Med.* 2011;62:347–360.
2. Ganz T, Olbina G, Girelli D, Nemeth E, Westerman M. Immunoassay for human serum hepcidin. *Blood.* 2008;112(10):4292–4297.
3. Piperno A, et al. Blunted hepcidin response to oral iron challenge in HFE-related hemochromatosis. *Blood.* 2007;110(12):4096–4100.
4. Origa R, et al. Liver iron concentrations and urinary hepcidin in beta-thalassemia. *Haematologica.* 2007; 92(5):583–588.
5. Kearney SL, et al. Urinary hepcidin in congenital chronic anemias. *Pediatr Blood Cancer.* 2007; 48(1):57–63.
6. Fujita N, et al. Patients with chronic hepatitis C achieving a sustained virological response to peginterferon and ribavirin therapy recover from impaired hepcidin secretion. *J Hepatol.* 2008;49(5):702–710.
7. Girelli D, et al. Reduced serum hepcidin levels in patients with chronic hepatitis C. *J Hepatol.* 2009; 51(5):845–852.
8. Barton JC. Chelation therapy for iron overload. *Curr Gastroenterol Rep.* 2007;9(1):74–82.
9. Porter JB. Optimizing iron chelation strategies in beta-thalassaemia major. *Blood Rev.* 2009; 23(suppl 1):S3–S7.
10. Bartnikas TB, Fleming MD. A tincture of hepcidin cures all: the potential for hepcidin therapeutics. *J Clin Invest.* 2010;120(12):4187–4190.
11. Rivera S, Liu L, Nemeth E, Gabayan V, Sorensen OE, Ganz T. Hepcidin excess induces the sequestration of iron and exacerbates tumor-associated anemia. *Blood.* 2005;105(4):1797–1802.
12. Fernandes A, et al. The molecular basis of hepcidin-resistant hereditary hemochromatosis. *Blood.* 2009;114(2):437–443.
13. Liu XB, Yang F, Haile DJ. Functional consequences of ferroportin 1 mutations. *Blood Cells Mol Dis.* 2005;35(1):33–46.
14. Rice AE, Mendez MJ, Hokanson CA, Rees DC, Bjorkman PJ. Investigation of the biophysical and cell biological properties of ferroportin, a multipass integral membrane protein iron exporter. *J Mol Biol.* 2009;386(3):717–732.
15. De Domenico I, et al. The hepcidin-binding site on ferroportin is evolutionarily conserved. *Cell Metab.* 2008;8(2):146–156.
16. Nemeth E, Preza GC, Jung CL, Kaplan J, Waring AJ, Ganz T. The N-terminus of hepcidin is essential for its interaction with ferroportin: structure-function study. *Blood.* 2006;107(1):328–333.
17. Clark RJ, Tan CC, Preza GC, Nemeth E, Ganz T, Craik DJ. Understanding the structure/activity relationships of the iron regulatory peptide hepcidin. *Chem Biol.* 2011 2011;18(3):336–343.
18. Jordan JB, et al. Hepcidin revisited, disulfide connectivity, dynamics, and structure. *J Biol Chem.* 2009; 284(36):24155–24167.
19. Wallace DF, Harris JM, Subramaniam VN. Functional analysis and theoretical modeling of ferroportin reveals clustering of mutations according to phenotype. *Am J Physiol Cell Physiol.* 2010;298(1):C75–C84.
20. Chen R, Li L, Weng Z. ZDOCK: an initial-stage protein-docking algorithm. *Proteins.* 2003;52(1):80–87.
21. Lyskov S, Gray JJ. The RosettaDock server for local proteinprotein docking. *Nucleic Acids Res.* 2008; 36(Web Server issue):W233–W238.
22. Sham RL, Phatak PD, Nemeth E, Ganz T. Hereditary hemochromatosis due to resistance to hepcidin: high hepcidin concentrations in a family with C326S ferroportin mutation. *Blood.* 2009; 114(2):493–494.
23. Resh MD. Palmitoylation of ligands, receptors, and intracellular signaling molecules. *Sci STKE.* 2006;2006(359):re14.
24. Roetto A, et al. Mutant antimicrobial peptide hepcidin is associated with severe juvenile hemochromatosis. *Nat Genet.* 2003;33(1):21–22.
25. Nemeth E, Roetto A, Garozzo G, Ganz T, Camaschella C. Hepcidin is decreased in TFR2 hemochromatosis. *Blood.* 2005;105(4):1803–1806.
26. Papanikolaou G, et al. Mutations in HFE2 cause iron overload in chromosome 1q-linked juvenile hemochromatosis. *Nat Genet.* 2004;36(1):77–82.
27. U.S. Preventive Services Task Force. Screening for Hemochromatosis: Recommendation Statement. *Ann Intern Med.* 2006;145(3):204–208.
28. Cunningham MJ. Update on thalassemia: clinical care and complications. *Pediatr Clin North Am.* 2008;55(2):447–460.
29. Taher A, Isma'eel H, Cappellini MD. Thalassemia intermedia: Revisited. *Blood Cells Mol Dis.* 2007; 37(1):12–20.
30. [No authors listed]. International BioIron society meeting. *Am J Hematol.* 2009;84(8):E236–E375.
31. Fujita N, et al. Hepcidin expression in the liver: relatively low level in patients with chronic hepatitis C. *Mol Med.* 2007;13(1–2):97–104.
32. Alla V, Bonkovsky HL. Iron in nonhemochromatotic liver disorders. *Semin Liver Dis.* 2005;25(4):461–472.
33. Nicolas G, et al. Constitutive hepcidin expression prevents iron overload in a mouse model of hemochromatosis. *Nat Genet.* 2003;34(1):97–101.
34. Viatte L, et al. Chronic hepcidin induction causes hyposideremia and alters the pattern of cellular iron accumulation in hemochromatotic mice. *Blood.* 2006;107(7):2952–2958.
35. Gualdi R, Casalgrandi G, Montosi G, Ventura E, Pietrangelo A. Excess iron into hepatocytes is required for activation of collagen type I gene during experimental siderosis. *Gastroenterology.* 1994; 107(4):1118–1124.
36. Pietrangelo A. The ferroportin disease. *Blood Cells Mol Dis.* 2004;32(1):131–138.
37. Gardenghi S, et al. Hepcidin as a therapeutic tool to limit iron overload and improve anemia in beta-thalassemic mice. *J Clin Invest.* 2010;120(12):4466–4477.
38. Nemeth E, et al. Hepcidin regulates cellular iron efflux by binding to ferroportin and inducing its internalization. *Science.* 2004;306(5704):2090–2093.
39. Wang W, et al. Retrocyclins kill bacilli and germinating spores of Bacillus anthracis and inactivate anthrax lethal toxin. *J Biol Chem.* 2006;281(43):32755–32764.
40. Sreerama N, Venyaminov SY, Woody RW. Estimation of the number of alpha-helical and beta-strand segments in proteins using circular dichroism spectroscopy. *Protein Sci.* 1999;8(2):370–380.
41. Nemeth E, et al. IL-6 mediates hypoferremia of inflammation by inducing the synthesis of the iron regulatory hormone hepcidin. *J Clin Invest.* 2004; 113(9):1271–1276.
42. Kim S, et al. Sorafenib inhibits the angiogenesis and growth of orthotopic anaplastic thyroid carcinoma xenografts in nude mice. *Mol Cancer Ther.* 2007; 6(6):1785–1792.
43. Lesbordes-Brion JC, et al. Targeted disruption of the hepcidin 1 gene results in severe hemochromatosis. *Blood.* 2006;108(4):1402–1405.
44. Pak M, Lopez MA, Gabayan V, Ganz T, Rivera S. Suppression of hepcidin during anemia requires erythropoietic activity. *Blood.* 2006;108(12):3730–3735.
45. Ramos E, et al. Evidence for distinct pathways of hepcidin regulation by acute and chronic iron loading in mice. *Hepatology.* 2011;53(4):1333–1341.

Supplemental Figure 1. Synthetic HBD does not bind hepcidin-25 specifically. Surface plasmon resonance analysis of HBD interaction with hepcidin: **A**. WT HBD or C326S HBD mutant was coated on the sensor surface, and bioactive hepcidin-25 or inactive hepcidin-20 were injected as analytes. There was no difference in hepcidin binding to HBD and mutated HBD-C326S. **B**. Hepcidin-25 but not hepcidin-20 aggregated on the sensor surface coated with hepcidin-25 itself, streptavidin (SA) or hepcidin biotinylated at K18 residue. **C**. The reverse configuration, with hepcidin-25 or -20 coated on the chip and HBD used as analyte, generated a negative binding signal, i.e. HBD bound to hepcidin less than it did to the uncoated reference sensor surface.

Although not shown in the figure, additional surface plasmon resonance experiments support the argument that HBD is not a hepcidin-binding domain: 1) Hepcidin bound similarly to unalkylated and alkylated HBD, whereas alkylation of cells expressing ferroportin-GFP prevented hepcidin binding. 2) Bioactive mouse hepcidin did not bind to HBD. 3) Non-aggregating but bioactive hepcidin derivatives (M21Y-hepcidin, F4Nleu-hepcidin, minihepcidin hep9) did not bind to HBD. 4) Aggregating mutant (hepcidin-protegrin chimera) which was inactive in cellular assays did bind HBD. Furthermore, using competitive ELISA format, we found no competition between unlabeled hepcidin and any of the three biotinylated hepcidins (N-terminal, K18 and K24-biotinylated) for HBD-coated plates. We did not detect any competition between unlabeled and ^{125}I-hepcidin for HBD-coated beads.

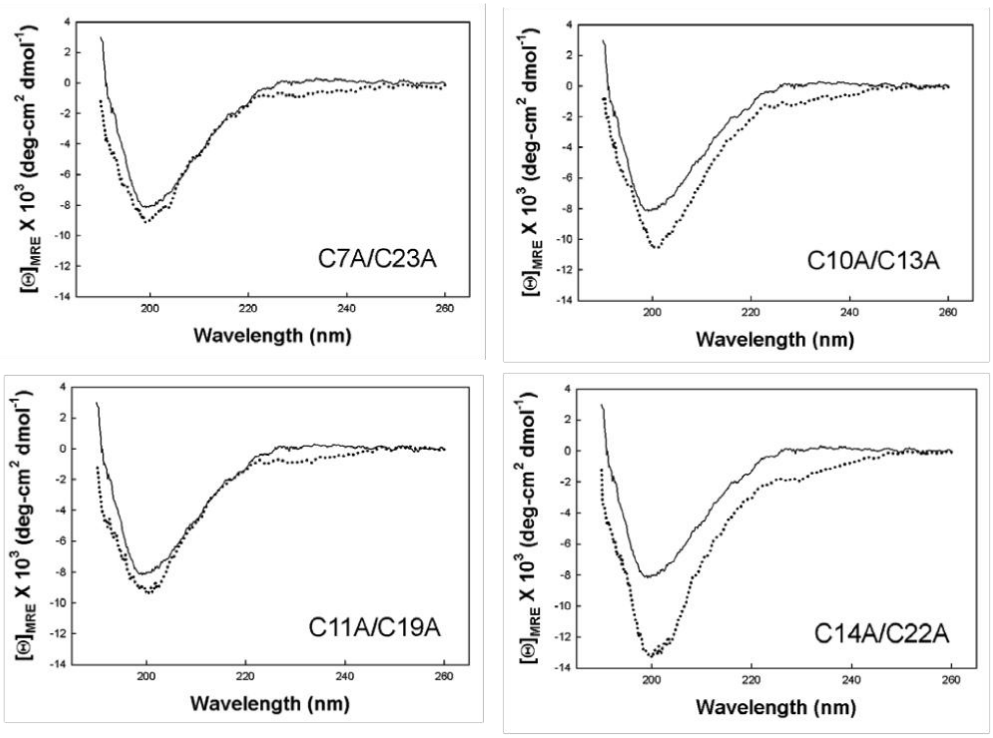

A
Hep25 and 20 binding to wt and C326S HBD
Response (RU)
Time (s)
Hep25 to wt HBD
Hep25 to C326S HBD
Hep20 to wt HBD
Hep20 to C326S HBD
B
Hep25 and 20 binding to Hep25, Hep25 binding to SA
Response (RU)
Time (s)
Hep25 to Hep25
Hep25 to SA
Hep25 to K18-biotin hepc
Hep20 to Hep25
C
HBD binding to Hep25
Response (RU)
Time (s)
HBD to Hep25
HBD to Hep20

Supplemental Figure 2. Fluorescent microscopy of Fpn-GFP mutants from Figure 1C/D. Most mutants were expressed on the plasma membrane, but some (D325N, I327A, A332D) had prominent intracellular localization.



Supplemental Figure 3. Circular dichroism spectroscopy of hepcidin disulfide mutants. Circular dichroism spectroscopy was used to assess changes in the secondary structure of hepcidin disulfide mutants. **A.** The solid line represents the spectrum of the native hepcidin, and dashed lines the spectra of hepcidin mutants. **B.** Quantitative analysis of the spectra. Estimates of the secondary structure were made with SELCON algorithm using the spectral basis set SP43, and results expressed as percentage of conformations.

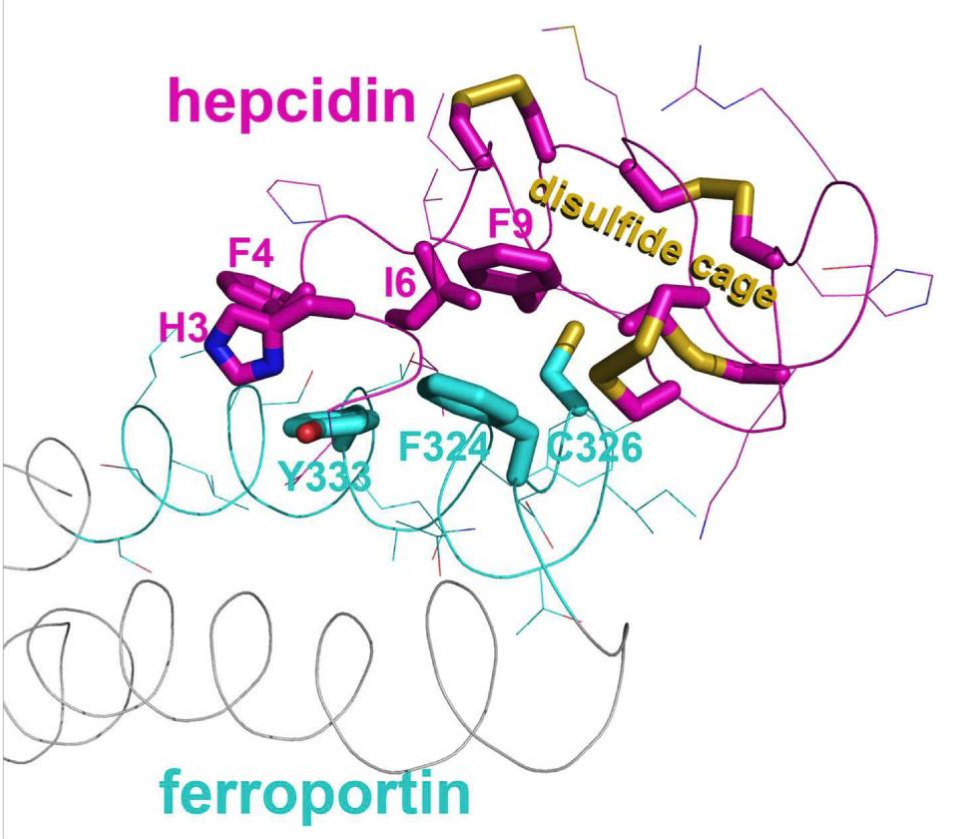
A.



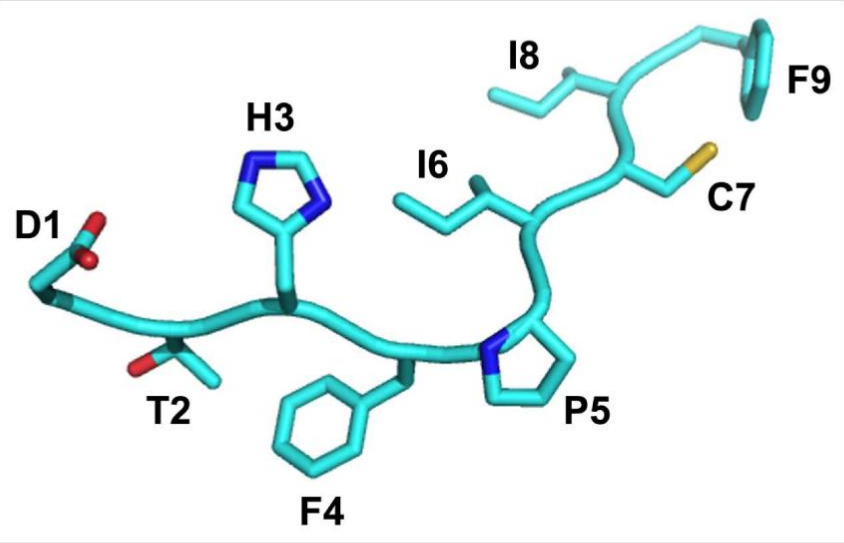
B.

Sample	% beta sheet	% disordered beta sheet	% disordered	% turn
Hepcidin25	29	14	36	21
C7A/C23A	27	14	40	19
C10A/C13A	27	14	40	19
C11A/C19A	27	14	40	19
C14A/C22A	26	14	41	19

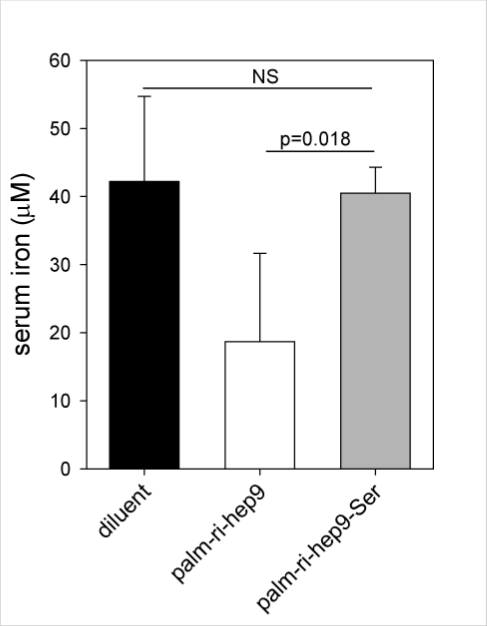
Supplemental Figure 4. A RosettaDock model of the hepcidin-ferroportin interface. The model is identical to the one in Figure 3, but is viewed parallel to the interface of the two molecules. Hepcidin on the top is shown in pink with yellow disulfide connectivities. Ferroportin extracellular loop on the bottom is shown in cyan, transmembrane helices in grey, and the sulfur of C326 in yellow. The strongly interacting side chain pairs are displayed in thicker lines.



Supplemental Figure 5. Modeled structure of the minihepcidin composed of 9 N-terminal residues of human hepcidin (DTHFPICIF). The structure was generated using PyMOL software.

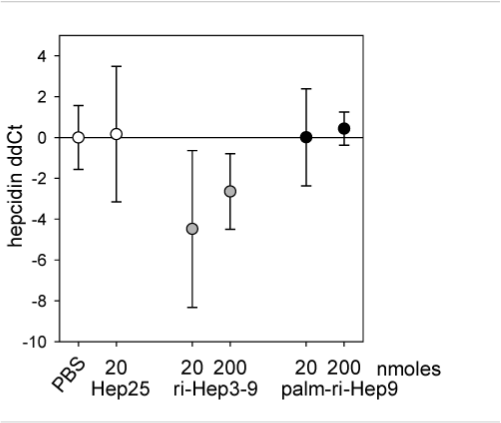


Supplemental Figure 6. Minihepcidin lacking cysteine is not active *in vivo*. Palmitoylated retroinverted hep9 (palm-ri-hep9) which contains a single cysteine was synthesized with the cysteine to serine substitution (palm-ri-hep9-Ser). Both peptides were injected intraperitoneally (20 nmoles per mouse, n=4 animals per treatment), mice were euthanized after 4 h, and non-heme iron levels determined in serum.

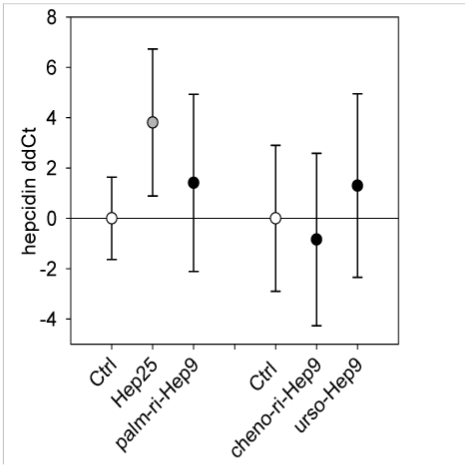


Supplemental Figure 7. Administration of minihepcidins in mice did not increase the expression of endogenous hepatic hepcidin mRNA. Hepcidin mRNA was measured by qPCR and normalized to the expression of actin mRNA. Graphs show mean and standard deviation of hepcidin ddCt. **A.** Hepcidin expression in mice from Figure 6B (intraperitoneal injection of minihepcidins). **B.** Hepcidin expression in mice from Figure 6C (oral administration by gavage). Only the gavage of full-length hepcidin-25 but not minihepcidins induced endogenous hepcidin mRNA (p=0.02).

A.



B.



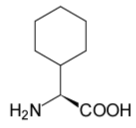
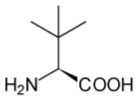
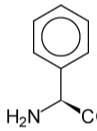
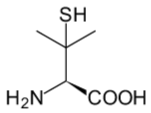
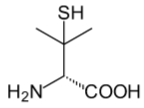
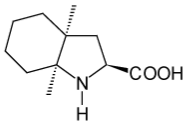
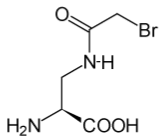
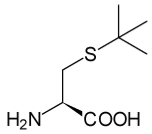
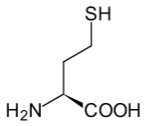
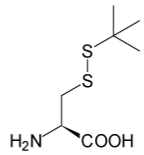
Supplemental Table 1. RosettaDock-derived pair energies across hepcidin-ferroportin interface showing strong association of ligand-receptor residues in the hypothetical molecular complex.

Fpn aa		Hep aa		total energy
323	GLY	18	LYS	0.15
323	GLY	19	CYS	0.01
324	PHE	1	ASP	-0.19
324	PHE	2	THR	-0.25
324	PHE	9	PHE	-1.93
324	PHE	11	CYS	0.71
324	PHE	19	CYS	-0.06
325	ASP	2	THR	-0.48
325	ASP	9	PHE	-0.05
325	ASP	10	CYS	-0.16
325	ASP	11	CYS	-1.96
325	ASP	12	GLY	0.01
325	ASP	13	CYS	0.01
326	CYS	2	THR	-0.23
326	CYS	6	ILE	0.10
326	CYS	9	PHE	0.04
326	CYS	10	CYS	-0.52
326	CYS	11	CYS	-0.05
326	CYS	13	CYS	-0.14
326	CYS	22	CYS	0.00
326	CYS	24	LYS	-0.15
327	ILE	10	CYS	-0.02
327	ILE	12	GLY	-0.01
327	ILE	13	CYS	-0.15
329	THR	1	ASP	0.01
329	THR	2	THR	-0.19
330	GLY	2	THR	-0.04
330	GLY	6	ILE	-0.32
331	TYR	24	LYS	-0.78
333	TYR	1	ASP	-0.28
333	TYR	2	THR	-0.28
333	TYR	3	HIS	-0.44
333	TYR	4	PHE	-1.60
333	TYR	6	ILE	-0.96
333	TYR	25	THR	0.00
334	THR	4	PHE	-0.03
334	THR	6	ILE	0.01
334	THR	24	LYS	0.02
337	LEU	4	PHE	-0.61

Supplemental Table 2. Design and bioassay of modified minihepcidins. Peptide sequences and IC50 values are displayed. IC50 was calculated from peptide dose response studies in which the activity was quantitated by measuring Fpn-GFP degradation by flow cytometry. Some peptides were synthesized as carboxyamides. D amino acids are represented by blue font. Unnatural amino acids are indicated in red and their structure is displayed in the Supplemental Table 3. ChenoD = chenodeoxycholic acid, or UrsoD = ursodeoxycholic acid, BetaP = Beta propeller, CD = collagen domain.

	Peptide Name	Sequence	IC50 (μM)
Minihepcidins	Hep1-9	DTHFPICIF	0.076
	Hep1-8	DTHFPICI	2.5
	Hep1-7	DTHFPIC	10
	Hep4-7	FPIC	7.5
	Hep3-7	HFPIC	10
	Hep3-8	HFPICI	1
	Hep3-9	HFPICIF	0.55
Cysteine Modifications of Hep1-9	Hep1-9 dC	DTHFPIdCIFamide	inactive (>10)
	Hep1-9 homoC	DTHFPIhomoCIFamide	0.3
	Hep1-9 Pen	DTHFPIPenIFamide	Inactive (>10)
	Hep1-9 dPen	DTHFPIdPenIFamide	Inactive (>10)
	Hep1-9 Dap(AcBr)	DTHFPIDap(AcBr)IFamide	Inactive (>10)
Cyclic peptides	Cyc-1	CDTHFPICIFamide	0.3
	Cyc-2	DTHFPICIF-$CONH_2$-CH_2-CH_2-S	Inactive (>10)
	Cyc-3	CHFPICIFamide	Inactive (>10)
	Cyc-4	HFPICIF-$CONH_2$-CH_2-CH_2-S	Inactive (>10)
Unnatural aa's	Un Pr10	DTIeHPhgOicChgCChgFamide	Inactive (>10)
	Un Pr11	DTIeHPOicChgCChgFamide	Inactive (>10)
Retro-Inverso Modifications	ri-Hep1-9	FICIPFHTD	0.8
	ri-Hep3-9	FICIPFH	0.2
	ChenoD-ri-Hep1-9	ChenoD(PEG11)**FICIPFHTD**amide	0.10
	UrsoD-ri-Hep1-9	UrsoD(PEG11)**FICIPFHTD**amide	1
	ri-Hep1-9 BetaP	**FICIPFHTD**(PEG11)-GYIPEAPRDGQAYVRKDGEWVLLSTFLamide	Inactive (>10)
	ri-Hep1-9 CD	**FICIPFHTD**(PEG11)-(GPHyp)10-amide	Inactive (>10)
	Palm-ri-Hep1-9	Palmitoyl-(PEG11)-**FICIPFHTD**amide	0.01
	Palm-ri-Hep1-9-	Palmitoyl-(PEG11)-**FISIPFHTD**amide	Inactive
	2Palmitoyl ri-	2(Palmitoyl)-Dap(PEG11)-**FICIPFHTD**amide	2

Supplemental Table 3. Uncommon or Unnatural Amino Acids

Chg  L-α-cyclohexylglycine	**Tle**  L-tert-leucine	**Phg**  L-phenylglycine	**Pen**  L-Penicillamine	**(D)Pen**  D-Penicillamine
Oic  octahydroindole-2-carboxylic acid	**Dap(AcBr)**  N^{γ}-(bromoacetyl)-L-2,3-diaminopropionic acid	**Cys(tBut)**  S-t-butyl-L-cysteine	**HomoC**  L-homocysteine	**Cys(S-tBut)**  S-t-Butylthio-L-cysteine

Manuscript in preparation:

Optimization of minihepcidins yields peptides that prevent iron overload in mouse models of hemochromatosis

Emilio Ramos, Piotr Ruchala, Julia Goodnough, Léon Kautz, Gloria Preza, Elizabeta Nemeth and Tomas Ganz

Abstract:

Hepcidin replacement therapy is a promising approach for preventing iron overload toxicity caused by hepcidin insufficiency in hereditary hemochromatosis and iron-loading anemias. In a previous study, we reported the development of synthetic hepcidin agonists (minihepcidins). To assess the feasibility of using minihepcidin therapy in humans we refined the design of minihepcidins to decrease the cost of synthesis and increase the peptide potency, and assessed the efficacy of the treatment in a mouse hemochromatosis model. **Methods:** Based on the human hepcidin N-terminus (DTHFPICIF, hepcidin-9), we designed over 50 hepcidin variants with substitutions that increased peptide activity and also tested the effect of functional groups on bioavailability (PEG, palmitoyl). Minihepcidins were administered to C57BL/6 mice by gavage, intraperitoneal, or subcutaneous injection and activity was assessed by the resulting decrease in serum iron. One of the optimized minihepcidins (PR65) was administered daily for 2 weeks to iron-depleted or iron-loaded hepcidin knockout mice and iron parameters were measured. **Results:** Compared to natural hepcidin, the hypoferremic activity of PR65 given by intraperitoneal or subcutaneous route was significantly greater. Chronic injections of PR65 prevented the development of iron overload in iron-depleted hepcidin knockout mice, and caused partial redistribution of iron from the liver to the spleen in iron-overloaded hepcidin knockout mice. **Conclusions**: We developed a hepcidin agonist that is more potent and less costly than

previous minihepcidins or native hepcidin. In a mouse model of hemochromatosis, a single daily injection of minihepcidin prevented iron accumulation but was less effective once severe iron overload was established. These results indicate that minihepcidins could be useful alone for the prevention of iron overload or as adjunctive therapy with phlebotomy or chelation.

Introduction:

Produced by the liver, hepcidin is a 25 amino acid peptide hormone that circulates in plasma and homeostatically controls body iron balance (1). In healthy individuals, hepcidin production is increased when plasma or tissue iron concentrations rise and decreased after iron depletion (2). The hormone binds to its receptor ferroportin which is prominently expressed in enterocytes, hepatocytes and iron-recycling macrophages, and functions as the sole exporter of cellular iron into plasma. Hepcidin binding initiates the endocytosis and proteolysis of ferroportin and thereby decreases iron flow into plasma (3). In the hereditary hemochromatoses (HH types I-III), mutations in hepcidin-regulating genes or the hepcidin gene itself diminish hepcidin synthesis, decreasing the inhibitory effect of hepcidin on duodenal iron absorption and thereby causing clinical iron overload (4).

Hepcidin deficiency and hyperabsorption of dietary iron are major factors not only in HH but also in the iron-loading syndromes associated with hereditary anemias characterized by ineffective erythropoiesis, and to a lesser extent in chronic hepatitis C infection and alcoholic liver disease (5)(6). Hepcidin replacement therapy with pharmacologically optimized agonists would provide a rational treatment for these disorders. In HH or β-thalassemia intermedia early diagnosis may allow preventive treatment with hepcidin agonists to reduce the potential for iron toxicity and the need for phlebotomy or chelation and hepcidin agonists could help improve iron control. Aside from preventing dietary iron absorption, minihepcidins may also have a protective

effect on the liver and other organs by causing redistribution of iron into macrophages of the liver and spleen which are more resistant to the toxic effects of iron. Moreover, in a mouse model of β-thalassemia intermedia, mild overexpresion of hepcidin not only prevented iron overload but increased hemoglobin and improved erythrocyte morphology (7), suggesting that minihepcidins could have broad beneficial effects in β-thalassemias.

In our previous studies, targeted amino acid substitution and computer modeling identified specific residues in hepcidin and ferroportin that were critical for the ligand-receptor interaction (8). We showed that the 9 N-terminal amino acids of human hepcidin (DTHFPICIF) were sufficient to degrade ferroportin in ferroportin-overexpressing cell lines. We then altered this hepcidin fragment to improve its pharmacological characteristics and developed several potent and bioavailable "minihepcidins."

In the current study, we designed more potent and less expensive minihepcidins and examined the benefits and potential side effects of hepcidin replacement therapy in a mouse model of hereditary hemochromatosis caused by hepcidin deficiency.

Materials and methods:

Peptide synthesis: Peptides were synthesized using standard solid-phase fmoc chemistry and were purified using reverse-phase HPLC. Minihepcidins were synthesized as carboxyamides (-$CONH_2$), which created a charge-neutral terminus more similar to a peptide bond than the negatively charged –COOH. The subset of peptides used for pharmacokinetic studies is listed in Table 2 and the entire list of peptides tested since our previous publication is provided in Tables 3-5.

Short-term animal studies: All studies were approved by the Animal Research Committee at UCLA. Six-week-old male C57BL/6 mice were obtained from The Jackson Laboratory. Mice were placed on an iron-deficient diet (~20 ppm iron, Harlan Teklad) for 1 week to suppress endogenous hepcidin and to decrease mouse-to-mouse variability. For intraperitoneal or subcutaneous injections, peptides were dissolved in 100 µl SL220 solubilization agent (NOF, Tokyo, Japan), and for gavage in a Cremophor-EL (BASF, Ludwigshafen, Germany) diluent (9). Mice were sacrificed 4 hours after administration for 20 nmol doses or 12, 24 and 36 hours after for 200 nmol does. Each timepoint and dose was tested in at least 4 animals.

Chronic animal studies: The effect of daily minihepcidin administration to iron-depleted and iron-loaded mice was studied in hepcidin-1 knockout mice (*Hamp1*$^{-/-}$), originally provided to our laboratory by Sophie Vaulont and modified by marker-assisted backcrossing onto C57B6 background (10). PR65 was administered subcutaneously in 100 µl of SL220.

To test the ability of PR65 to prevent iron loading ("prevention" studies), iron-depleted *Hamp1*$^{-/-}$ mice were prepared by placing 5–6 week old animals on a low-iron diet (4 ppm iron) for 2 months. A group of mice was sacrificed at this time (baseline group), and the remaining animals were switched to an iron-loading diet (standard chow, 336 ppm Fe) and received daily subcutaneous injection of solvent, or 20, 50 or 100 nmoles of PR-65 for 2 weeks.

To test the effect of PR65 on iron-loaded *Hamp1*$^{-/-}$ mice ("redistribution" studies), the animals were kept on the standard diet for their entire lifespan. Beginning at 12-14 weeks of age, 50 nmoles of PR65 or solvent was injected daily by subcutaneous route for 2 weeks.

Measurement of Iron and Hematological Parameters: Serum iron and non-heme iron concentrations were determined as described (11), using acid protein precipitation followed by a

colorimetric assay for iron quantitation (Diagnostic Chemicals). Deparaffinized sections were stained with the Perls Prussian blue stain for non-heme iron and enhanced with the SG peroxidase substrate kit from Vector labs and counterstained with nuclear fast red. Complete blood counts were obtained using a HemaVet blood analyzer.

Western blots:

Ferroportin levels were measured in spleen samples from mice injected with PR65 from 1-48 hours. 20-30 mg of spleen tissue was mechanically homogenized in ice-cold RIPA buffer (Sigma-Aldrich) and rotated for 2 hours at 4ºC. 50 ug of total protein was loaded per well and electrophoresed on a 7.5% Mini-Protean (Bio-Rad) then transferred to a nitrocellulose membrane which was blocked with 2.5% non-fat dry milk in TTBS (.1% Tween-20). Blots were incubated with rat 1:200 anti-mouse ferroportin (Amgen, Thousand Oaks, California) and incubated with 1:10,000 goat anti-rat human and mouse pre-adsorbed IgG (Santa Cruz Biotechnology, Santa Cruz, California). Western blots were visualized by chemiluminescence using the West Pico SuperSignal Chemiluminescent Substrate (ThermoScientific/Pierce).

Results:

Peptide screening and Optimization

In preparation for potential human applications, we aimed to improve the potency of minihepcidins as well as reduce reagent costs and facilitate large-scale synthesis. We tested the introduction of different unnatural amino acids in L-amino acid peptides (Tables 1, 3 and 5), substitution of residues in both L- and retroinverted peptides (Table 4), and elimination of non-essential pharmacology-enhancing functional groups (Table 2). Activity of peptides PR29-PR61 was tested *in vitro*, by flow cytometric measurements of Fpn-GFP degradation (8). Substitution

of F4 with Dpa in L-amino acid peptides greatly improved activity (PR30) presumably by increasing hydrophobic interactions between hepcidin and ferroportin (Table 3). Substitution of an additional two or three residues with unnatural amino acids (D1, P5, I6/8 or F9) further increased activity (peptides PR53-61, Table 5), reaching or even exceeding the potency of native hepcidin *in vitro* (EC50 ~10 nM). Shorter retroinverted peptides (7 amino acids) with Dpa substitutions also displayed high *in vitro* activity (PR49-50, Table 4), but were not as active in our *in vivo* screen (data not shown).

We next tested select minihepcidins *in vivo* and found that PR61 demonstrated high bioactivity through i.p. injection which is presumably dependent on Ile to Arg substitutions at positions 6 and 8 (Table 1, Figure 1A). PR61 caused more profound hypoferremia after intraperitoneal administration than native hepcidin at a dose of 20 nmoles per mouse ($p=0.023$, Figure 1B). The ease and low cost of synthesis due to its exclusively L-amino acid sequence made PR61 ideal for further optimization and *in vivo* testing.

The following experiments tested whether elimination of PR61 functional groups such as the solubility enhancing polyethylene glycol (PEG) linker or palmitoyl fatty acid group affected activity *in vivo* (Table 2). Four hours after a 20 nmole i.p. dose (Figure 1C), the PEG/palmitoyl-containing variants (PR61, 65) were slightly more active (80% drop in serum Fe, $p<.001$ for both) than minihepcidin variants lacking both PEG and palmitoyl group (PR66, 50% drop in serum Fe, $p<0.001$) or PEG only (PR71, 65% drop in serum Fe, $p=0.011$). We thus determined that both PEG and palmitoyl groups contribute to peptide activity *in vivo*.

Subcutaneous administration, due to its ease and safety compared to intravenous administration, is widely used to deliver peptide therapeutics such as insulin. Unlike native hepcidin,

minihepcidins were active after s.c. injection although the onset and duration of the effect varied (Figure 1C, D). This is not surprising as subcutaneous absorption of drugs is generally slower than in the intraperitoneal cavity which has a larger surface area for capillary absorption. PR66 (no PEG/palmitoyl) caused an 80% drop in serum iron after 4 hours (Figure 1C) but no effect was observed after 12 hours at a 10-fold higher dose (Figure 1D). The palmitoyl/PEG combination (PR61 and 65) caused prolonged hypoferremia over a 36 hour period after a single injection. Retroinverted peptides, as shown in previous studies, were active at 4 hours through i.p. injection, but not through the subcutaneous route (data not shown).

We also tested the effect of PEG/palmitoyl on oral activity by gavage. Mice were gavaged with 200 nmoles (10-15 mg/kg) and euthanized after 4 hours. Animals that received PR61 showed a 30% drop in serum Fe (Figure 1E, $p=0.017$). No other peptide showed significant oral ability, which indicates the importance of the extra PEG group at the C-terminus. Because of the cost-prohibitive amount of peptide required to achieve a modest drop in serum iron, subsequent experiments were conducted using only i.p. or s.c. administration.

Some hepcidin deficiency models (HFE, TfR2 and to some extent HJV and BMP6) retain residual hepcidin production and we elected instead to use hepcidin KO mice to eliminate the possibility of endogenous hepcidin regulation by our synthetic analogues. PR61 was more effective than native hepcidin at lowering serum iron in hepcidin knockout mice. We collected 75 ul blood from the retroorbital plexus 48 hrs before injection and again at 4 and 24 hours after i.p. injection from the same mouse and alternating the draw site. Compared to hepcidin-25 at 4 hours, hepcidin KO injected with 20 nmoles PR61 showed a 61% drop in serum Fe ($p=0.001$), while hepcidin-25 injected mice showed no significant changes (Figure 2A). After 24 hours, serum iron levels normalized in PR61 injected mice much faster than in wild-type mice,

indicating that a higher dose of peptide would be required to allow a single daily dose treatment regimen in hepcidin knockout mice. Mice injected with PR71, a PR61 derivative with a fatty acid group but no PEG linker was not active in hepcidin knockouts ($p=0.955$)

Development of a PR65 treatment regimen

We selected PR65 for pharmacokinetic studies in hepcidin-null mice. PR65 retains full activity through i.p. and s.c. administration compared to PR61 and does not contain a mini-PEG group, thus decreasing reagent cost and synthesis time. To establish optimal treatment parameters for a long-term minihepcidin treatment regimen, we performed dose response (Figure 2B) and time course (Figure 2C) experiments in iron-loaded hepcidin knockout mice. After 24 h, subcutaneous injection of 20 and 50 nmoles of PR65 showed 15% and 10% ($p=0.005$, $p=0.004$) decreases in serum iron, while 100 and 200 nmole doses showed an 85% and 95% ($p<0.001$ for both) reduction. Selecting 100 nmoles as the optimal dose, we conducted a time course experiment to determine the peak effect. The maximal drop (88%) in serum Fe occured 12 hours after injection ($p<.001$), serum Fe remained severely suppressed (82%) at 24 hours but returned to solvent control levels 48 hours after.

We also measured activity of PR65 from 1-48 hours through its effect on ferroportin and the resultant changes in tissue iron retention. Analysis of lysates from spleen tissue indicated that a drop Fpn levels precedes iron retention in the organ. Splenic ferroportin levels drop by 60% 4 hours after injection (Figure 3A). Ferroportin signal intensity was quantitated and normalized to the housekeeping gene GAPDH (Figure 3B). Interestingly, we did not observe significant differences in spleen iron content (Figure 2D, Figure 4) until 48 hours after PR65 injection and observed no change in liver iron content (enhanced Perls stain) through the course of the

experiment (Figure 4). From 1-4 hours after injection, duodenal sections showed distinct iron staining in villi capillary networks which indicated high ferroportin activity and uncurbed iron transfer. From 12-24 hours after PR65 injection, iron accumulates within enterocytes consistent with the expected inhibition by minihepcidin of iron transfer to plasma. As minihepcidin effects wear off 48 hours after minihepcidin injection, iron is no longer retained.

Minihepcidin can prevent iron loading in hepcidin-deficient mice

In the first set of experiments, we first placed hepcidin KO mice on an iron-deficient diet to lower their iron stores to a level comparable to WT, then examined the effect of PR65 on iron reloading after the mice were returned to a standard diet. After 8 weeks on a 4 ppm Fe diet, a group of mice was analyzed to obtain baseline iron parameters and blood counts and the rest of the mice were put on a 336 ppm Fe diet for 2 weeks. To assess the ability of minihepcidins to prevent body iron loading during a 14 day dietary iron challenge, mice received daily subcutaneous doses of 20, 50 or 100 nmoles of PR65 and a group of solvent-injected controls was used for each concentration of peptide. We hypothesized that PR65 would cause iron retention in the spleen and cause a reduction in liver and serum iron. Because cardiac iron overload is a marker for poor prognosis in iron-loaded patients, we also measured heart iron. Hemoglobin levels were monitored to detect potential iron-restrictive effects of hepcidin excess on erythropoiesis.

Hepcidin agonist activity of minihepcidins was confirmed in all treated groups by the increased retention of iron in macrophages manifested as increases in spleen iron content. Compared to the almost undetectable non-heme iron content in solvent-injected control spleens, all three minihepcidin doses showed 15-30 fold increases in spleen iron content ($p=0.010$ for all) (Figure

5A). Serum Fe did not change in mice that received 20 nmoles daily doses (p=0.257), but decreased by 69% and 83% in mice that received 50 and 100 nmoles doses per day (p=0.010 for both)(Figure 5B). The decrease in circulating iron concentrations was also reflected as a dose-dependent 3 and 5 g/dL drop in hemoglobin concentration in the 50 and 100 nmoles groups, respectively (p<.001 for both), but hemoglobin levels did not change significantly at 20 nmoles (p=0.130)(Figure 5C). Heart iron levels dropped 33%, 60% and 47% in mice treated with 20, 50 and 100 nmoles of PR65 (p=0.081, 0.007, 0.050)(Figure 5D). Additionally, PR65-treated mice showed 76%, 53% and 68% less liver iron than solvent treated controls (p=0.001, 0.060, 0.010) and no statistically significant increases compared to mice examined at the beginning of the experiment were observed.

Perls staining of liver and spleen sections showed no detectable liver iron in PR65- treated mice, but significant deposition into the red pulp of the spleen (Figure 6). Duodenal sections at baseline before dietary iron challenge show no iron staining, while solvent-treated mice show staining in the stroma of the villus, containing the blood supply. Only PR65-treated mice showed iron retention in the duodenum, again confirming peptide activity (inhibition of iron transfer to plasma) in these mice. Additionally, as mice received more peptide the total body iron load decreased as evidenced by the lack of iron staining in the heart and liver in mice that received 100 nmoles of peptide. Conversely, solvent treated mice accumulated large amounts of iron in the liver, but did not retain iron in the spleen.

Minihepcidin effect in iron-overloaded hepcidin knockout mice

Inducible overexpression of hepcidin in iron-loaded HFE-deficient mice was previously reported to be beneficial by causing redistribution of excess iron to hepatic macrophages (12). To assess

the potential of minihepcidins as a standalone treatment for iron overload, we injected 12 week old hepcidin deficient mice with 50 nmoles PR65 per day for 14 days. This dose was chosen as the maximal tolerated dose because mice that received 100 nmoles in the previous experiment became anemic. Peptide activity was confirmed by the 15-fold increase in spleen iron content ($p<0.001$)(Figure 7A). In contrast to mice that were iron depleted before injection, serum iron levels at day 14 were not decreased compared to solvent ($p=0.682$)(Figure 7B). However, considering a 2 g/dL decrease in hemoglobin ($p=0.012$)(Figure 7C), serum iron was likely transiently decreased during the treatment. PR65-treated iron-loaded mice showed a trend ($p=0.085$) toward decreased heart iron (Figure 7D). Liver iron levels decreased mildly by 4 μmoles/g ($p=0.009$) in PR65-injected mice (Figure 7E).

Enhanced Perls staining demonstrated iron retention in the spleen and duodenum in PR65-treated mice and a change in the iron distribution pattern in the liver (Figure 8). Additionally, heart iron staining appeared to be decreased but the decrease was not statistically significant in the quantitative iron assay ($p=0.085$). Iron staining of the pancreas also showed less intense staining in treated mice. In the aggregate, staining and quantitative analysis indicate that minihepcidin treatment alone can not only inhibit dietary iron absorption but also redistribute a modest amount of iron from vulnerable organs to the spleen.

Discussion

The goal of this study was to assess the feasibility of minihepcidins for the treatment of iron overload associated with hepcidin deficiency. Hepcidin deficiency is a common factor underlying the iron-loading syndromes associated with HH, β-thalassemia and certain viral or alcohol-induced liver diseases (13). Excess iron can be efficiently removed by phlebotomy or

chelation though treatment efficacy is compromised by suboptimal compliance, significant toxicity in the case of chelation, and the unwanted suppressive effects of these treatments on hepcidin. Hepcidin replacement or hepcidin agonist therapy is a potentially useful modality for inhibiting iron absorption and promoting redistribution of iron from the liver parenchyma and other vulnerable tissues to macrophages where it can be safely stored. The decrease of plasma iron could also reduce the levels of toxic non-transferrin bound iron (NTBI) and promote the mobilization of iron from the heart and endocrine organs where iron excess is not tolerated.

We previously reported that intraperitoneal administration (8 mg/kg/d) of a retro-inverso 9 amino acid hepcidin analogue prevented iron overload in hepcidin knockout mice without causing iron-restricted anemia (8). Because of the relatively large dose of hepcidin required to achieve therapeutic efficacy, it is important to develop more potent and less costly hepcidin mimetics. In the new set of analogues described in this study, the exclusive use of L-amino acids reduced peptide production costs significantly and the strategic incorporation of unnatural and highly aromatic residues reduced the minimal effective dose to 1.3 mg/kg/d.

According to FDA dosing adjustment guidelines, the difference in metabolic rates between mouse and human necessitates a conversion based on the Km factor which normalizes doses to body surface area (14). A human equivalent dose (HED) can be estimated by HED = animal dose (mg/kg) * (animal Km/human Km), where the Km for mouse and an adult human are 3 and 37, respectively. Thus, an expected subcutaneous dose of minihepcidin in a human could be in the range of 100 μg/kg/d, an amount of peptide roughly equivalent two to three times the typical dose of subcutaneous insulin 45 μg/kg/d in type 1 diabetics (15).

Our data are the first to demonstrate that minihepcidins could have a beneficial effect in the prevention of iron overload in patients at risk due to genetic defects or those who have already undergone iron depletion, but no longer tolerate chelation or venesection therapy. The potential benefit of minihepcidins in β-thalassemia major, where transfusions are major contributors to iron overload, remains to be explored. In these patients hepcidin levels are higher than in normal controls but are lower than appropriate for the degree of iron overload, and hepcidin concentrations decrease further as patients become more anemic before each transfusion (16)(17). It is possible that hyperabsorption of dietary iron contributes significantly to iron overload at least in patients who do not receive frequent transfusions. Moreover, minihepcidins could partially reverse ineffective erythropoiesis and improve anemia, as suggested by studies of the effects of transgenic hepcidin in a mouse model of β-thalassemia (7).

Unlike phlebotomy or chelation, minihepcidins will not appreciably increase iron losses from the body. In a relatively mild model of iron overload in HFE null mice (12), transgenic hepcidin expression was reported to cause significant redistribution of iron into hepatic macrophages, a location where iron accumulation is relatively nontoxic. In our more overloaded *Hamp1*$^{-/-}$ mice, red pulp macrophages in minihepcidin-treated mice retained iron but the small resulting decrease in liver and heart iron stores suggests that minihepcidins alone confer a minor therapeutic benefit once the liver iron burden is high.

Finally, the small size of minihepcidins raises the possibility that appropriately formulated and optimized peptides can be administered orally (8) or by other noninvasive means used for insulin delivery (18), further increasing their potential convenience and acceptability.

References

1. Ganz T, Nemeth E. Hepcidin and iron homeostasis. Biochimica Et Biophysica Acta [Internet]. 2012 [cited 2012 Mar 18];Available from: http://www.ncbi.nlm.nih.gov/pubmed/22306005

2. Rivera S, Nemeth E, Gabayan V, Lopez MA, Farshidi D, Ganz T. Synthetic hepcidin causes rapid dose-dependent hypoferremia and is concentrated in ferroportin-containing organs. Blood. 2005;106:2196–2199.

3. Nemeth E, Tuttle MS, Powelson J, Vaughn MB, Donovan A, Ward DM, et al. Hepcidin regulates cellular iron efflux by binding to ferroportin and inducing its internalization. Science. 2004;306:2090–2093.

4. Brissot P, Troadec M-B, Bardou-Jacquet E, Le Lan C, Jouanolle A-M, Deugnier Y, et al. Current approach to hemochromatosis. Blood Rev. 2008;22:195–210.

5. Girelli D, Pasino M, Goodnough JB, Nemeth E, Guido M, Castagna A, et al. Reduced serum hepcidin levels in patients with chronic hepatitis C. J. Hepatol. 2009;51:845–852.

6. Harrison-Findik DD, Schafer D, Klein E, Timchenko NA, Kulaksiz H, Clemens D, et al. Alcohol Metabolism-mediated Oxidative Stress Down-regulates Hepcidin Transcription and Leads to Increased Duodenal Iron Transporter Expression. J.Biol.Chem. 2006;281:22974–22982.

7. Gardenghi S, Ramos P, Marongiu MF, Melchiori L, Breda L, Guy E, et al. Hepcidin as a therapeutic tool to limit iron overload and improve anemia in β-thalassemic mice. J. Clin. Invest. 2010;120:4466–4477.

8. Preza GC, Ruchala P, Pinon R, Ramos E, Qiao B, Peralta MA, et al. Minihepcidins are rationally designed small peptides that mimic hepcidin activity in mice and may be useful for the treatment of iron overload. J. Clin. Invest. 2011;121:4880–4888.

9. Preza GC, Ruchala P, Pinon R, Ramos E, Qiao B, Peralta MA, et al. Minihepcidins are rationally designed small peptides that mimic hepcidin activity in mice and may be useful for the treatment of iron overload. J Clin Invest. 2011;

10. Nicolas G, Bennoun M, Devaux I, Beaumont C, Grandchamp B, Kahn A, et al. Lack of hepcidin gene expression and severe tissue iron overload in upstream stimulatory factor 2 (USF2) knockout mice. Proceedings of the National Academy of Sciences. 2001;98:8780–8785.

11. Ramos E, Kautz L, Rodriguez R, Hansen M, Gabayan V, Ginzburg Y, et al. Evidence for distinct pathways of hepcidin regulation by acute and chronic iron loading in mice. Hepatology. 2011;53:1333–1341.

12. Viatte L, Nicolas G, Lou DQ, Bennoun M, Lesbordes-Brion JC, Canonne-Hergaux F, et al. Chronic hepcidin induction causes hyposideremia and alters the pattern of cellular iron accumulation in hemochromatotic mice. Blood. 2006;107:2952–2958.

13. Goodnough JB, Ramos E, Nemeth E, Ganz T. Inhibition of hepcidin transcription by growth factors. Hepatology (Baltimore, Md.) [Internet]. 2012 [cited 2012 Mar 18];Available from: http://www.ncbi.nlm.nih.gov/pubmed/22278715

14. Reagan-Shaw S, Nihal M, Ahmad N. Dose translation from animal to human studies revisited. FASEB J. 2008;22:659–661.

15. Margeirsdottir HD, Stensaeth KH, Larsen JR, Brunborg C, Dahl-Jørgensen K. Early Signs of Atherosclerosis in Diabetic Children on Intensive Insulin Treatment A Population-Based Study. Dia Care. 2010;33:2043–2048.

16. Origa R, Galanello R, Ganz T, Giagu N, Maccioni L, Faa G, et al. Liver iron concentrations and urinary hepcidin in beta-thalassemia. Haematologica. 2007;92:583–588.

17. Kearney SL, Nemeth E, Neufeld EJ, Thapa D, Ganz T, Weinstein DA, et al. Urinary hepcidin in congenital chronic anemias. Pediatr.Blood Cancer. 2007;48:57–63.

18. Khafagy E-S, Morishita M, Onuki Y, Takayama K. Current challenges in non-invasive insulin delivery systems: a comparative review. Adv. Drug Deliv. Rev. 2007;59:1521–1546.

Table 1. **Example of minihepcidin primary sequence optimization**. We tested substitution of Aspartic acid with an achiral homologue Ida in PR59-61. Phenylalanine 4 substitution with Diphenylalanine increased hydrophobicity and Phenylalanine 9 with a beta-homo analogue increased resitance to proteolysis. Proline 5 was also substititued with its beta-homo equivalent to increase resistance to proteolysis. Isoleucine 6 and 8 were substituted with arginine or aminocyclohexanoic acid to increase hydrophobic interactions with ferroportin. α-aminocyclohexanoic acid substitution increases hydrophobicity and resistance to proteolytic degradation.

Abbreviations: D- Aspartic acid T- Threonine H- Histidine F- Phenylalanine P- Proline I- Isoleucine C- Cysteine PEG- polyethylene glycol

Ida- Iminodiacetic acid Dpa- Diphenylalanine bhPro- beta-homo Proline R- Arginine Ach- Aminocyclohexanoic acid

bhPhe- beta-homo Phenylalanine

Sequence Name	*In vitro* EC 50 nM	i.p. Activity	N-terminus								Carboxy-amide terminus	Linker	Fatty Acid
Hepcidin 9			D	T	H	F	P	I	C^{SH}	I	F	-	-
PR59	<10	Partial	Ida	T	H	Dpa	bhPro	Ile	C^{SH}	Ile	bhPhe	PEG+ miniPEG3	Palmitoyl
PR60	<10	Partial	Ida	T	H	Dpa	P	Ach	C^{SH}	Ach	Phe	PEG+ miniPEG3	Palmitoyl
PR61	10	Full	Ida	T	H	Dpa	bhPro	R	C^{SH}	R	bhPhe	PEG+ miniPEG3	Palmitoyl

Table 2**. Example of minihepcidin functional group optimization**. Selecting PR61 for its high activity *in vivo*, we eliminated the mini PEG3 moiety (PR 65), both PEG groups and fatty acid (PR 65) or both PEG groups while retaining the fatty acid (PR 71).

Abbreviations not used in Table I: PEG- polyethylene glycol

i.p.-intraperitoneal activity s.c.- subcutaneous activity

Sequence Name	Gavage	i.p.	s.c.	N-terminus								Carboxy-amide terminus	Linker	Fatty Acid
Hepcidin 9				D	T	H	F	P	I	C^{SH}	I	F	-	-
PR61	Yes	Yes	Yes	Ida	T	H	Dpa	bhPro	R	C^{SH}	R	bhPhe	mini-PEG3+ PEG11	Palmitoyl
PR65	No	Yes	Yes	Ida	T	H	Dpa	bhPro	R	C^{SH}	R	bhPhe	PEG11	Palmitoyl
PR66	No	Yes	No	Ida	T	H	Dpa	bhPro	R	C^{SH}	R	bhPhe	-	-
PR71	No	Yes	Yes	Palmitl-Ida	T	H	Dpa	bhPro	R	C^{SH}	R	bhPhe	-	On N-terminus

Table 3. **List of minihepcidins without fatty acid or linker enhancement screened *in vitro***. We made substitutions in the following manner: PR 29-33 F 4 substitution, PR33-39 F 9 substitution, PR40-41 D 1 and T 2 elimination, PR42-46 F4,9 I 6,8 P5 substitution.

Abbreviations not used in Tables I or II: 1Nal- 1-Naphthyl-alanine, Bip- Biphenylalanine, Oic- Octahydroindole-2-carboxylic acid, (D) indicates the D- version of an amino acid was used.

In vitro EC50 (nM)	Name	N-terminus								Carboxy-amide terminus
700	PR29	D	T	H	bhPhe	P	I	C^{SH}	I	F
30	PR30	D	T	H	Dpa	P	I	C^{SH}	I	F
150	PR31	D	T	H	Bip	P	I	C^{SH}	I	F
110	PR32	D	T	H	1Nal	P	I	C^{SH}	I	F
80	PR33	D	T	H	bhDpa	P	I	C^{SH}	I	F
150	PR34	D	T	H	F	P	I	C^{SH}	I	bhPhe
70	PR35	D	T	H	F	P	I	C^{SH}	I	Dpa
150	PR36	D	T	H	F	P	I	C^{SH}	I	Bip
200	PR37	D	T	H	F	P	I	C^{SH}	I	1Nal
100	PR38	D	T	H	F	P	I	C^{SH}	I	bhDpa
35	PR39	D	T	H	Dpa	P	I	C^{SH}	I	Dpa
70	PR40			H	Dpa	P	I	C^{SH}	I	F
300	PR41			H	Dpa	P	I	C^{SH}	I	Dpa
30	PR42	D	T	H	Dpa	P	R	C^{SH}	R	Dpa
200	PR43	D	T	H	Dpa	P	(D)R	C^{SH}	(D)R	Dpa
30	PR44	D	T	H	Dpa	Oic	I	C^{SH}	I	F
150	PR45	D	T	H	Dpa	Oic	I	C^{SH}	I	Dpa
80	PR46	D	T	H	Dpa	P	C^{SH}	C^{SH}	C^{SH}	Dpa

Table 4. **Retroinverso "all D-amino acid" peptides with fatty acid and linker enhancement screened *in vitro* or *in vivo***. A retroinverso peptide is synthesized only with D-amino acids and in reverse order (aspartic acid first instead of F9 for hepcidin 9) to make a highly resistant mirror image of the parent peptide. PR47 tested retroinversion of hepcidin 9 with substitution of F4, PR48 substitution of F4 and F9 together, PR 49-PR50 elimination of D and T, PR51 V for I substitution, and PR52 L for I substitution. PR76-79 tested the effect of different fatty acid chain lengths from 4-24 carbons as well as substitution of t-butyl blocked cysteine and substitution of F with tryptophan for possible quantification of peptide absorption through spectrophotometric methods.

Abbreviations not used in Tables I-III: tBut- tertiary-butyl, Trp- tryptophan, V- Valine, L- Leucine

EC50 nM	Name	Fatty Acid	Linker	N-terminus								Carboxy-amide terminus	
	Hepcidin 9	-	-	D	T	H	F	P	I	C^{SH}	I	F	
50	PR47	Palmitoyl	PEG11	F	I	C^{SH}	I	P	Dpa	His	T	D	"all D"
50	PR48	Palmitoyl	PEG11	Dpa	I	C^{SH}	I	P	Dpa	His	T	D	"all D"
<10	PR49	Palmitoyl	PEG11	F	I	C^{SH}	I	P	Dpa	His			"all D"
<10	PR50	Palmitoyl	PEG11	Dpa	I	C^{SH}	I	P	Dpa	His			"all D"
100	PR51	Palmitoyl	PEG11	F	V	C^{SH}	V	P	Dpa	His	T	D	"all D"
<10	PR52	Palmitoyl	PEG11	F	L	C^{SH}	L	P	Dpa	His	T	D	"all D"
	PR76	Butanoyl (C4)	PEG11	Trp	R	$C^{S\text{-}StBut}$	R	P	F	His	T	D	"all D"
	PR77	Octanoyl (C8, Caprylic)	PEG11	Trp	R	$C^{S\text{-}StBut}$	R	P	F	His	T	D	"all D"
	PR78	Palmitoyl (C16)	PEG11	Trp	R	$C^{S\text{-}StBut}$	R	P	F	His	T	D	"all D"
	PR79	Tetra-cosanoyl (C24, Lignoceric)	PEG11	Trp	R	$C^{S\text{-}StBut}$	R	P	F	His	T	D	"all D"

Table 5, Part I. L-amino acid peptides containing fatty acid or linker enhancement tested *in vitro* or *in vivo*: PR53-57 increased resistance to proteolysis by the introduction of methylated and beta-homo amino amino acids. The extra methyl or eythl groups in these amino acids are not recognized as well by cellular proteolytic machinery. PR58-61 improved proteolytic resistance with an achiral aspartic acid homologue, iminodiacetic acid, as well as hydrophobic substitutions.

Abbreviation not used in Tables I-IV: N-MeAsp- N-methyl-aspartic acid, N-MeR- N-Methyl Arginine

In vitro EC50 (nM)	Name	N-terminus								Carboxy-amide terminus	Linker	Fatty Acid
10	PR53	N-MeAsp	T	H	Dpa	P	Ile	C^{SH}	Ile	bhPhe	PEG + miniPEG3	Palmitoyl
10	PR54	N-MeAsp	T	H	Dpa	bhPro	Ile	C^{SH}	Ile	bhPhe	PEG + miniPEG3	Palmitoyl
10	PR55	N-MeAsp	T	H	Dpa	P	Ach	C^{SH}	Ach	Phe	PEG + miniPEG3	Palmitoyl
15	PR56	N-MeAsp	T	H	Dpa	Oic	R	C^{SH}	R	bhPhe	PEG + miniPEG3	Palmitoyl
<10	PR57	N-MeAsp	T	H	Dpa	bhPro	R	C^{SH}	R	bhPhe	PEG + miniPEG3	Palmitoyl
<10	PR58	Ida	T	H	Dpa	P	Ile	C^{SH}	Ile	bhPhe	PEG + miniPEG3	Palmitoyl
<10	PR59	Ida	T	H	Dpa	bhPro	Ile	C^{SH}	Ile	bhPhe	PEG + miniPEG3	Palmitoyl
<10	PR60	Ida	T	H	Dpa	P	Ach	C^{SH}	Ach	Phe	PEG + miniPEG3	Palmitoyl
10	PR61	Ida	T	H	Dpa	bhPro	R	C^{SH}	R	bhPhe	PEG + miniPEG3	Palmitoyl

Table 5 Part II**. L-amino acid peptides screened only *in vivo***. PR62-64 tested resistance to proteolysis with D-amino or methylated amino acid substitutions. PR67-70 tested different methods of attaching the fatty acid group to cysteine to facilitate synthesis.

Abbreviations not used previously: Pal- palmitoyl, N-Me-R- N-Methyl-Arginine, bh-R- beta-homo Arginine

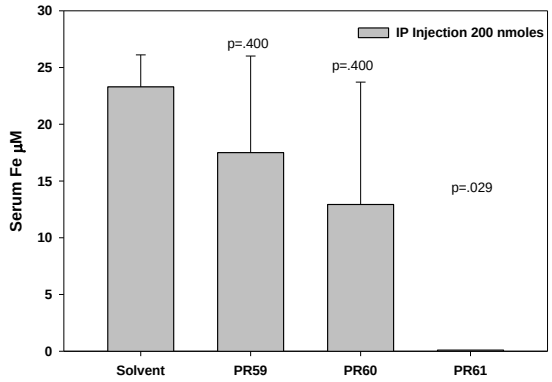
Name	N-terminus								Carboxy-amide terminus	Linker	Fatty Acid
PR62	Ida	T	H	Dpa	bhPro	(D) R	C^{SH}	(D) R	bhPhe	PEG+ miniPEG3	Palmitoyl
PR63	Ida	T	H	Dpa	bhPro	N-Me-R	C^{SH}	N-Me-R	bhPhe	PEG+ miniPEG3	Palmitoyl
PR64	Ida	T	H	Dpa	bhPro	bhR	C^{SH}	bh-R	bhPhe	PEG + miniPEG3	Palmitoyl
PR65	Ida	T	H	Dpa	bhPro	R	C^{SH}	R	bhPhe	PEG	Palmitoyl
PR66	Ida	T	H	Dpa	bhPro	R	C^{SH}	R	bhPhe	-	-
PR67	Ida	T	H	Dpa	bhPro	R	C(S-S-C16H33)	R	bhPhe		On Cysteine
PR68	Ida	T	H	Dpa	bhPro	R	C(S-S-CH2CH2NH-Pal)	R	bhPhe		On Cysteine
PR69	Ida	T	H	Dpa	bhPro	R	C(S-S-C-NHPal)	R	bhPhe		On Cysteine
PR70	Ida	T	H	Dpa	bhPro	R	C(S-S-C)	R	bhPhe	PEG + miniPEG3	Palmitoyl

Table 5, Part III. **List of L-amino acid mini hepcidins tested *in vivo***. PR 71 tested attachment of fatty acid directly to the N-terminus. PR72-73 tested attachment of the fatty acid to the C-terminus with different amin acid linkers. PR 74 substituted the 16 carbon fatty acid with N,N-dibenzylamide. PR75 tested attachment of the fatty through thioglycolic acid. PR 80-82 tested peptide activity with substitution of beta-homo amino acids with less expensive counterparts.

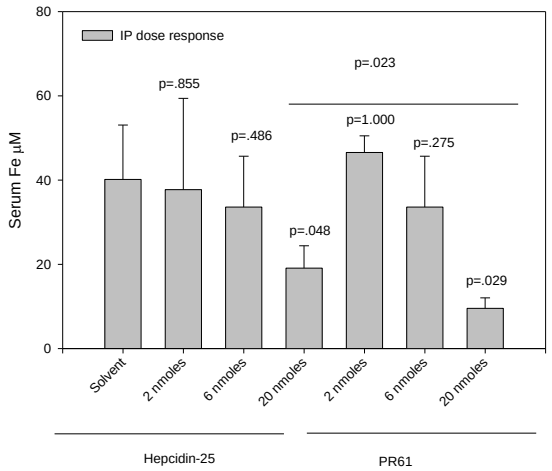
Abbreviations not used previously: Ahx- Aminohexanoic acid Ac-S-Pal - (S-palmityl) thioglycolic acid, NBzl2- N,N-dibenzylamide

Name	N-terminus								Carboxy-amide terminus	Linker	Fatty Acid
PR71	Ida-NHPal	T	H	Dpa	bhPro	R	C^{SH}	R	bhPhe		On N-terminal Ida
PR72	Ida	T	H	Dpa	bhPro	R	C^{SH}	R	bhPhe	Ida	NHPal
PR73	Ida	T	H	Dpa	bhPro	R	C^{SH}	R	bhPhe	Ahx	Ida-NHPal
PR74	Ida	T	H	Dpa	bhPro	R	C^{SH}	R	bhPhe	Ahx	Ida-NBzl2
PR75	Ida	T	H	Dpa	bhPro	R	C^{SH}	R	bhPhe	-	Ac-S-Pal
PR80	Ida	T	H	Dpa	bhPro	R	C^{SH}	R	Phe	Ahx	Ida-NHPal
PR81	Ida	T	H	Dpa	Pro	R	C^{SH}	R	Phe	Ahx	Ida-NHPal
PR82	Ida	T	H	Dpa	bhPro	R	C^{SH}	R	Trp	Ahx	Ida-NHPal

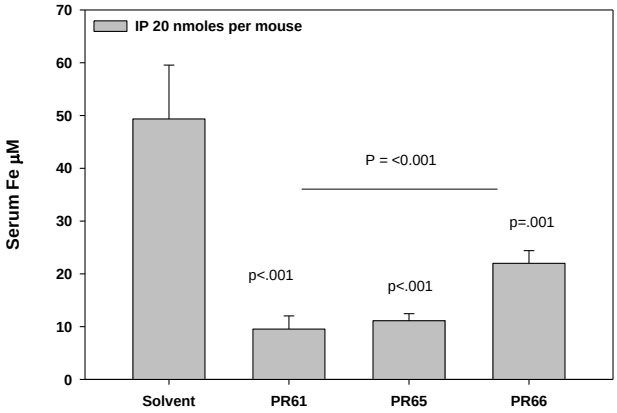
1A)


IP Injection 200 nmoles
Serum Fe µM
30
25
20
15
10
5
0
p=.400
p=.400
p=.029
Solvent
PR59
PR60
PR61

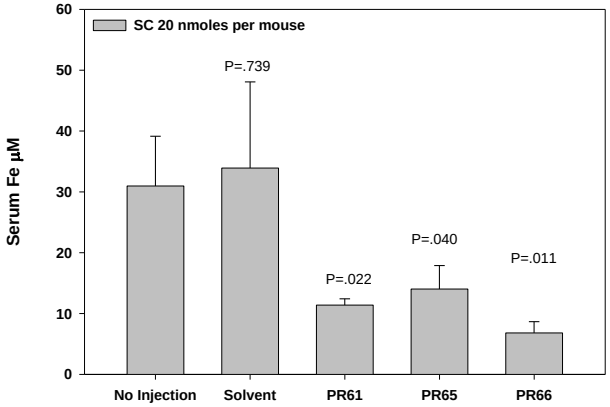
1B)


IP dose response
Serum Fe µM
80
60
40
20
0
p=.023
p=.855
p=.486
p=1.000
p=.275
p=.048
p=.029
Solvent
2 nmoles
6 nmoles
20 nmoles
2 nmoles
6 nmoles
20 nmoles
Hepcidin-25
PR61

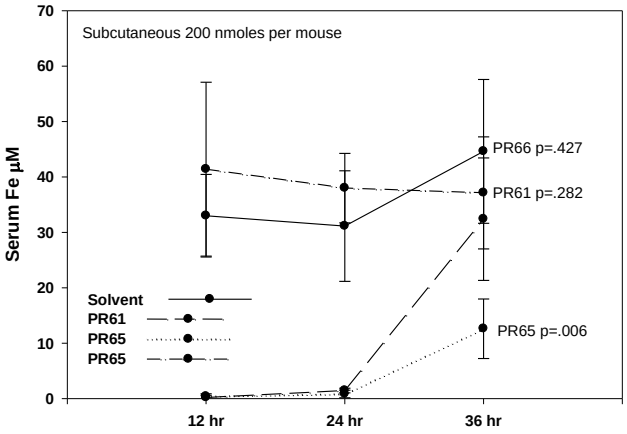
1C)


IP 20 nmoles per mouse
Serum Fe µM
70
60
50
40
30
20
10
0
P = <0.001
p<.001
p<.001
p=.001
Solvent
PR61
PR65
PR66

1D)


SC 20 nmoles per mouse
Serum Fe µM
60
50
40
30
20
10
0
P=.739
P=.022
P=.040
P=.011
No Injection
Solvent
PR61
PR65
PR66

1E)



1F)

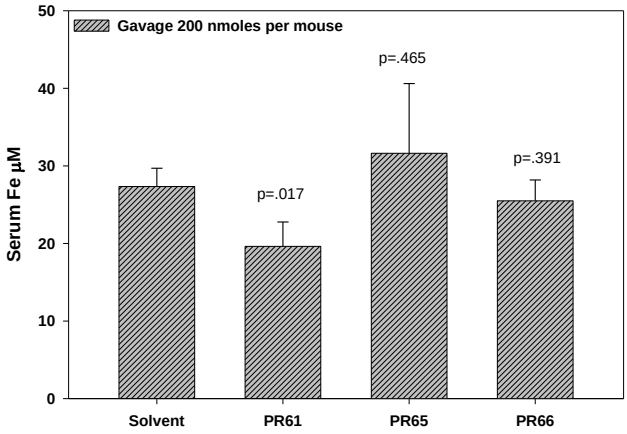


Figure 1A-F. Optimization of minihepcidins. A) We substituted various amino acids to improve mini hepcidin potency and resistance to proteolysis. Substitution of Ile 6 and 8 with Arg was important for *in vivo* activity. B) In the comparison of PR61 to full length hepcidin through i.p. injection and found that PR61 was more active (p=0.023). C) Selecting PR61 as a candidate for optimization, we eliminated hydrophobic functional groups and found that both PEG and palmitoyl groups were important for activity. D) We tested subcutaneous injection as an alternative route of administration and found that at 4 hours and 20 nmoles dose PR61 and its derivatives were active. E) At a 200 nmoles dose, PR66, lacking PEG and fatty acid groups, was not active after 12, 24 or 36 hours. F) As a proof of principle, we tested PR61 and variants for oral activity and found that only PR61 was active, indicating that the extra mini-PEG 3 group was crucial for oral absorption.

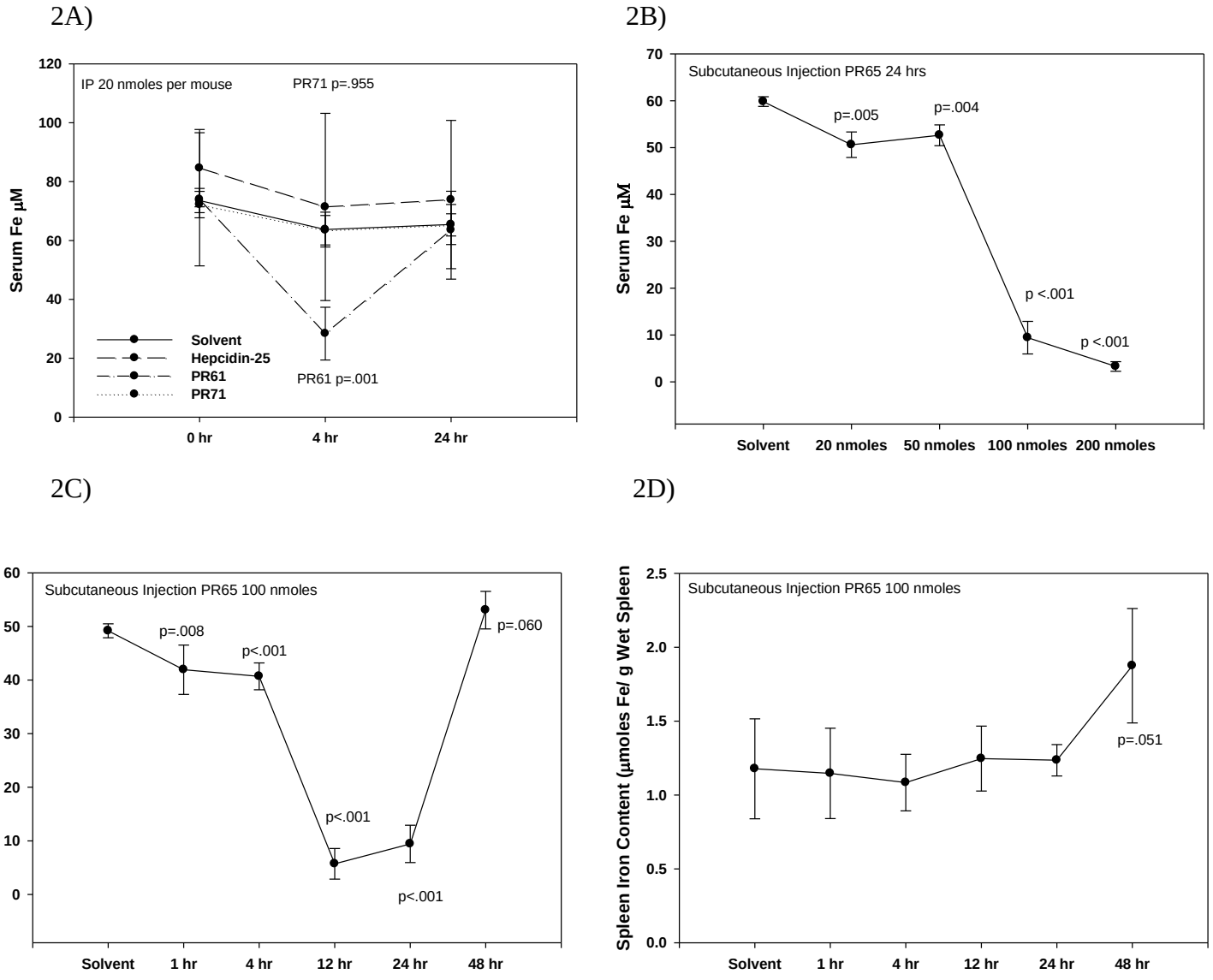
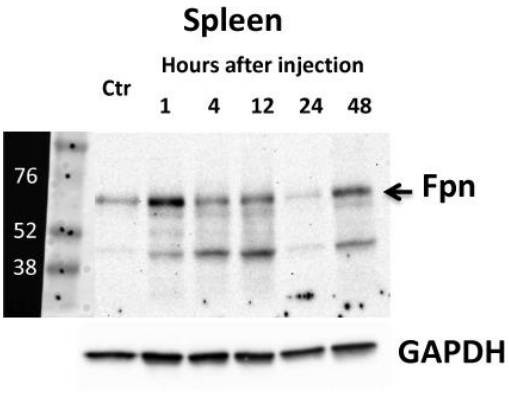


Figure 2A-D. Characterization of minihepcidin kinetics in hepcidin deficient mice. A) We measured serum iron before peptide injection and 4 and 24 hours after and found that only PR61 was active but not full length hepcidin nor PR71. B) Selecting PR66, a close derivative of PR61, as the most active hepcidin mimetic, we determined that 100 nmoles through s.c. injection was sufficient to maintain serum iron levels low for at least 24 hours. C) A time course of 100 nmoles of PR65 determined that the nadir in serum iron was at 12 hours, similar at 24 and returns to baseline 48 hours after injection. D) Measurement of spleen iron content showed that iron retention in macrophages begins to increase measurably 48 hours after injection.

3A)



3B)



Figure 3A-C. Modulation of ferroportin levels by mini hepcidin. A) We measured ferroportin (Fpn) levels in spleen lysates at intervals from 1-48 hours after mini hepcidin treatment and an initial drop at 4 hours, nadir at 24 and trend toward normal after 48 hours. B) Quantitation of chemiluminescent signal using Image Lab software (BioRad).

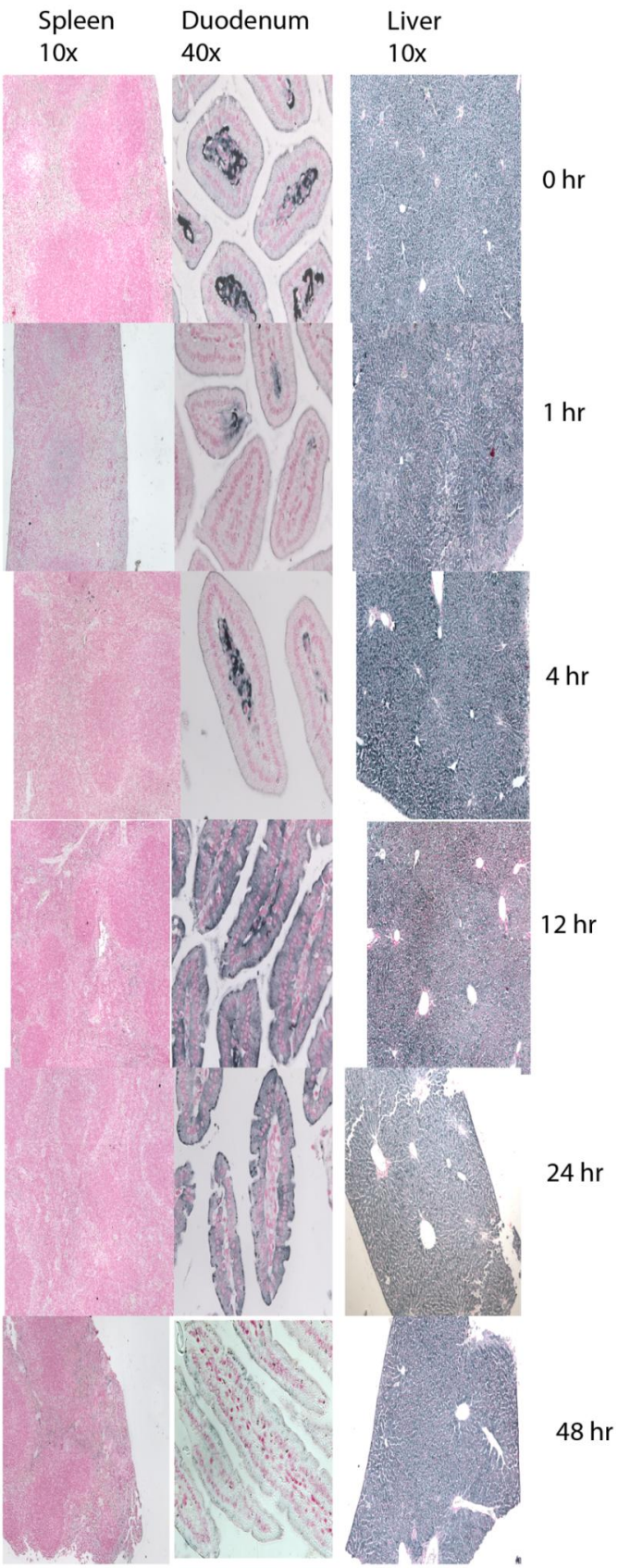
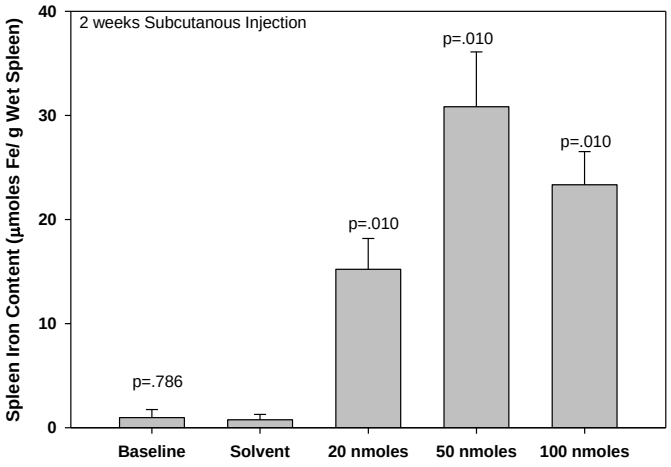
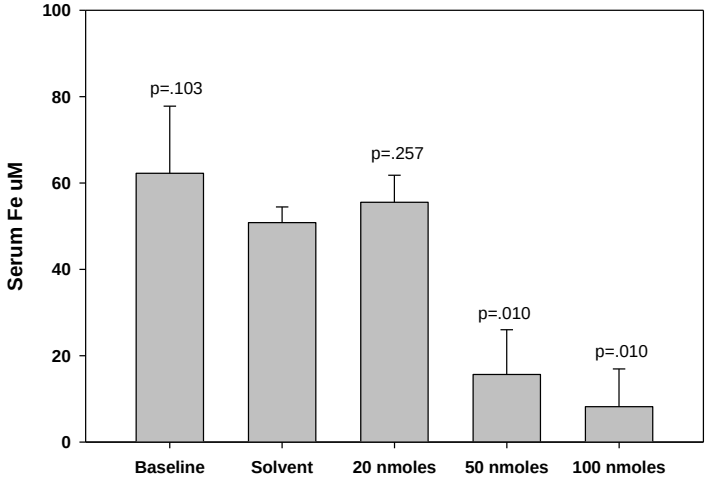

Spleen
10x
Duodenum
40x
Liver
10x
0 hr
1 hr
4 hr
12 hr
24 hr
48 hr

Figure 4. Iron distribution kinetics in minihepcidin treated mice. We used an enhanced Perls stain (Vector labs) to visualize iron at intervals from 1-48 hours after PR65 injection and show representative sections from individual mice (Solvent n=5,1 hr n=6,4 hr n=5,12 hr n=4, 24 hr n=5 and 48 hr n=3). We found that spleen iron begins to accumulate 48 hours after injection. We did not observe any significant changes in liver iron staining. We did, however, observe iron in villus stroma in solvent and 1-4 hour PR65 treated mice, indicating high ferroportin activity. From 12-24 hours, we observed iron retention in enterocytes as expected when ferroportin degradation occurs. 48 hours after injection, iron was no longer retained by enterocytes.

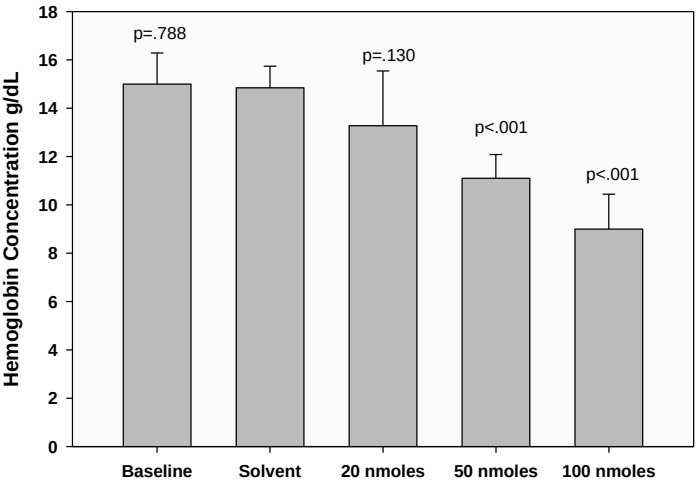
5A)


2 weeks Subcutanous Injection
Spleen Iron Content (µmoles Fe/ g Wet Spleen)
40
30
20
10
0
p=.786
p=.010
p=.010
p=.010
Baseline
Solvent
20 nmoles
50 nmoles
100 nmoles

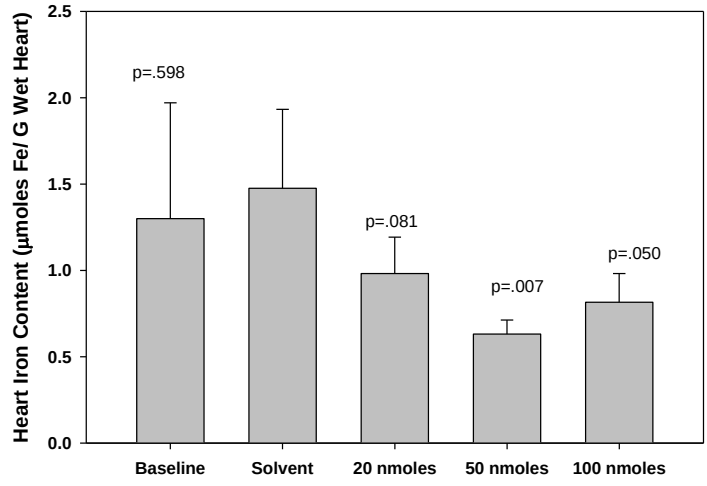
5B)


Serum Fe uM
100
80
60
40
20
0
p=.103
p=.257
p=.010
p=.010
Baseline
Solvent
20 nmoles
50 nmoles
100 nmoles

5C)


Hemoglobin Concentration g/dL
18
16
14
12
10
8
6
4
2
0
p=.788
p=.130
p<.001
p<.001
Baseline
Solvent
20 nmoles
50 nmoles
100 nmoles

5D)


Heart Iron Content (µmoles Fe/ G Wet Heart)
2.5
2.0
1.5
1.0
0.5
0.0
p=.598
p=.081
p=.007
p=.050
Baseline
Solvent
20 nmoles
50 nmoles
100 nmoles

5E)

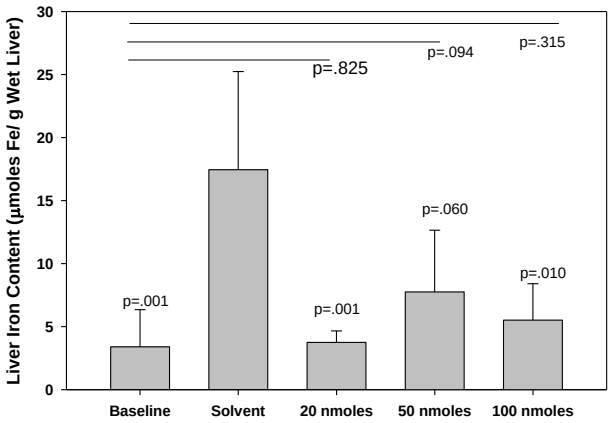

Liver Iron Content (µmoles Fe/ g Wet Liver)
30
25
20
15
10
5
0
p=.825
p=.094
p=.315
p=.001
p=.001
p=.060
p=.010
Baseline
Solvent
20 nmoles
50 nmoles
100 nmoles

Figure 5A-E. Daily hepcidin injection prevents iron loading in iron-depleted hepcidin knockout mice. All mice were placed on an iron-deficient 4 ppm iron diet from 4-12 weeks of age. The "baseline" group was sacrificed at 12 weeks of age, while the rest of the mice were challenged with a 336 ppm iron diet for 2 weeks and divided into groups receiving solvent, 20, 50 or 100 nmoles of PR65 at 24 hour intervals for the rest of the experiment. A) Spleen iron assay indicated that only PR65-treated mice retained iron. B) In mice that received PR65, dose-dependent decrease in serum iron levels was seen. C) In PR65-treated mice, an analogous dose-dependent decrease in Hb levels was observed. D) Heart iron levels trended to decrease in all PR65-treated mice, but statistical significance was achieved only in mice that received 50 nmoles. E) Liver iron was lower in all PR65-treated mice and not significantly different from the group of mice sacrificed before the iron challenge indicating that little to no new iron was absorbed.

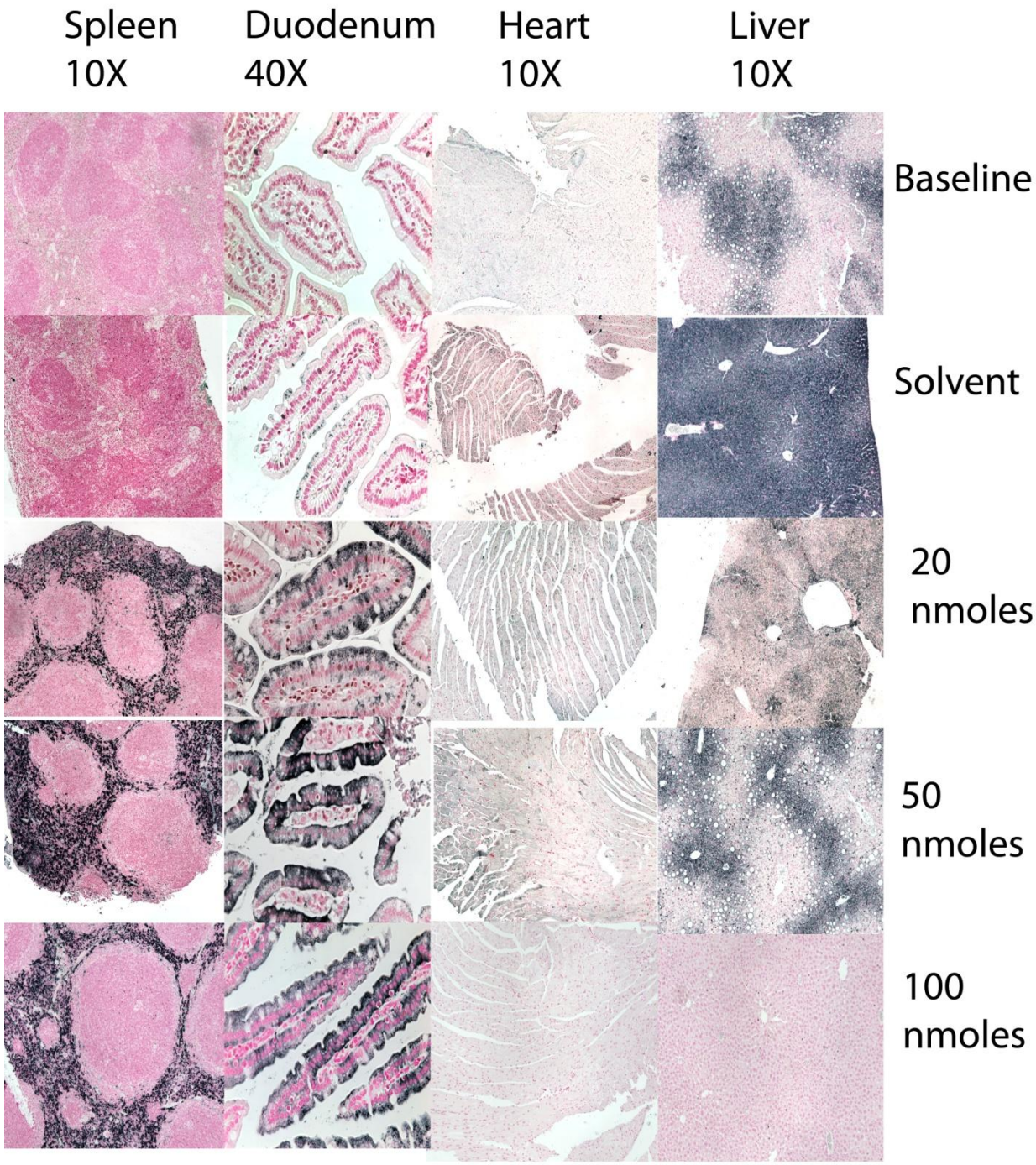
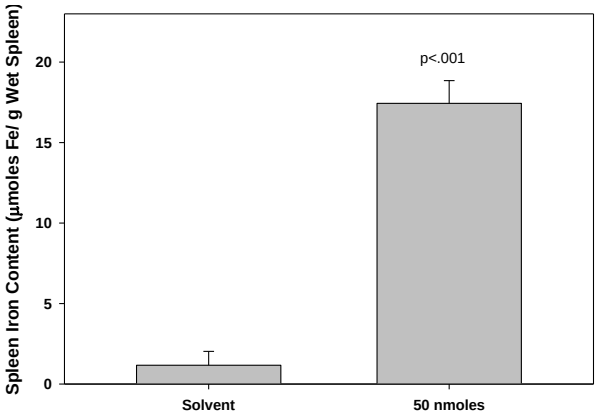
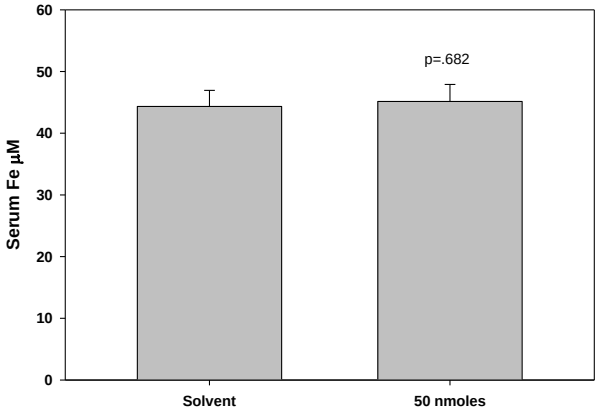

Spleen
10X
Duodenum
40X
Heart
10X
Liver
10X
Baseline
Solvent
20
nmoles
50
nmoles
100
nmoles

Figure 6. Enhanced Perls stain of organs in the iron overload prevention study.
Representative sections show iron staining in the spleens of peptide treated iron-depleted mice only in mice that received PR65 (Baseline n=7, Solvent n=6, 20,50 and 100 nmoles n=4). Similarly, iron accumulation in duodenal enterocytes was seen only in PR65-treated mice. Compared to baseline heart iron staining, mice that received 50 and 100 nmoles of PR65 showed less iron accumulation corroborating the quantitative method in Figure 5. Heart iron content in mice treated with 20 and 50 nmoles of PR65 was not significantly different from baseline, and no iron was detectable in mice that received the highest dose, indicating that mice were able to mobilize cardiac iron despite high minihepcidin activity.

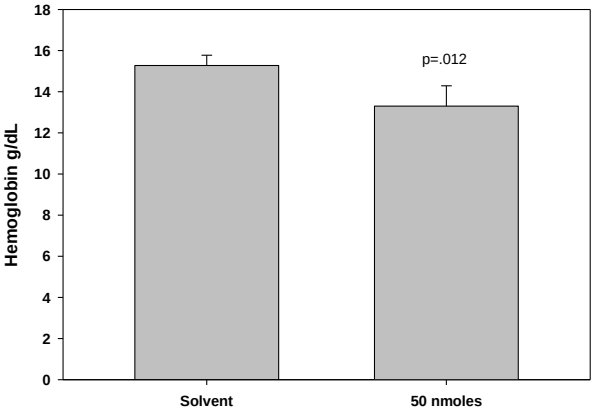
7A)


Spleen Iron Content (µmoles Fe/ g Wet Spleen)
0
5
10
15
20
p<.001
Solvent
50 nmoles

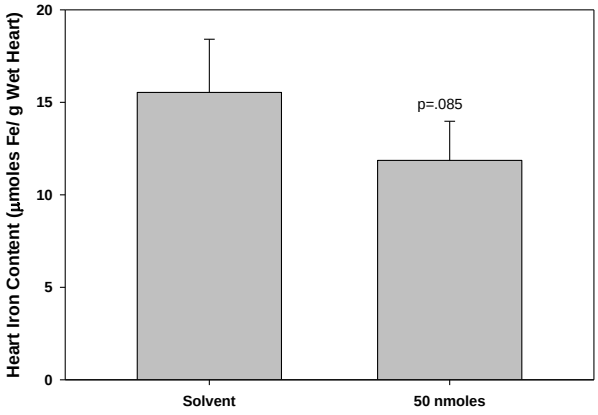
7B)


Serum Fe µM
0
10
20
30
40
50
60
p=.682
Solvent
50 nmoles

7C)


Hemoglobin g/dL
0
2
4
6
8
10
12
14
16
18
p=.012
Solvent
50 nmoles

7D)


Heart Iron Content (µmoles Fe/ g Wet Heart)
0
5
10
15
20
p=.085
Solvent
50 nmoles

7E)

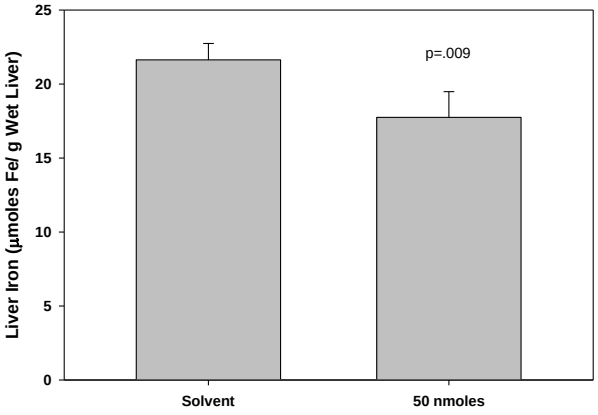

Liver Iron (µmoles Fe/ g Wet Liver)
0
5
10
15
20
25
p=.009
Solvent
50 nmoles

Figure 7. Daily minihepcidin injection in iron-loaded mice causes modest redistribution of iron. Two groups of hepcidin knockout mice were kept on a 336 ppm iron diet for their entire lifespan. One group of mice was injected with solvent and the other with 50 nmoles of PR65 daily for 24 days during weeks 12-14. A) Peptide activity was confirmed by the greater than 15-fold increase in spleen iron. B) In contrast to mice that were iron-depleted before iron challenge, mice that received 50 nmoles of PR65 did not change their serum iron levels. C) Hemoglobin levels decreased by 2 g/dL in PR65-treated mice. D) Heart iron levels tended to decrease in peptide treated mice, though the difference was not statistically significant. E) Liver iron decreased modestly in PR65-treated mice.

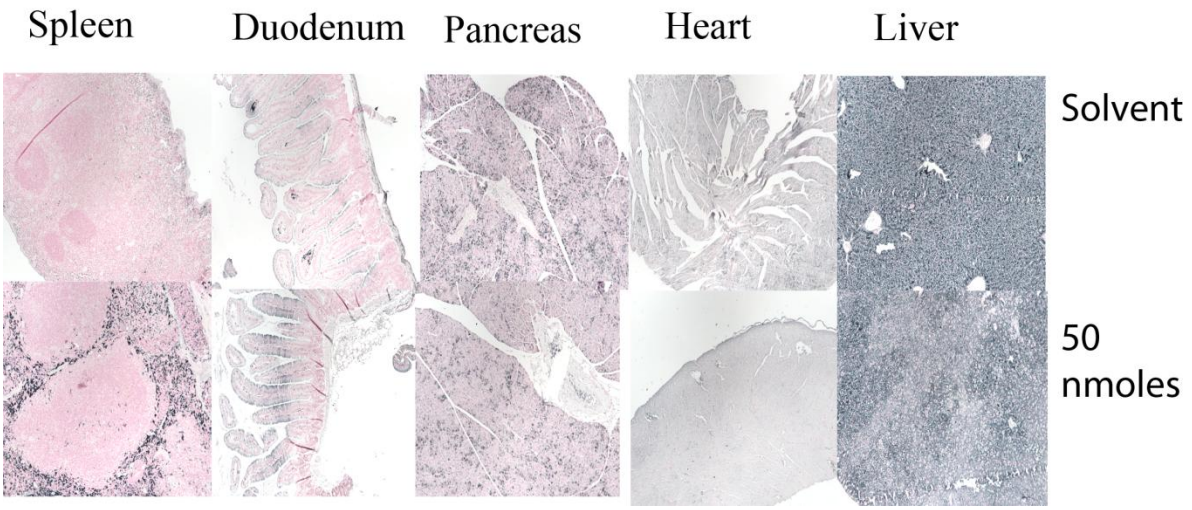


Figure 8. Enhanced Perls stain of redistribution study. Representative iron stains of tissue samples from the redistribution study corroborated the quantitative iron measurements. Splenic macrophage and enterocyte iron was visible only in PR65-treated mice (n=4). Compared to solvent-treated controls (n=4), less intense iron staining was observed in the pancreas, heart and liver of mice treated with PR65.

Concluding remarks

One of the two foci of this dissertation was to characterize the nature of hepcidin deficiency and the ensuing misdistribution of iron. We studied the physiology and cellular mechanisms of hepcidin deficiency due to genetic maladies as in hereditary hemochromatosis (HH) (Chapter 1) or liver injury (Chapter 2). Each chapter presents novel insights into the pathophysiological regulation of hepcidin.

In chapter 1, evidence for a new level of hepcidin regulation by iron stores was presented. Much of the prior work focused on how circulating iron induces hepcidin production. In this study we studied the effect of increasing iron stored on hepcidin and found that extracellular and intracellular iron regulate hepcidin production independently. The extracellular pathway senses changes in transferrin levels and requires at least the HFE, TfR2, HJV and BMP6 proteins for proper hepcidin production. We also found that as liver iron stores increased in mice that suffer from hemochromatosis, hepcidin levels increased proportionately. Interestingly, hepcidin responds to increases in stored iron despite ablation of crucial hepcidin producing genes, HFE, TfR2, HJV and BMP6. Though it is not clear how iron stores regulate hepcidin production, a recent study suggests that soluble ferritin, which is not as iron rich as cytosolic ferritin, can induce hepcidin transcription (1). Thus, in states of liver iron overload such as hereditary hemochromatosis which is typically diagnosed by high soluble ferritin levels in the serum, hepatocytes may respond to increased ferritin to increase hepcidin. Though iron stores play an important role in regulating hepcidin production in iron overloaded states, the significance of this pathway has yet to be determined in normal physiology.

Chapter 2 is the first study to detail a signaling pathway that suppresses hepcidin production. Most of the in depth understanding of hepcidin regulation relates to stimulatory pathways such as iron and inflammation, but little was known about the pathways that down-regulate hepcidin. We identified hepatocyte growth factor (HGF), which is increased during liver repair, as a likely physiological hepcidin suppressor. Importantly, in this chapter we describe how HGF or related hormones suppress hepcidin transcription by blocking the nuclear translocation of SMAD transcription factors which are required for hepcidin stimulation in response to iron. When the PI3 kinase pathway was inhibited chemically, HGF no longer suppressed hepcidin, suggesting that PI3 kinases at least partially mediate the suppressive effect. Ultimately, this study provides novel molecular insights into the pathogenesis of hepcidin deficiency in chronic liver diseases. Future studies may determine whether the HGF pathway acts physiologically to suppress hepcidin during development to allow iron uptake during periods of rapid growth early in life.

Our second research focus was to develop a novel treatment for hepcidin deficiency. Though there are varying degrees of hepcidin deficiency in HH, liver damage as well as β-thalassemia intermedia, re-establishing normal hepcidin levels would be the most direct method to prevent the body from accumulating toxic levels of iron in the first place. Through the rational design (Chapter 3) and thorough testing of (Chapter 4) minihepcidins in mouse models of iron overload, our group has devised a new approach to the treatment or prevention of iron overload. Our experiments in mouse models have shown that hepcidin replacement therapy with minihepcidins is effective as well as economically feasible when scaled up to humans, providing strong justification for testing minihepcidins in humans. Though hepcidin replacement therapy is directly suited to patients who suffer from hereditary hemochromatosis, the current treatment,

phlebotomy, is safe, inexpensive and effective. For these reasons, the financial incentives may be too small for companies to undertake the expense of developing minihepcidins into a clinical product for this indication alone (2).

Thus, initial trials of minihepcidins would require a patient population that suffers from hepcidin deficiency, but cannot be phlebotomized. Though not as common as hereditary hemochromatosis, close to 5% of the world's population carries globin chain variants and approximately 1.6% are heterozygous for α or β-thalassemia (3). Due to inheritance of a mutated copy of the alpha or beta chain of hemoglobin leading to unbalanced production of hemoglobin chains and apoptosis of most erythrocyte precursors, thalassemic individuals suffer from massively expanded but ineffective erythropoiesis and develop varying degrees of anemia. The expansion of the erythropoietic machinery inappropriately signals that more iron is needed for hemoglobin synthesis and results in hepcidin suppression. Thalassemia intermedia patients become iron overloaded which is the main cause of morbidity and mortality in this disease (4) and may cause hepatocellular carcinoma (5). In mouse models of β-thalassemia transgenic increase in hepcidin restricts iron absorption and iron supply to the developing erythrocytes, improves the efficiency of erythropoiesis and prevents iron overload. Because these patients are diagnosed within the first 2 years of life (6), there is a strong chance that minihepcidin therapy could help these patients achieve an erythropoietic balance and avoid iron overload.

Exploration of minihepcidin administration is still in its infancy, but we have shown that minihepcidins are safe and effective in mouse models. Our data indicate that minihepcidins can also be active through the oral route, though a large amount of peptide is required to reach therapeutic efficacy. Oral administration of peptides in general is difficult to achieve because of the proteolytic environment of the stomach and the small bowel (7). Even if a peptide is able to

escape proteolysis, it must still cross a number of hydrophilic and lipophilic barriers including distinct mucous and water layers that protect epithelial cells (8). The peptide must then traverse the enterocyte and subsequently, the basement membrane before entering the bloodstream.

Overcoming these challenges to make an orally available form of insulin has been the goal of many researchers over the past 80 years (9). While there are no forms currently available on the market, there are several promising candidates in clinical trials. This raises the question, "Are minihepcidins more likely to make it to clinical trials as an injectable or orally available drug?" One entity that may provide an answer is the newly formed Merganser Biotechnology which recently purchased the rights to develop minihepcidins from UCLA (10). The company will optimize minihepcidin pharmacokinetics and pharmacodynamics for injectable versions of the drug as well as explore possible oral formulations. Though there are not many orally active peptides, Linaclotide is a recently developed 14 amino acid peptide similar in size to minihepcidins that has progressed to phase III trials for the treatment of chronic constipation (11).

Chronic administration of peptide therapeutics is eventually immunogenic which presents another important area of future research with hepcidin replacement therapy (12). Because of the highly modified structure of minihepcidin PR65, the immunogenic potential of chronic minihepcidin administration must be studied. The immunogenicity of insulin and erythropoietin replacement has been studied extensively though the frequency of occurrence and physiological relevance of neutralizing antibodies is disputed. During the early years of subcutaneous insulin administration, extracts from bovine or porcine pancreases caused local reactions in 55% of recipients which were later shown to be caused the development insulin antibodies (13). These preparations contained large amounts of non-insulin peptides including glucagon and

somatostatin. The use of chromatographic techniques and recombinant DNA technology to produce highly pure human insulin has almost, but not entirely, eliminated the development of immunogenic responses. Insulin auto antibodies are found even in insulin-naïve patients and there is no consensus on whether insulin antibodies have a measurable effect on glycemic control (13).Genetic predispositions, route of administration and dosing amount and frequency are all thought to determine whether antibodies develop to exogenous proteins. In the case of recombinant erythropoietin administration (Epogen), a subset of patients can develop antibodies against human erythropoietin which blocks red blood cell production and causes pure red cell aplasia (PRCA) and necessitates ceasing Epogen treatment (14). Thus, future studies must address the immunogenic character of highly modified minihepcidins, but if all goes well, human trials of injectable and oral minihepcidins could begin in the near future.

1. Feng Q, Migas MC, Waheed A, Britton RS, Fleming RE. Ferritin Upregulates Hepatic Expression of Bone Morphogenetic Protein 6 and Hepcidin in Mice. American journal of physiology. Gastrointestinal and liver physiology [Internet]. 2012 [cited 2012 May 23];Available from: http://www.ncbi.nlm.nih.gov/pubmed/22517766

2. Andrews NC. Closing the iron gate. N. Engl. J. Med. 2012;366:376–377.

3. Rund D, Rachmilewitz E. Beta-thalassemia. N. Engl. J. Med. 2005;353:1135–1146.

4. Musallam KM, Cappellini MD, Wood JC, Motta I, Graziadei G, Tamim H, et al. Elevated liver iron concentration is a marker of increased morbidity in patients with β thalassemia intermedia. Haematologica. 2011;96:1605–1612.

5. Restivo Pantalone G, Renda D, Valenza F, D'Amato F, Vitrano A, Cassarà F, et al. Hepatocellular carcinoma in patients with thalassaemia syndromes: clinical characteristics and outcome in a long term single centre experience. Br. J. Haematol. 2010;150:245–247.

6. Musallam KM, Sankaran VG, Cappellini MD, Duca L, Nathan DG, Taher AT. Fetal hemoglobin levels and morbidity in untransfused patients with β-thalassemia intermedia. Blood. 2012;119:364–367.

7. Soltero R. Oral Protein and Peptide Drug Delivery [Internet]. In: Wang B, Siahaan TJ, Soltero R, editors. Drug Delivery: Principles and Applications. John Wiley & Sons, Inc.; 2005 [cited 2012 Apr 26]. p. 189–200.Available from: http://onlinelibrary.wiley.com/doi/10.1002/0471475734.ch10/summary

8. Soltero R. The oral delivery of protein and peptide drugs [Internet]. [cited 2012 Apr 26];Available from: http://www.iptonline.com/pdf_viewarticle.asp?cat=6&article=91

9. Heinemann L, Jacques Y. Oral insulin and buccal insulin: a critical reappraisal. J Diabetes Sci Technol. 2009;3:568–584.

10. Merganser Biotech Announces Signing of Option to License Minihepcidin Technology from UCLA | Business Wire [Internet]. [cited 2012 Apr 26];Available from: http://www.businesswire.com/news/home/20111212005209/en/Merganser-Biotech-Announces-Signing-Option-License-Minihepcidin

11. Lembo AJ, Schneier HA, Shiff SJ, Kurtz CB, MacDougall JE, Jia XD, et al. Two randomized trials of linaclotide for chronic constipation. N. Engl. J. Med. 2011;365:527–536.

12. Vlieghe P, Lisowski V, Martinez J, Khrestchatisky M. Synthetic therapeutic peptides: science and market. Drug Discov. Today. 2010;15:40–56.

13. Fineberg SE, Kawabata TT, Finco-Kent D, Fountaine RJ, Finch GL, Krasner AS. Immunological responses to exogenous insulin. Endocr. Rev. 2007;28:625–652.

14. Casadevall N, Nataf J, Viron B, Kolta A, Kiladjian J-J, Martin-Dupont P, et al. Pure red-cell aplasia and antierythropoietin antibodies in patients treated with recombinant erythropoietin. N. Engl. J. Med. 2002;346:469–475.